

Discovering optimal fermion—qubit mappings through algorithmic enumeration

Mitchell Chiew and Sergii Strelchuk

DAMTP, Centre for Mathematical Sciences, University of Cambridge, Cambridge CB30WA, UK

Abstract

Simulating fermionic systems on a quantum computer requires a high-performing mapping of fermionic states to qubits. A key characteristic of an efficient mapping is its ability to translate local fermionic interactions into local qubit interactions, leading to easy-to-simulate qubit Hamiltonians.

All fermion–qubit mappings must use a numbering scheme for the fermionic modes in order for translation to qubit operations. We make a distinction between the unordered, symbolic labelling of fermions and the ordered, numeric labelling of the qubits to which the fermionic system maps. This separation shines light on a new way to design fermion–qubit mappings by making use of the extra degree of freedom – the enumeration scheme for the fermionic modes. The purpose of this paper is to demonstrate that this concept allows for notions of fermion–qubit mappings that are *optimal*, with regard to any cost function one might choose. Our main example is the minimisation of the average number of Pauli matrices in the Jordan–Wigner transformations of Hamiltonians for fermions interacting in square lattice–type arrangements. In choosing the best ordering of fermionic modes for the Jordan–Wigner transformation, and unlike other popular modifications, our prescription does not cost additional resources such as ancilla qubits.

We demonstrate how Mitchison and Durbin’s enumeration pattern is optimal for minimising the average Pauli weight of Jordan–Wigner transformations of systems interacting in square fermionic lattices. This leads to qubit Hamiltonians consisting of terms with average Pauli weights 13.9% shorter than previously known. Furthermore, by adding only two ancilla qubits we introduce a new class of fermion–qubit mappings, and reduce the average Pauli weight of Hamiltonian terms by 37.9% compared to previous methods. For n -mode fermionic systems of cellular arrangements of square lattices, we find enumeration patterns which result in $n^{1/4}$ improvement in average Pauli weight over naïve enumeration schemes.

1 Introduction

Simulating physical systems is one of the most promising applications of quantum computers. Fermionic systems are essential components in several fields of theoretical and experimental physics, from quantum physics [1, 2, 3, 4] to quantum chemistry and condensed matter [5, 6, 7] to quantum field theories [8]. Fermions pose complex, often intractable computational challenges when studied with the aid of classical computers, such as the electronic structure problem [9], studying properties of gauge theories that govern strong interactions between quarks and gluons [10], determining ground state properties of fermionic Hamiltonians [11] and many others.

One can break down all quantum algorithms for fermionic simulation into three sequential steps: 1) initialising the quantum register, 2) applying unitary gates to the qubits, and 3) measuring the result to obtain an estimate for the desired molecular property or other quantity of interest. Within this framework, algorithms may encode the fermionic Hamiltonian via first or second quantisation. Fermi–Dirac statistics impose asymmetry on fermionic systems’ wavefunctions, and using first quantisation of the system’s Hamiltonian, one can incorporate this asymmetry into the qubit basis itself or use the qubits to directly encode the wavefunction into real–time and real–space [12, 13, 14, 15]. In contrast, second quantisation encodes the asymmetry into the qubit operators rather than the quantum states [16], and provides a number of distinct advantages over representations in the first quantisation [17, 18].

Quantum algorithms employing second quantisation require an important fourth, preemptive step: the fermion–qubit mapping, which we label 0). In the second quantisation picture, a quantum algorithm must map each term of the fermionic Hamiltonian into a sequence of Pauli matrices acting on qubits. The original problem thus becomes a k –local Hamiltonian problem, where k depends on the choice of fermion–qubit mapping.

This work introduces a new approach to defining and designing fermion–qubit mappings, which directly leads to a significant reduction in the complexity of some quantum simulation algorithms. There is practical value in any improvement to the sleekness of quantum simulation algorithms’ designs. While the k –local Hamiltonian problem is QMA–complete [19], enormous value remains in finding or approximating solutions in the average case–scenarios for practical problems, such as molecular electronic structure [20]. Turning from complexity theory, then, to focus on the more practical elimination of redundant costs in steps 0)–3) of existing fermionic simulation algorithms, there have been a number of recent developments in quantum computing that could make solutions to the above problems feasible [12, 16, 15, 14, 21, 20, 13]. Many of these approaches [12, 13] rely on phase estimation [22, 23] and thus require an impractically large number of qubits and operations in order to keep the register of the quantum computer coherent [24]. Algorithms for near–term quantum computers have sprung up in answer to these challenges, such as the variational quantum eigensolver [24, 25, 16], which is only just coming within reach of current technology.

Some improvements to quantum simulation algorithms come with no caveats: for example, careful parallelisation of Hamiltonian terms during Trotterisation in step 2) of a phase estimation algorithm can cancel out long strings of Pauli matrices, a simple adjustment that does not come at the expense of any additional resources [26]. However, the search for the best fermion–qubit mapping has largely not been met with much progress because the task of simulating fermionic interactions in a complexity–theoretic sense is very difficult to formalise. To bring the problem of fermionic simulation closer to meeting constraints of near–term quantum technology, it is crucially important to establish optimal

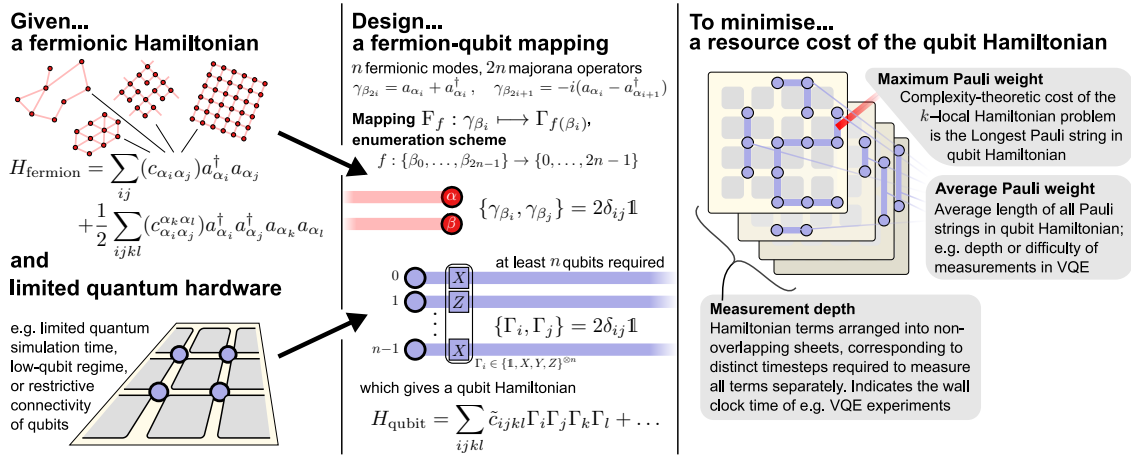


Figure 1: Schematic showing the purpose of a fermion–qubit mapping, the factors that influence its effectiveness, and various cost functions under which one might judge the effectiveness of a mapping.

protocols that strike a balance between competing resources, such as the number of qubits, local quantum operation counts, or quantum circuit depth. This is a complex challenge, as the definition of an optimal protocol may depend on the topology of the physical system to be simulated (e.g. the optimal strategy for simulating a fermionic square lattice may be different to that of a molecule), or the limitations of the quantum hardware at hand (e.g. only permitting nearest-neighbour interactions between qubits).

The century-old work of Jordan and Wigner [27] inspired the idea of fermion–qubit mappings, when Lieb et al. used their method to solve the XY -model Hamiltonian classically in 1961 [28]. In 2001, Ortiz employed the transformation as a fermion–qubit mapping in the first explicit proposal of a quantum simulation of a fermionic Hamiltonian [21]. The Jordan–Wigner transformation is intuitive and performs well in simulating nearest-neighbour Hamiltonians acting on 1D chains of fermionic modes, but experiences impracticably large overheads in higher dimensions.

Fermionic systems that permit only local interactions on a 2D or 3D lattice are a major focus of study [29, 30, 31, 32, 33]. These systems are difficult to simulate, even for quantum computers, because an overwhelming number of local fermionic interactions become non-local – and hence timely and costly to simulate – once mapped to the qubit picture. In recent years, there have been a flurry of results tackling this challenge introducing new fermion–qubit mappings as well as generalising the existing ones to higher dimensions [30, 31, 32, 34, 35, 36, 37, 38]. A common theme among these proposals is the use of ancilla qubits [36, 17, 37]. Such mappings can produce local qubit Hamiltonians, and could make small instances of a problem within reach of modest quantum computers.

Our approach makes use of a new degree of freedom in fermion–qubit mappings: the ability to index the fermionic modes in any order, a process we dub *choosing the fermionic enumeration scheme*. While trivial for a string of fermions interacting only with nearest-neighbours modes, the choice of enumeration scheme has the potential to dramatically improve the average locality of the fermion–qubit mappings for fermionic systems in 2D and above. Examining enumeration schemes, and finding the most efficient ones, we show how to reduce various cost functions of the target qubit Hamiltonian relating to scarce physical resources. This requires no additional resources such as additional Hamiltonian terms or ancilla qubits!

Thus, we arrive at the crux of our work: for a given fermionic system and a given quantum computing technology, a fermion–qubit mapping *cannot* be considered optimal

unless its fermionic enumeration scheme minimises the scarcest physical resource. Many innovations in fermion–qubit mappings have been in aid of reducing the maximum number of qubits upon which any one term in the Hamiltonian acts [39, 35, 37, 36]. This is an important metric in a complexity–theoretic sense – it is the ‘ k ’ in ‘ k –local Hamiltonian’.

Other metrics may be more practical in near–term quantum algorithms. For example, the number of Pauli measurements in a variational quantum eigensolver depends on the overall number of Pauli matrices appearing in all terms in the qubit Hamiltonian, not just the longest term. While our method could be tailored to improve many metrics of fermion–qubit mappings, the focus of this work is on improving the average locality of the qubit Hamiltonian terms. The only other work that has used this metric for fermion–qubit mappings is [38], which we discuss and incorporate into our work in Section 2.6.

In a broad class of problem fermionic Hamiltonians with non–local hopping terms, we show that minimising the average Pauli weight of a Jordan–Wigner type mapping is equivalent to the edgesum problem from graph theory [40, 41, 42, 43]. When compared to the only other ancilla–free mapping for the 2D fermionic lattice – which uses the S–pattern enumeration scheme, introduced by Verstraete and Cirac [17] – our method directly reduces the average Pauli weight of the terms in the qubit Hamiltonian by a constant factor ($\approx 13.9\%$). Our optimal fermion–qubit mapping uses a carefully selected enumeration scheme based on a special pattern recognised by Mitchison and Durbin in their seminal work [40], and culminates in:

Theorem 1 [Informal] *For a fermionic Hamiltonian acting on a system of $n = N^2$ local fermionic modes with interactions only between nearest neighbours on the square $N \times N$ lattice, the Jordan–Wigner transformation that uses the Mitchison–Durbin pattern to enumerate the modes minimises the average Pauli weight of the qubit Hamiltonian.*

The structure of the paper is as follows: in Section 2 we provide a self–contained introduction to fermion–qubit mappings and identify the role that fermionic enumeration schemes play. We give a new, broad definition that encapsulates all n –mode to n –qubit mappings before narrowing our focus to the Jordan–Wigner transformation. We follow with results from complexity theory that will be used to prove our main result.

In Section 3, we discuss the maximum Pauli weight and measurement depth of qubit Hamiltonians, which are practical figures of merit worth minimising in fermion–qubit mappings. We present Theorem 1 for constructing Jordan–Wigner transformations for 2D fermionic lattice systems that they minimise the average Pauli weight of qubit Hamiltonian terms. We argue that our approach can improve simulations for many fermionic systems, and use an heuristic approach to find Jordan–Wigner transformations for certain n –mode fermionic systems that provide average Pauli weights shorter than those of naïve alternatives by a factor of $\mathcal{O}(n^{1/4})$.

In Section 4, we explain auxiliary qubit mapping techniques and modify our fermion–qubit mapping to improve Theorem 1’s 13.9% advantage over the Z– and S–patterns to nearly 38% using just two ancilla qubits.

Finally, in Section 5 we discuss open problems and directions for further research. We also mention the qubit routing problem as a potential generalisation of the optimisation problems described in this paper.

2 Defining fermion–qubit mappings

This section outlines the theory of fermion–qubit mappings: Section 2.1 describes the motivation, while Section 2.2 the requirements of a mapping. The naïve definition of the Jordan–Wigner transformation appears in Section 2.3, before we introduce the Jordan–

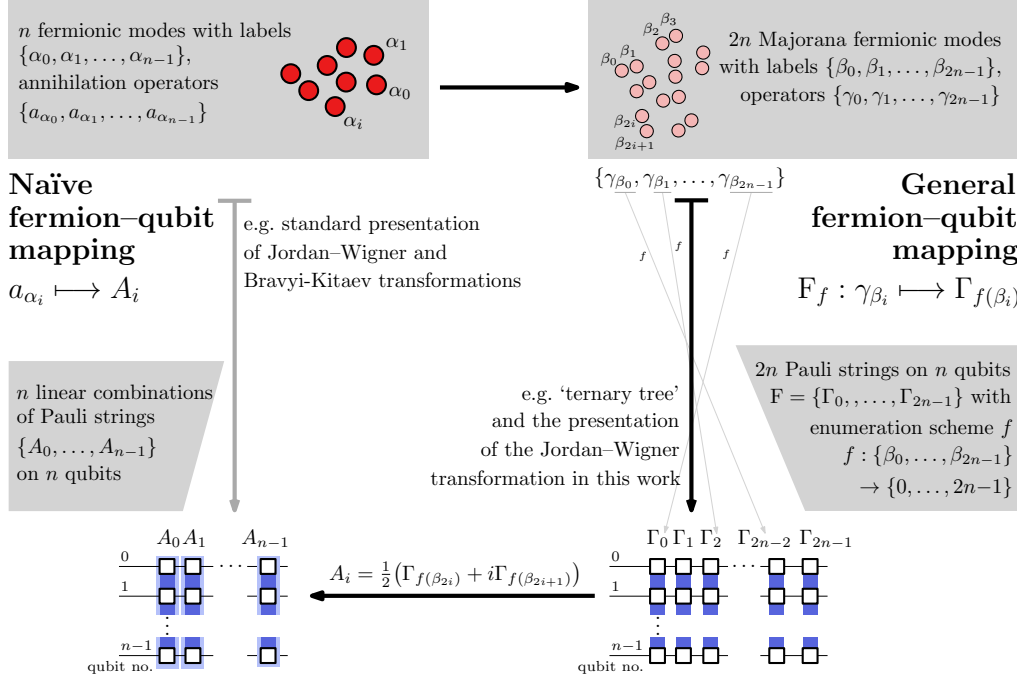


Figure 2: The role of enumeration schemes is hidden in naïve descriptions of fermion–qubit mappings, but becomes apparent in our general definition; it is also recognisable in the ternary tree transformation.

Wigner transformation with fermion enumeration schemes in Section 2.4, which is the working definition we use for the rest of the paper. We generalise our definition of fermion–qubit mappings in Section 2.5 to demonstrate that the principle of optimising over enumeration schemes is a valid for improving all fermion–qubit mappings, with a specific example in Section 2.6. In Section 2.7 we detail the graph theory related to the problem of finding optimal Jordan–Wigner transformations with fermion enumeration schemes.

2.1 Goal of fermion–qubit mappings

Typical second–quantised fermionic Hamiltonians of interest, such as molecular electronic Hamiltonians, describe the energy of quantum systems with n sites, or *modes*, each of which can be either occupied or unoccupied by a fermion. Use the distinct, unordered, symbolic labels $\{\alpha_0, \alpha_1, \dots, \alpha_{n-1}\}$ to distinguish the n fermionic modes, and denoting the annihilation operator of a fermion in mode α_i by a_{α_i} , physical Hamiltonians take the form

$$H_{\text{fermion}} = \sum_{i,j=0}^{n-1} (c_{\alpha_i \alpha_j}) a_{\alpha_i}^\dagger a_{\alpha_j} + \frac{1}{2} \sum_{i,j,k,l=0}^{n-1} (c_{\alpha_i \alpha_j}^{\alpha_k \alpha_l}) a_{\alpha_i}^\dagger a_{\alpha_j}^\dagger a_{\alpha_k} a_{\alpha_l}, \quad (1)$$

where the c are complex coefficients that ensure the hermiticity of the Hamiltonian. As an example, in the Fermi–Hubbard model [44] the fermions are electrons, and the coefficients $c_{\alpha_i \alpha_j}$ and $c_{\alpha_i \alpha_j}^{\alpha_k \alpha_l}$ are respectively one– and two–electron overlap integrals. A fermionic Hamiltonian consisting just of quadratic single–particle terms $a_{\alpha_i}^\dagger a_{\alpha_j}$ may easily be diagonalised and its eigenvalues simply read off [45]. The presence of quartic terms $a_{\alpha_i}^\dagger a_{\alpha_j}^\dagger a_{\alpha_k} a_{\alpha_l}$ usually makes simulation of the Hamiltonian classically intractable, and as such an object of interest for prospective quantum algorithms.

The intended use of a fermion–qubit mapping is as a tool to translate from the fermionic

picture into Hamiltonians that can be implemented on qubits in a laboratory:

$$H_{\text{fermion}} \mapsto H_{\text{qubit}} = \sum_{ij} (c_{\alpha_i \alpha_j}) A_i^\dagger A_j + \frac{1}{2} \sum_{ijkl} (c_{\alpha_i \alpha_j}^{\alpha_k \alpha_l}) A_i^\dagger A_j^\dagger A_k A_l. \quad (2)$$

A fermion–qubit mapping is a representation of the fermionic algebra in Equation 3, characterised by the set $\{A_i\}_{i=0}^{n-1}$ of complex matrix representations of the annihilation operators $\{a_{\alpha_i}\}_{i=0}^{n-1}$.

The operators should be straightforward to write in the basis of n –qubit Pauli operators $\{\{\mathbb{1}, X, Y, Z\}^{\otimes n}\}$, to be practical for real–world quantum technology. We use the notation $X_i = \sigma_i^x$, $Y_i = \sigma_i^y$, $Z_i = \sigma_i^z$ for the Pauli operators on the qubit with label i .

A further practical caveat is that the fermionic vacuum state $|\Omega\rangle$, which uniquely satisfies $a_{\alpha_i} |\Omega\rangle = 0$ for all i , becomes a product state such as $|0\rangle^{\otimes n}$ on the qubits. The name for this property is *product–preserving*. The popular fermion–qubit mappings – Jordan–Wigner, Bravyi–Kitaev and ternary tree – all satisfy this constraint [46].

2.2 Canonical anticommutation relations

As in [39], our convention is to treat fermionic modes as either occupied or unoccupied, treating any spin–up and spin–down modes as distinct. Thus, a system of n identical fermionic modes inhabits a 2^n –dimensional complex–valued Hilbert space.

Given a quantum system with n fermionic modes, its Hamiltonian H_{fermion} is of the form of Equation 1. The *canonical anticommutation relations* fully describe the fermionic operators:

$$\{a_{\alpha_i}, a_{\alpha_j}\} = 0, \{a_{\alpha_i}^\dagger, a_{\alpha_j}^\dagger\} = 0, \{a_{\alpha_i}, a_{\alpha_j}^\dagger\} = \delta_{ij} \mathbb{1}. \quad (3)$$

For each fermionic label $\alpha_i \in \{\alpha_0, \dots, \alpha_{n-1}\}$, there are two labels $\beta_{2i}, \beta_{2i+1} \in \{\beta_0, \dots, \beta_{2n-1}\}$ which relate the operators a_{α_i} and $a_{\alpha_i}^\dagger$ via the *Majorana operators*:

$$\gamma_{\beta_{2i}} = a_{\alpha_i} + a_{\alpha_i}^\dagger \quad (4)$$

$$\gamma_{\beta_{2i+1}} = -i(a_{\alpha_i} - a_{\alpha_i}^\dagger). \quad (5)$$

The Majorana operators $\{\gamma_{\beta_0}, \gamma_{\beta_1}, \dots, \gamma_{\beta_{2n-1}}\}$ form an alternative set of fermionic operators, equivalent to the complete set of creation and annihilation operators $\{a_{\alpha_0}, a_{\alpha_0}^\dagger, \dots, a_{\alpha_{n-1}}, a_{\alpha_{n-1}}^\dagger\}$. Each of the Majorana operators is its own Hermitian conjugate, and, by construction, neither $\gamma_{\beta_{2i}}$ nor $\gamma_{\beta_{2i+1}}$ are involved in the definition of any other a_{α_j} for $j \neq i$. The Majoranic equivalent to the anticommutation relations in Equation 3 is thus simply

$$\gamma_{\beta_i} = \gamma_{\beta_i}^\dagger, \quad \{\gamma_{\beta_i}, \gamma_{\beta_j}\} = 2\delta_{ij} \mathbb{1}. \quad (6)$$

for $i, j \in \{0, 1, \dots, 2n - 1\}$.

In Sections 3 and 4, we use the language of creation and annihilation operators $a_\alpha^\dagger, a_\alpha$, since they are the ingredients of the Jordan–Wigner transformation. However, Majorana operators are necessary to explore the complete picture of enumeration schemes’ role within fermion–qubit mappings, as we explain in Section 2.5.

2.3 The standard (naïve) definition of the Jordan–Wigner transformation

Suppose that the labels for the fermionic modes were ordered via the scheme $\alpha_0 \mapsto 0, \alpha_1 \mapsto 1, \dots, \alpha_{n-1} \mapsto n - 1$. Then, with the notion of order for the fermionic modes, we could define the system’s Fock space with the occupancy number basis $\{|j_0, j_1, \dots, j_{n-1}\rangle : j_i \in$

$\{0, 1\}$, where j_i denotes the occupancy of the i th fermionic mode. The annihilation operators act as

$$a_{\alpha_i} |j_0 \dots \underbrace{0}_{i\text{th mode}} \dots j_{n-1}\rangle = 0 \quad (7)$$

$$a_{\alpha_i} |j_0 \dots \underbrace{1}_{i\text{th mode}} \dots j_{n-1}\rangle = (-1)^{\sum_{k=1}^{i-1} j_k} |j_0 \dots \underbrace{0}_{i\text{th mode}} \dots j_{n-1}\rangle, \quad (8)$$

while $a_{\alpha_i}^\dagger$ acts as the Hermitian conjugate of a_i . Equations 7 and 8 are equivalent to Equation 3 [45]. This formulation allows us to define the Jordan–Wigner transformation in the original way [27], as a map from an n -mode fermionic system to an n -qubit system, where the qubits also have ordered labels $0, 1, \dots, n-1$:

Definition 1. (*Naïve Jordan–Wigner transformation.*) The naïve Jordan–Wigner transformation for a system with n fermionic modes is a 2^n -dimensional representation $\overline{\text{JW}}_{\text{naïve}}$ of the fermionic algebra. In particular, $\overline{\text{JW}}_{\text{naïve}}$ restricts to a bijection between the annihilation operators and a set $\overline{\text{JW}} = \{A_0, A_1, \dots, A_{n-1}\}$:

$$\overline{\text{JW}}_{\text{naïve}} : a_{\alpha_i} \mapsto A_i = \left(\bigotimes_{k=0}^{i-1} Z_k \right) \frac{1}{2} (X + iY)_i. \quad (9)$$

To verify that this is a valid fermion–qubit mapping, i.e. that the A_i replicate Equation 3, observe that $\{Z_i, X_i\} = \{Z_i, Y_i\} = 0$. Therefore, the $\{A_i\}_{i=0}^{n-1}$ that characterise $\overline{\text{JW}}_{\text{naïve}}$ satisfy

$$\{A_i^{(\dagger)}, A_j^{(\dagger)}\} = 0, \{A_i, A_j^\dagger\} = \delta_{ij} \mathbb{1}. \quad (10)$$

2.4 A definition for the Jordan–Wigner transformation that incorporates enumeration schemes

The standard description of the Jordan–Wigner transformation does not make clear that one of its inherent components is an *enumeration scheme* for the fermionic modes, a bijective mapping from unordered fermionic labels to the natural number labels of qubits. The following definition makes the role of the enumeration scheme explicit:

Definition 2. The *Jordan–Wigner transformation with a fermionic enumeration scheme* for a system with n fermionic modes is a 2^n -dimensional representation $\overline{\text{JW}}_f$ of the fermionic algebra, equipped with a bijective enumeration scheme f for the fermionic modes:

$$f : \{\alpha_0, \dots, \alpha_{n-1}\} \longrightarrow \{0, \dots, n-1\}. \quad (11)$$

In particular, $\overline{\text{JW}}_f$ restricts to a bijection between the annihilation operators and a set $\overline{\text{JW}} = \{A_0, \dots, A_{n-1}\}$:

$$\overline{\text{JW}}_f : a_{\alpha_i} \mapsto A_{f(\alpha_i)}, \quad (12)$$

where A_i has the same expression as in Definition 1.

The purpose of generalising the Jordan–Wigner transformation to Definition 2 is to demonstrate that there is complete freedom in labelling the fermionic modes: no matter the ordering f , we recover the canonical anticommutation relations of Equation 3. The operators A_i are still drawn from the set $\overline{\text{JW}}$, which satisfies Equation 10. For example, the enumeration scheme $f(\alpha_i) = i$ recovers the naïve mapping from Definition 1.

The topic of discussion of Sections 3 and 4 is defining the degree of freedom f in $\overline{\text{JW}}_f$ and how to exploit it for material gain. Before we come to that, first let us fully generalise the concept of fermion–qubit mappings.

2.5 A general definition for fermion–qubit mappings that incorporates enumeration schemes

As it turns out, the freedom of choice to associate each of the annihilation operators a_{α_i} with a unique linear combination of Pauli strings $A_{f(\alpha_i)}$ in Definition 2 does not capture the full degree of freedom in the choice of enumeration schemes in general. The Majorana fermionic operators $\{\gamma_{\beta_0}, \dots, \gamma_{\beta_{2n-1}}\}$ from Equations 4 and 5 are equivalent building blocks for any fermionic system described by Equation 3, and have the benefit of obeying the more concise anticommutation relations of Equation 6.

We propose that the broadest definition of a fermion–qubit mapping from n modes to n qubits is as follows:

Definition 3. (*General fermion–qubit mapping.*) A fermion–qubit mapping for a system with n fermionic modes system is a 2^n –dimensional representation F_f of the fermionic algebra, equipped with a bijective enumeration scheme f for the Majorana modes

$$f : \{\beta_0, \dots, \beta_{2n-1}\} \longrightarrow \{0, 1, \dots, 2n-1\}. \quad (13)$$

The restriction of F_f to the Majorana operators is a bijection to $2n$ pairwise–anticommuting Pauli strings $F = \{\Gamma_0, \dots, \Gamma_{2n-1}\}$, with $\Gamma_i \in \{\mathbb{1}, X, Y, Z\}^{\otimes n}$. That is,

$$F_f : \gamma_{\beta_i} \longmapsto \Gamma_{f(\beta_i)}. \quad (14)$$

Since the elements Γ_i of F are Pauli strings, they are Hermitian. Thus, with their pairwise–anticommutation,

$$\Gamma_i = \Gamma_i^\dagger, \quad \{\Gamma_i, \Gamma_j\} = 2\delta_{ij}\mathbb{1} \quad (15)$$

for all $i, j = 0, 1, \dots, 2n-1$, reproducing the fermionic system described by Equation 6 as required.

Corollary 1. The restriction of the fermion–qubit mapping F_f to the annihilation operators $\{a_{\alpha_0}, \dots, a_{\alpha_{n-1}}\}$ is a bijection to a set $\{A_0, \dots, A_{n-1}\}$ defined by

$$F_f : a_{\alpha_i} \longmapsto A_i = \frac{1}{2} \left(\Gamma_{f(\beta_{2i})} + i\Gamma_{f(\beta_{2i+1})} \right), \quad (16)$$

for $i = 0, 1, \dots, n-1$. This arises from Equations 4 and 5, which give for $i = 0, 1, \dots, n-1$

$$a_{\alpha_i} = \frac{1}{2} (\gamma_{\beta_{2i}} + i\gamma_{\beta_{2i+1}}). \quad (17)$$

The A_i satisfy Equation 10 by construction.

Figure 2 visualises the relation between the operators A_i arising from a general fermion–qubit mapping in Definition 3 and the A_i operators that arise from naïve mappings such as the Jordan–Wigner transformation in Definition 1. The most general form of the Jordan–Wigner transformation is thus:

Example 1. (*General Jordan–Wigner transformation*) The *general Jordan–Wigner transformation* for a system with n fermionic modes is a fermion–qubit mapping JW_f which restricts to a bijection between the Majorana operators and a set of $2n$ pairwise–anticommuting Pauli strings $JW = \{\Gamma_0, \dots, \Gamma_{2n-1}\}$, defined for $i = 0, \dots, n-1$ by

$$\Gamma_{2i} = \left(\bigotimes_{k=0}^{i-1} Z_k \right) X_i, \quad (18)$$

$$\Gamma_{2i+1} = \left(\bigotimes_{k=0}^{i-1} Z_k \right) Y_i. \quad (19)$$

That is,

$$\text{JW}_f : \gamma_{\beta_i} \mapsto \Gamma_{f(\beta_i)}. \quad (20)$$

Note that the Pauli strings Γ_i have length $\mathcal{O}(n)$. The annihilation operators of the general Jordan–Wigner transformation map to:

$$\text{JW}_f : a_{\alpha_i} \mapsto A_i = \frac{1}{2} \left(\Gamma_{f(\beta_{2i})} + i\Gamma_{f(\beta_{2i+1})} \right), \quad (21)$$

which satisfy Equation 10 by construction.

Remark 1. If the fermionic enumeration scheme for the Majorana modes f satisfies $f(\beta_{2i+1}) = f(\beta_{2i}) + 1$ for all $i = 0, \dots, n-1$, then JW_f reduces to $\overline{\text{JW}}_f$ from Definition 2. Thus, the Jordan–Wigner transformation with a fermionic enumeration scheme in Definition 2 does not capture the true degree of freedom in enumeration schemes – it is only a special case of the general Jordan–Wigner transformation described in Example 1.

Remark 2. (*Notation.*) The most general form of a fermion–qubit mapping, which we write as F_f , maps Majorana operators to Pauli strings. We use the overline notation \overline{F}_f for mappings that enumerate the n fermionic modes. The expression $\overline{F}_{\text{naïve}}$ denotes mappings that unnecessarily force a specific enumeration scheme such as $f(\alpha_i) = i$, with the aim to highlight the naïveté. For example, the relation between these different classes of mappings for the Jordan–Wigner transformation is:

$$\overline{\text{JW}}_{\text{naïve}} = \overline{\text{JW}}_f \text{ where } f(\alpha_i) = i; \quad (22)$$

$$\overline{\text{JW}}_f = \text{JW}_g \text{ where } g(\beta_{2i}) = f(\alpha_i) \text{ and} \quad (23)$$

$$g(\beta_{2i+1}) = f(\alpha_i + 1).$$

Definition 3 encapsulates all forms of the Jordan–Wigner, Bravyi–Kitaev [39], ternary tree [38], and other n -qubit transformations, and thus allows a fair comparison between them as in Section 2.6 and [47]. By expanding the definition of the pairwise–anticommuting Pauli strings to $\Gamma_i \in \{\mathbf{1}, X, Y, Z\}^{\otimes m}$ for $m \geq n$ such that 15 still holds, the general definition here could be extended to include mappings with ancilla qubits such as [17, 37, 36]; we leave such extension for future work.

2.6 Comparison between different mapping types and the notion of an optimal fermion–qubit mapping

Through the lens of Definition 3, the feature that identifies a mapping as being of Jordan–Wigner type is that it associates Majorana fermionic operators with a set of Pauli strings JW of the forms in Equations 18 and 19.

In the literature, the search for more efficient mappings beyond the Jordan–Wigner transformation resulted in the Bravyi–Kitaev transformation [39], which yields exponentially shorter Pauli strings in the asymptotic limit. The Bravyi–Kitaev transformation does not outperform the Jordan–Wigner on modest fermionic systems, however, and has a similar T–gate count [48]. Aside from its intuitive definition, the Jordan–Wigner mapping has also gained widespread use because it demands far fewer degrees of connectivity from the qubit architecture [37].

We can construct the most general definition for other types of fermion–qubit mappings, where the identifying feature of each mapping type is the unique set of Pauli strings to which it maps the Majorana fermionic operators. For example, the most general definition for the Bravyi–Kitaev transformation [39] is:

Example 2. (*General Bravyi–Kitaev transformation.*) The general Bravyi–Kitaev transformation for a system with n fermionic modes is a fermion–qubit mapping BK_f which restricts to a bijection between the Majorana operators and a set of $2n$ pairwise–anticommuting Pauli strings $\text{BK} = \{\Gamma_0, \dots, \Gamma_{2n-1}\}$, defined for $i = 0, \dots, n-1$ by

$$\Gamma_{2i} = X_{U(i)} X_i Z_{P(i)}, \quad (24)$$

$$\Gamma_{2i+1} = \begin{cases} X_{U(i)} Y_i Z_{P(i)}, & i \text{ even,} \\ X_{U(i)} Y_i Z_{R(i)}, & i \text{ odd.} \end{cases} \quad (25)$$

That is,

$$\text{BK}_f : \gamma_{\beta_i} \mapsto \Gamma_{f(\beta_i)} \quad (26)$$

Here, using the notation of Seeley et al. [49], the sets $U(i)$, $P(i)$ and $R(i)$ are subsets of $\{0, 1, \dots, n-1\}$ of size $\sim \log_2 n$.

Much like the Jordan–Wigner transformation, this general definition of the Bravyi–Kitaev transformation is more extensive than the usual naïve presentation, which simply maps annihilation operators to their qubit equivalents $\overline{\text{BK}}$ with the trivial enumeration scheme $f : \alpha_i \mapsto i$:

$$\overline{\text{BK}}_{\text{naïve}} : a_{\alpha_i} \mapsto A_i = \frac{1}{2} (\Gamma_{2i} + i\Gamma_{2i+1}). \quad (27)$$

Example 3. (*Ternary tree transformation.*) Unlike the naïve versions of the Bravyi–Kitaev and Jordan–Wigner transformations, the base definition of the ternary tree transformation [38] is already similar to Definition 3: it is a map TT_f that identifies the Majorana fermionic operators $\{\gamma_{\beta_0}, \dots, \gamma_{\beta_{2n-1}}\}$ with Hermitian, pairwise–anticommuting Pauli strings $\text{TT} = \{\Gamma_0, \dots, \Gamma_{2n-1}\}$ defined by

$$\begin{aligned} \text{TT} = \{ & \Gamma_0 = X_0 X_1 X_4 \dots X_{\frac{n-1}{3}}, \\ & \Gamma_1 = X_0 X_1 X_4 \dots Y_{\frac{n-1}{3}}, \\ & \Gamma_2 = X_0 X_1 X_4 \dots Z_{\frac{n-1}{3}}, \\ & \dots, \\ & \Gamma_{2n-2} = Z_0 Z_3 Z_{12} \dots X_{n-1}, \\ & \Gamma_{2n-1} = Z_0 Z_3 Z_{12} \dots Y_{n-1} \}. \end{aligned} \quad (28)$$

We mention the mapping here for the purpose of making its dependence on an enumeration scheme f explicit, rather than implicit as in its initial presentation in [38]:

$$\text{TT}_f : \gamma_{\beta_i} \mapsto \Gamma_{f(\beta_i)}. \quad (29)$$

Strictly speaking, Equation 28 only describes TT if $2n+1$ is a power of 3. The mapping can be altered slightly to accommodate other values of n without suffering any ill effects: namely, the remarkable $\sim \log_3(2n)$ Pauli weight of each of the Γ_i qubit operators, which is the provably optimal average Pauli weight of any such set of Pauli strings F in an n -fermion to n -qubit mapping [38].

Examples 1–3 demonstrate that the Pauli strings Γ_i in the Jordan–Wigner, Bravyi–Kitaev and ternary tree mappings have maximum weight n , $\sim \log_2(n)$ and $\sim \log_3(2n)$. This might incline one to declare the Bravyi–Kitaev transformation to be an improvement on Jordan–Wigner, and the ternary tree mapping to be the best of all possible mappings.

Role of enumeration schemes $f : \{\beta_0, \dots, \beta_{2n-1}\} \rightarrow \{0, \dots, 2n-1\}$ in zero-ancilla fermion-qubit mappings

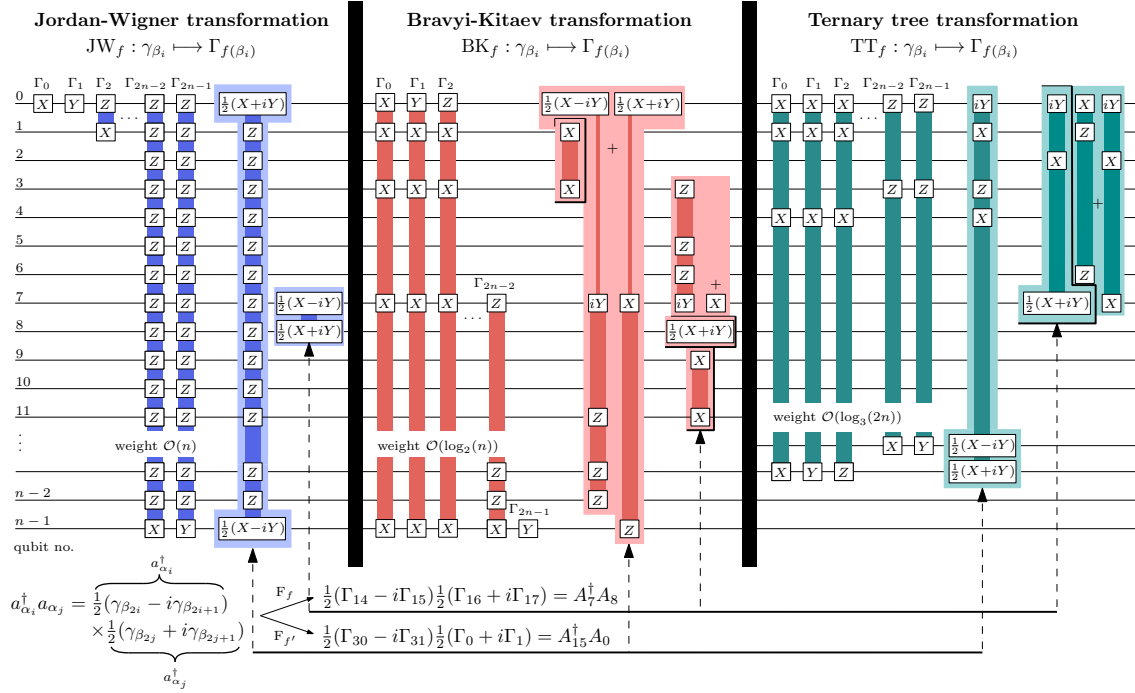


Figure 3: A general fermion-qubit mapping F_f for a system with n fermionic modes described by Majorana operators $\{\gamma_{\beta_0}, \gamma_{\beta_1}, \dots, \gamma_{\beta_{2n-1}}\}$ consists of a set of pairwise-anticommuting Pauli strings $F = \{\Gamma_0, \Gamma_1, \dots, \Gamma_{2n-1}\}$ along with an enumeration scheme $f : \{\beta_0, \dots, \beta_{2n-1}\} \mapsto \{0, 1, \dots, 2n-1\}$. This diagram displays three well-known fermion-qubit mappings: the Jordan-Wigner, Bravyi-Kitaev, and ternary tree mappings, and shows how the enumeration scheme dictates the properties physical operators, which are products of $a_{\alpha_i}^\dagger = \frac{1}{2}(\gamma_{\beta_{2i}} - i\gamma_{\beta_{2i+1}})$ and $a_{\alpha_j} = \frac{1}{2}(\gamma_{\beta_{2j}} + i\gamma_{\beta_{2j+1}})$ for $i, j \in \{0, 1, \dots, n-1\}$. Suppose that f and f' are two distinct Majorana enumeration schemes with $f(\{\beta_{2i}, \beta_{2i+1}, \beta_{2j}, \beta_{2j+1}\}) = \{14, 15, 16, 17\}$ respectively, and $f'(\{\beta_{2i}, \beta_{2i+1}, \beta_{2j}, \beta_{2j+1}\}) = \{30, 31, 0, 1\}$ respectively. The interaction terms $A_7^\dagger A_8$ and $A_{15}^\dagger A_0$ are noticeably distinct under f compared to f' , for all three fermion-qubit mapping types.

However, recall from Section 2.1 that the goal of any fermion–qubit mapping is to simulate a fermionic Hamiltonian H_{fermion} with physical interaction terms of the form $a_{\alpha_i}^\dagger a_{\alpha_j}$ and $a_{\alpha_i}^\dagger a_{\alpha_j}^\dagger a_{\alpha_k} a_{\alpha_l}$. These terms are linear combinations of products of particular Majorana operators γ_{β_i} . Given a fermion–qubit mapping F_f , the terms in the qubit Hamiltonian H_{qubit} are of the form $A_i^\dagger A_j$ and $A_i^\dagger A_j^\dagger A_k A_l$, which are linear combinations of products of the Pauli strings $\Gamma_i \in F = \{\Gamma_0, \dots, \Gamma_{2n-1}\}$. Even for the ternary tree mapping, the Pauli weight of the physical interaction terms varies depending on the enumeration scheme f , as Figure 3 demonstrates.

Moreover, there are a multitude of properties of the qubit Hamiltonian H_{qubit} that one might want to minimise depending on the quantum technology at hand. For example, the *average Pauli weight* or the *Pauli measurement depth* of the terms in H_{qubit} are quantities that can determine the resource cost in near–term algorithms such as the variational quantum eigensolver. The *maximum Pauli weight* of any one term in H_{qubit} is the ‘ k ’ in its k –local Hamiltonian problem, and hence a measure of computational complexity. Thus, it could be an appropriate target to minimise for long–term algorithms such as those involving phase estimation.

Therefore, we argue that the notion of an optimal fermion–qubit mapping is only well–defined given these two contexts: the problem Hamiltonian H_{fermion} , and a physical resource cost C to minimise in H_{qubit} . Given these inputs, the total search space for an optimal fermion–qubit mapping F_f of the form given in Definition 3 is characterised by:

1. The set of mutually–anticommuting Pauli strings $F = \{\Gamma_0, \dots, \Gamma_{2n-1}\}$, determined by the type of fermion–qubit mapping, e.g. Jordan–Wigner, Bravyi–Kitaev, or ternary tree; and,
2. The enumeration scheme $f : \{\beta_0, \dots, \beta_{2n-1}\} \rightarrow \{0, \dots, 2n - 1\}$.

A brute–force search over all the enumeration schemes for one set of Pauli strings F must reckon with a $(2n)!$ –size dataset; once we include the search over all mapping types for F , the task will become even more unwieldy.

In this work, we argue that it *is* possible to make meaningful headway in the search for an optimal fermion–qubit mapping. In this paper, we propose the approach of fixing the mapping type F and searching for the optimal fermion enumeration scheme f .

Definition 4. (*Optimal fermion–qubit mapping of type F .*) Let H_{fermion} be a fermionic Hamiltonian on n modes, let F be a fermion–qubit mapping type, and suppose we possess a qubit architecture with some limiting resource. Then for any fermion–qubit mapping F_f , let $C = C(f)$ be the cost function of the qubit Hamiltonian $H_{\text{qubit}} := H_{\text{qubit}}(f) = F_f(H_{\text{fermion}})$ with respect to that resource. The C –*optimal fermion–qubit mapping of type F for H_{fermion}* is the fermion–qubit mapping F_{f^*} , where f^* is a Majorana fermionic enumeration scheme satisfying

$$f^* = \arg \min_f C(f). \quad (30)$$

In Section 3, we find optimal fermion–qubit mappings of Jordan–Wigner type $\overline{\text{JW}}_f$ for various common problem Hamiltonians H_{fermion} , and various common cost functions C such as the average and maximum Pauli weight of terms in H_{qubit} . In Section 4, we loosen Definition 2 of the Jordan–Wigner transformation $\overline{\text{JW}}_f$ to find fermion–qubit with two ancilla qubits that outperform the optimal mappings from Section 3.

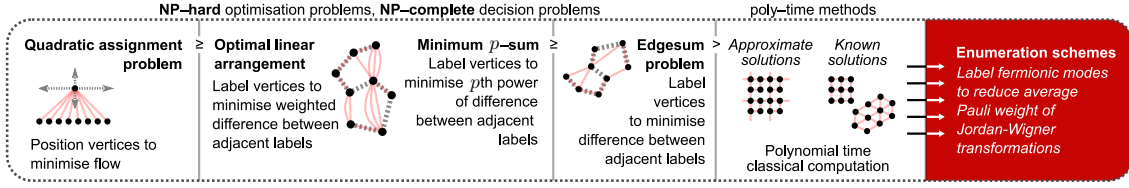


Figure 4: Complexity-theoretic hierarchy of problems generalising the edgesum problem.

2.7 Complexity-theoretical preliminaries

This section introduces the notation and complexity theoretic problems that underpin the results of Section 3. Awareness of these problems is necessary to find optimal fermion-qubit mappings of Jordan-Wigner type as described in Definition 4. Figure 4 gives a summary of the hierarchy of these problems, all of which start with some variation of the following ingredients:

1. A **graph** $G = (V, E)$ with $|V| = n$ vertices and edge set $E \subseteq V \times V$, and
2. a **weight function** $w : E \rightarrow \mathbb{R}$ which assigns a value $w(\alpha, \beta)$ to the edge (α, β) between vertices $\alpha, \beta \in V$, and
3. a list L of possible **locations** for the vertices, and
4. a **distance function** $d : L \times L \rightarrow \mathbb{R}$ describing the spatial separation between the locations.

All optimisation problems in this section have NP-complete decision versions, and are thus NP-hard. They share the objective of finding an injective *assignment function* $f : V \rightarrow L$ to place the vertices in locations so as to minimise a cost function. We call f a *vertex enumeration scheme* when $L = \{0, 1, \dots, n-1\}$.

The problems in this section appear in order of descending complexity, in that subsequent problems are special cases of earlier problems. The following problem was introduced by Koopmans and Beckmann [50]

QUADRATIC ASSIGNMENT

INSTANCE: Graph $G = (V, E)$, weight function $w : E \rightarrow \mathbb{R}$, vertex locations L , distance function $d : L \times L \rightarrow \mathbb{R}$.

PROBLEM: Find the location assignment function $f : V \rightarrow L$ in such a way as to minimise the assignment function

$$C(f) = \sum_{(\alpha, \beta) \in E} w(\alpha, \beta) \cdot d(f(\alpha), f(\beta)) . \quad (31)$$

The optimal linear arrangement problem was first studied by Garey and Johnson [41]. Note that it is different to the “optimal linear arrangement” in their book [43].

OPTIMAL LINEAR ARRANGEMENT

INSTANCE: Graph $G = (V, E)$, weight function $w : E \rightarrow \mathbb{Z}$.

PROBLEM: Find the enumeration scheme $f : V \rightarrow \{0, 1, \dots, n-1\}$ that minimises the assignment function

$$C(f) = \sum_{(\alpha, \beta) \in E} w(\alpha, \beta) \cdot |f(\alpha) - f(\beta)|. \quad (32)$$

This is a special case of the quadratic assignment problem: the weight function w is restricted to integer values, the vertex locations L are $\{1, 2, \dots, n\}$, and the distance metric is $d(i, j) = |i - j|$.

The minimum p -sum problem was studied by Mitchison and Durbin [40], Garey and Johnson [42], and Juvan and Mohar [51].

MINIMUM p -SUM

INSTANCE: Graph $G = (V, E)$, integer $p \in \mathbb{Z}$.

PROBLEM: Find the enumeration scheme $f : V \rightarrow \{0, 1, \dots, n-1\}$ that minimises the assignment function

$$C^p(f) = \left(\sum_{(\alpha, \beta) \in E} |f(\alpha) - f(\beta)|^p \right)^{1/p}. \quad (33)$$

This is a special case of the optimal linear arrangement problem, because its weight function is effectively $w(\alpha, \beta) = |f(\alpha) - f(\beta)|^{p-1} \in \mathbb{Z}$. The decision version of the problem is NP-complete for $p = 1$ [41], $p = 2$ [52] and $p \rightarrow \infty$ [53]. One could also consider the broader class of problems where $p \in \mathbb{R}^+$, as done by Mitchison and Durbin [40]. These problems are likely to be at least as hard as their integer- p equivalents.

2.7.1 Special cases of minimum p -sum

The edgesum problem was introduced in [41], and the study of this problem is the key ingredient to our optimal Jordan–Wigner transformations in Section 3:

EDGESUM (or SIMPLE OPTIMAL LINEAR ARRANGEMENT, MINIMUM 1-SUM)

INSTANCE: Graph $G = (V, E)$.

PROBLEM: Find the enumeration scheme $f : V \rightarrow \{0, 1, \dots, n-1\}$ that minimises the assignment function

$$C(f) = \sum_{(\alpha, \beta) \in E} |f(\alpha) - f(\beta)|. \quad (34)$$

The decision version of this problem is known to be NP-complete via a reduction to the simple max-cut problem [41]. Figure 5 surveys the graphs with known solutions, as of the date of publication of Horton’s PhD thesis [53] which cites a solution for outerplanar graphs by Frederickson and Hambruch [55]. Other sources include a survey by Lai [54], and solution for tree graphs by Chung [56].

As an example of a comparable problem, consider the following:

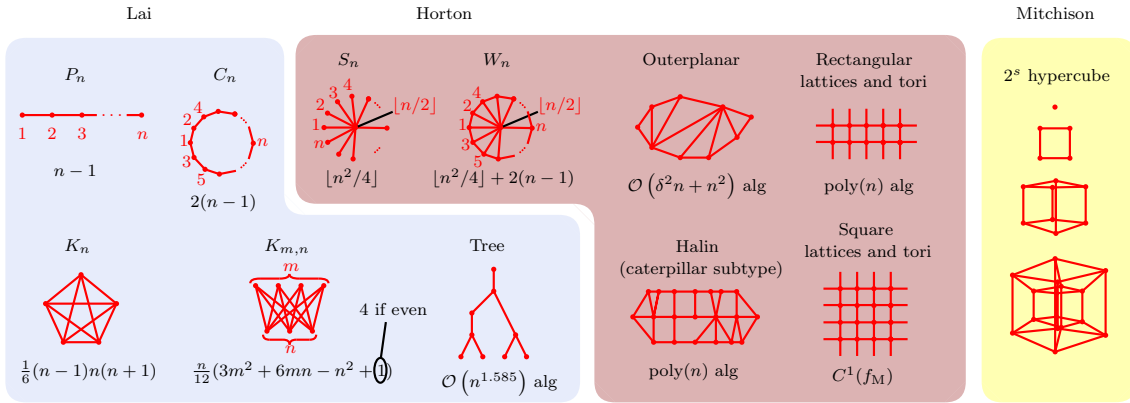


Figure 5: Graph families with known solutions to their edgesum problems. The formula for the minimum edgesum appears beneath each graph's image, if it exists, or the cost of the best-known classical algorithm for solving that graph's edgesum problem if not. References for the solution of these graphs appear in Lai [54], Horton [53], and Mitchison's [40] works as indicated.

BANDWIDTH (or MINIMUM ∞ -SUM)

INSTANCE: Graph $G = (V, E)$.
PROBLEM: Find the enumeration scheme $f : V \rightarrow \{0, 1, \dots, n-1\}$ that minimises cost function

$$C^\infty(f) = \max_{(\alpha, \beta) \in E} |f(\alpha) - f(\beta)|. \quad (35)$$

This is the minimum p -sum problem as $p \rightarrow \infty$. The decision version of the bandwidth problem is NP-complete for e.g. an arbitrary tree graph [42]; conversely, Saxe proves that the decision problem as to whether the bandwidth is less than or equal to $k = O(1)$ is efficiently solvable [57].

3 Optimal fermion-qubit mappings of Jordan-Wigner type

This section demonstrates the key idea of our approach: using enumeration schemes to optimise fermion-qubit mappings for practical cost functions. Section 3.1 establishes the scope of the search for optimal Jordan-Wigner mappings in this work, defining optimality in terms of practical cost functions for quantum computers. Section 3.2 sets out the broad class of problem Hamiltonians that this search will consider. Section 3.3 derives expressions for the cost functions of the search, which are related to problems in graph theory. Section 3.4 states Theorem 1 for minimising the average Pauli weight of a Jordan-Wigner transformation of a system of fermions interacting in a square lattice, with proof in Section B. In Section 3.5, we consider an heuristic approach to minimising the average Pauli weight of a Jordan-Wigner transformation of cellular lattice fermionic systems. In Section 3.6, we consider the task of minimising the average p th power of Pauli weight of a Jordan-Wigner transformation of square lattice fermionic systems, for $p > 1$.

3.1 Objective

In practice, it is very difficult to find the optimal fermion-qubit mapping for a given Hamiltonian H_{fermion} as defined in Definition 4. Within the scope of this paper, instead

consider the subproblem of finding the optimal Jordan–Wigner transformation with a fermionic enumeration scheme as in Definition 2:

Definition 5. (*Optimal Jordan–Wigner transformations with fermionic enumeration schemes.*)

Let H_{fermion} be a fermionic Hamiltonian on n modes. Let $C = C(f)$ be the cost function of the qubit Hamiltonian $H_{\text{qubit}} = H_{\text{qubit}}(f) := \overline{\text{JW}}_f(H_{\text{fermion}})$ with respect to some scarce physical resource. The C -optimal Jordan–Wigner transformation with a fermionic enumeration scheme for H_{fermion} is the fermion–qubit mapping $\overline{\text{JW}}_{f^*}$, where f^* is a fermionic enumeration scheme satisfying

$$f^* = \arg \min_f C(f). \quad (36)$$

In this work, we discuss optimal Jordan–Wigner transformations with fermionic enumeration schemes for three example cost functions:

Example 4. ($C = \text{APV}$, *average Pauli weight.*) Given a fermionic Hamiltonian H_{fermion} , a Jordan–Wigner mapping with minimum average Pauli weight is a fermion–qubit mapping $\overline{\text{JW}}_{f^*}$ where the fermionic enumeration scheme f^* satisfies

$$f^* = \arg \min_f (\text{APV}(H_{\text{qubit}}(f))), \quad (37)$$

where $\text{APV}(H_{\text{qubit}})$ is the average Pauli weight of all terms in $H_{\text{qubit}}(f) = \overline{\text{JW}}_f(H_{\text{fermion}})$.

The average Pauli weight of a qubit Hamiltonian could be a limiting resource in near-term algorithms such as the variational quantum eigensolver (VQE), where $\text{APV}(H_{\text{qubit}})$ represents the total number of single–qubit measurements involved in each step of the VQE.

Example 5. ($C = \text{MPV}$, *maximum Pauli weight.*) As in Example 4, except that f^* satisfies

$$f^* = \arg \min_f (\text{MPV}(H_{\text{qubit}}(f))), \quad (38)$$

where $\text{MPV}(H_{\text{qubit}})$ is the maximum Pauli weight of any one term in the qubit Hamiltonian.

The maximum Pauli weight of H_{qubit} is a complexity–theoretic measure of the cost of simulating H_{qubit} via long–term algorithms such as phase estimation. In the k -local Hamiltonian problem for H_{qubit} , the quantity $\text{MPV}(H_{\text{qubit}})$ is the value k .

Example 6. ($C = \text{MD}$, *Pauli measurement depth*) As in Example 4, except that f^* satisfies

$$f^* = \arg \min_f (\text{MD}(H_{\text{qubit}}(f))), \quad (39)$$

where $\text{MD}(H_{\text{qubit}})$ is the minimum number of groupings of the terms in H_{qubit} such that each group contains no terms that act on shared qubits.

The quantity $\text{MD}(H_{\text{qubit}})$ corresponds to the number of distinct timesteps required to run all Hamiltonian terms in parallel, indicating, for example, the total clock time required to perform all measurements during an iteration of a variational quantum eigensolver algorithm.

3.2 Problem Hamiltonians

The terms in a general fermionic Hamiltonian H_{fermion} as specified in Equation 1 represent quadratic one-particle and quartic two-particle interactions. The Jordan–Wigner transformation $\overline{\text{JW}}_f$ maps each of the one-particle terms to

$$\overline{\text{JW}}_f : a_{\alpha_i}^\dagger a_{\alpha_i} \mapsto \frac{1}{2} (\mathbb{1} - Z)_{f(\alpha_i)} \quad (40)$$

$$\overline{\text{JW}}_f : a_{\alpha_i}^\dagger a_{\alpha_j} \mapsto \frac{1}{2} (X - iY)_{f(\alpha_i)} \left(\bigotimes_{k=f(\alpha_i)}^{f(\alpha_j)-1} Z_k \right) \frac{1}{2} (X + iY)_{f(\alpha_j)}, \quad (41)$$

where $f(\alpha_i) < f(\alpha_j)$ in Equation 41. However, the term $c_{\alpha_i \alpha_j} a_{\alpha_i}^\dagger a_{\alpha_j}$ will always appear in H alongside its conjugate term $(c_{\alpha_i \alpha_j})^* a_{\alpha_j}^\dagger a_{\alpha_i}$. The expression $c_{\alpha_i \alpha_j} a_{\alpha_i}^\dagger a_{\alpha_j} + (c_{\alpha_i \alpha_j})^* a_{\alpha_j}^\dagger a_{\alpha_i}$ is the *hopping term* between fermionic modes α_i and α_j . The hopping terms of H_{fermion} lead to non-local terms in the qubit Hamiltonian of the form

$$\begin{aligned} \overline{\text{JW}}_f : c_{\alpha_i \alpha_j} a_{\alpha_i}^\dagger a_{\alpha_j} + (c_{\alpha_i \alpha_j})^* a_{\alpha_j}^\dagger a_{\alpha_i} & \quad (42) \\ \mapsto \frac{\text{Re}(c_{\alpha_i \alpha_j})}{2} \left(\bigotimes_{k=f(\alpha_i)+1}^{f(\alpha_j)-1} Z_k \right) \times (X_{f(\alpha_i)} \otimes X_{f(\alpha_j)} + Y_{f(\alpha_i)} \otimes Y_{f(\alpha_j)}) \\ + \frac{\text{Im}(c_{\alpha_i \alpha_j})}{2} \left(\bigotimes_{k=f(\alpha_i)+1}^{f(\alpha_j)-1} Z_k \right) \times (X_{f(\alpha_i)} \otimes Y_{f(\alpha_j)} + Y_{f(\alpha_i)} \otimes X_{f(\alpha_j)}). \end{aligned}$$

In the case where the coefficients of the conjugate one-particle interaction terms are $c_{ij} = (c_{ij})^* = 1$, the transformation of the hopping term is simply

$$\overline{\text{JW}}_f : a_{\alpha_i}^\dagger a_{\alpha_j} + a_{\alpha_j}^\dagger a_{\alpha_i} \mapsto \frac{1}{2} \left(\bigotimes_{k=f(\alpha_i)+1}^{f(\alpha_j)-1} Z_k \right) (X_{f(\alpha_i)} \otimes X_{f(\alpha_j)} + Y_{f(\alpha_i)} \otimes Y_{f(\alpha_j)}). \quad (43)$$

Figure 6 illustrates the conversion of these simpler hopping terms into qubit Hamiltonian terms.

Literature on quantum simulation algorithms tends to permit quartic terms in the fermionic Hamiltonian that transform into local qubit operations. For example, Verstraete and Cirac [17] and Derby and Klassen [36] consider terms of the form

$$\overline{\text{JW}}_f : a_{\alpha_i}^\dagger a_{\alpha_i} a_{\alpha_j}^\dagger a_{\alpha_j} \mapsto \frac{1}{4} (\mathbb{1} - Z)_{f(\alpha_i)} (\mathbb{1} - Z)_{f(\alpha_j)}. \quad (44)$$

The quartic terms make diagonalisation of the fermionic Hamiltonian H_{fermion} exponentially difficult to solve on a classical computer. However, they become simple 1- or 2-local Pauli operations after the Jordan–Wigner transformation maps them into the local Pauli operations in Equation 44. Thus, a fermionic Hamiltonian H_{fermion} consisting of self-interactions $a_{\alpha_i}^\dagger a_{\alpha_i}$, hopping terms, and quartic terms of the form $a_{\alpha_i}^\dagger a_{\alpha_i} a_{\alpha_j}^\dagger a_{\alpha_j}$ transforms under $\overline{\text{JW}}_f$ to a qubit Hamiltonian H_{qubit} where the only non-local terms are of the form in Equation 41. Moreover, the hopping terms are the only Pauli strings with weight dependent on the enumeration scheme f of the Jordan–Wigner mapping.

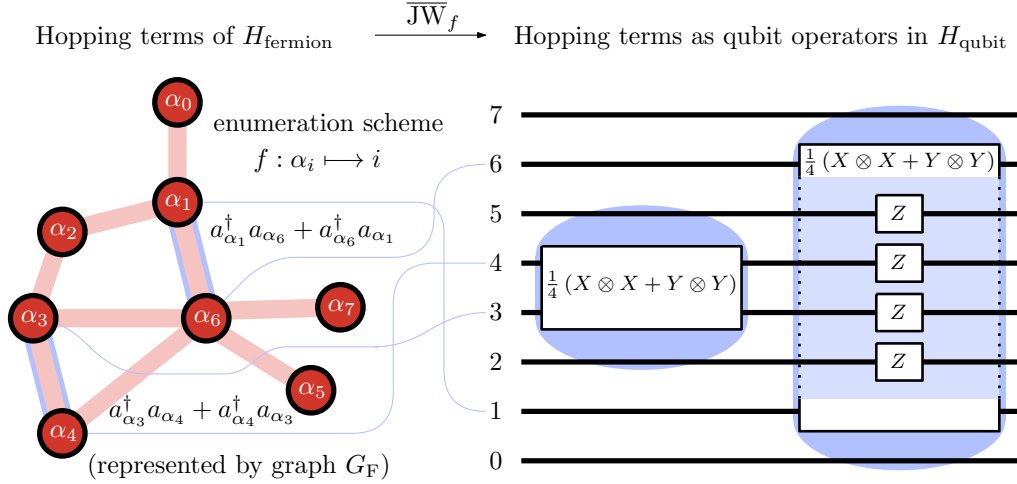


Figure 6: Jordan–Wigner transformation with a fermionic enumeration scheme $\overline{\text{JW}}_f$, in this diagram with the naïve enumeration scheme $f : \alpha_i \mapsto i$. For any enumeration scheme f , the fermion–qubit mapping $\overline{\text{JW}}_f$ transforms hopping terms $a_{\alpha_i}^\dagger a_{\alpha_j} + a_{\alpha_j}^\dagger a_{\alpha_i} \mapsto A_{f(\alpha_i)}^\dagger A_{f(\alpha_j)} + A_{f(\alpha_j)}^\dagger A_{f(\alpha_i)}$.

Consider fermionic Hamiltonians of the general form

$$H_{\text{fermion}} = \sum_{i,j=0}^{n-1} (c_{\alpha_i \alpha_j}) a_{\alpha_i}^\dagger a_{\alpha_j} + \sum_{i,j=0}^{n-1} (c'_{\alpha_i \alpha_j}) a_{\alpha_i}^\dagger a_{\alpha_i} a_{\alpha_j}^\dagger a_{\alpha_j} \quad (45)$$

(hereon referred to as Eqn. 44 terms)

$$= \sum_{\text{pairs } (i,j)} \left((c_{\alpha_i \alpha_j}) a_{\alpha_i}^\dagger a_{\alpha_j} + (c_{\alpha_i \alpha_j}^*) a_{\alpha_i} a_{\alpha_j}^\dagger \right) + \text{Eqn. 44 terms} \quad (46)$$

$$= \sum_{(\alpha,\beta) \in E} \left((c_{\alpha\beta}) a_\alpha^\dagger a_\beta + (c_{\alpha\beta}^*) a_\alpha a_\beta^\dagger \right) + \text{Eqn. 44 terms}, \quad (47)$$

where E is the edge set of the graph $G_F(V, E)$ with $V = \{\alpha_0, \dots, \alpha_{n-1}\}$ and $(\alpha, \beta) \in E \subseteq V \times V$ if and only if $c_{\alpha\beta} \neq 0$.

For convenience of notation, assume that $c_{\alpha\beta} = 1$ for all $(\alpha, \beta) \in E$, so that only hopping terms of the form in Equation 41 are of concern. If our task were to find the optimal fermion–qubit mapping as in Definition 4, this assumption would reduce the variety of problem Hamiltonians described by Equation 47. However, focused as we are on finding optimal Jordan–Wigner transformation as defined in Examples 4–6, the assumption $c_{\alpha\beta} = 1$ comes with no loss of generality in the form of the problem Hamiltonians. This is because the weights of the Pauli strings of $H_{\text{qubit}} = \overline{\text{JW}}_f(H_{\text{fermion}})$ in Equation 42 with coefficients $\text{Re}(c_{\alpha\beta})$ and $\text{Im}(c_{\alpha\beta})$ are equal. Properties that are only concerned with the length of Hamiltonian terms such as APV, MPV and MD are unchanged by setting all nonzero $c_{\alpha\beta}$ to 1. For the remainder of this paper, we can thus assume problem Hamiltonians take the form:

$$H_{\text{fermion}} = \sum_{(\alpha,\beta) \in E} \left(a_\alpha^\dagger a_\beta + a_\alpha a_\beta^\dagger \right) + \text{Eqn. 44 terms}. \quad (48)$$

This assumption would not hold if instead the task were to find, for example, the optimal enumeration scheme for Bravyi–Kitaev type mappings $\overline{\text{BK}}_f$. This is because the Bravyi–Kitaev transformation does not transform the hopping terms of H_{fermion} in Equation 47 into a sum of Pauli strings of equal length [49, 47].

3.3 Expressions for cost functions of qubit Hamiltonians

For problem Hamiltonians of the form in Equation 48, there is a simple relation for the Pauli weight of the Jordan–Wigner transformation of hopping terms:

$$\text{Pauli weight}(\overline{\text{JW}}_f(a_\alpha^\dagger a_\beta + a_\alpha a_\beta^\dagger)) = |f(\alpha) - f(\beta)| + 1, \quad (49)$$

since the Pauli strings of $\overline{\text{JW}}_f(a_\alpha^\dagger a_\beta + a_\alpha a_\beta^\dagger)$ contain $(|f(\alpha) - f(\beta)| - 1)$ Z matrices and two X or Y matrices, from Equation 41.

Recall from Section 2.7 that $C^p(f)$, the p -sum of a graph $G(V, E)$ with vertex enumeration scheme f , is

$$C^p(f) := \left(\sum_{(\alpha, \beta) \in E} |f(\alpha) - f(\beta)|^p \right)^{1/p}. \quad (50)$$

This notation, along with Equation 49, allows for simple expressions for the cost functions APV and MPV from Examples 4 and 5, respectively.

Average Pauli weight (Example 4). The formula for the average Pauli weight of a Jordan–Wigner transformation $\overline{\text{JW}}_f$ of a problem Hamiltonian H_{fermion} of the form in Equation 48 is

$$\text{APV}(f) := \frac{C^1(f)}{|G_F|} + 1, \quad (51)$$

where G_F is the number of edges in G_F . In fact, Equation 51 neglects the contribution of the quartic terms from Equation 44 to the average Pauli weight of H_{fermion} , because they are independent of the fermion enumeration scheme f and hence have no effect in determining the optimal enumeration scheme f^* as described in Example 4. The extra term of 1 accounts for the fact that the weight of a Pauli string between qubits with labels i and j is $|i - j| + 1$.

Figure 7 lists the average Pauli weight of the Jordan–Wigner transformation $\overline{\text{JW}}_f$ of a fermionic Hamiltonian H_{fermion} with fermionic interaction graph G_F equal to the 6×6 lattice for three enumeration schemes: the S-pattern f_S , the Z-pattern f_Z , and the Mitchison–Durbin pattern, f_M , which underlies the results of Section 3.4.

Finding Jordan–Wigner transformations with minimum average Pauli weight is equivalent to finding enumeration scheme of G_F that minimise $C^1(f)$, which is the NP-hard edgesum problem from Section 2.7. In Section 3.4, we present Theorem 1 for an enumeration scheme f_M that minimises the average Pauli weight of a Jordan–Wigner transformation of H_{fermion} where if G_F is the $N \times N$ square lattice. Through Corollary 2, this is an improvement of up to $\approx 13.9\%$ upon existing methods.

Average p th power of Pauli weight. One might want to penalise the qubit Hamiltonian via some other measure, such as the average p th power of the Pauli weights where $p \in \mathbb{R}^+$. Minimising this property corresponds to the NP-hard minimum p -sum problem of minimising $C^p(f)$ from Section 2.7. In Section 3.6, we present numerical results for the minimum p -sum problem to illustrate how one might optimise Jordan–Wigner transformations for this objective function.

Maximum Pauli weight (Example 5) The cost function for the maximum Pauli weight of a Jordan–Wigner transformation $\overline{\text{JW}}_f$ is

$$\text{MPV}(f) = C^\infty(f) + 1, \quad (52)$$

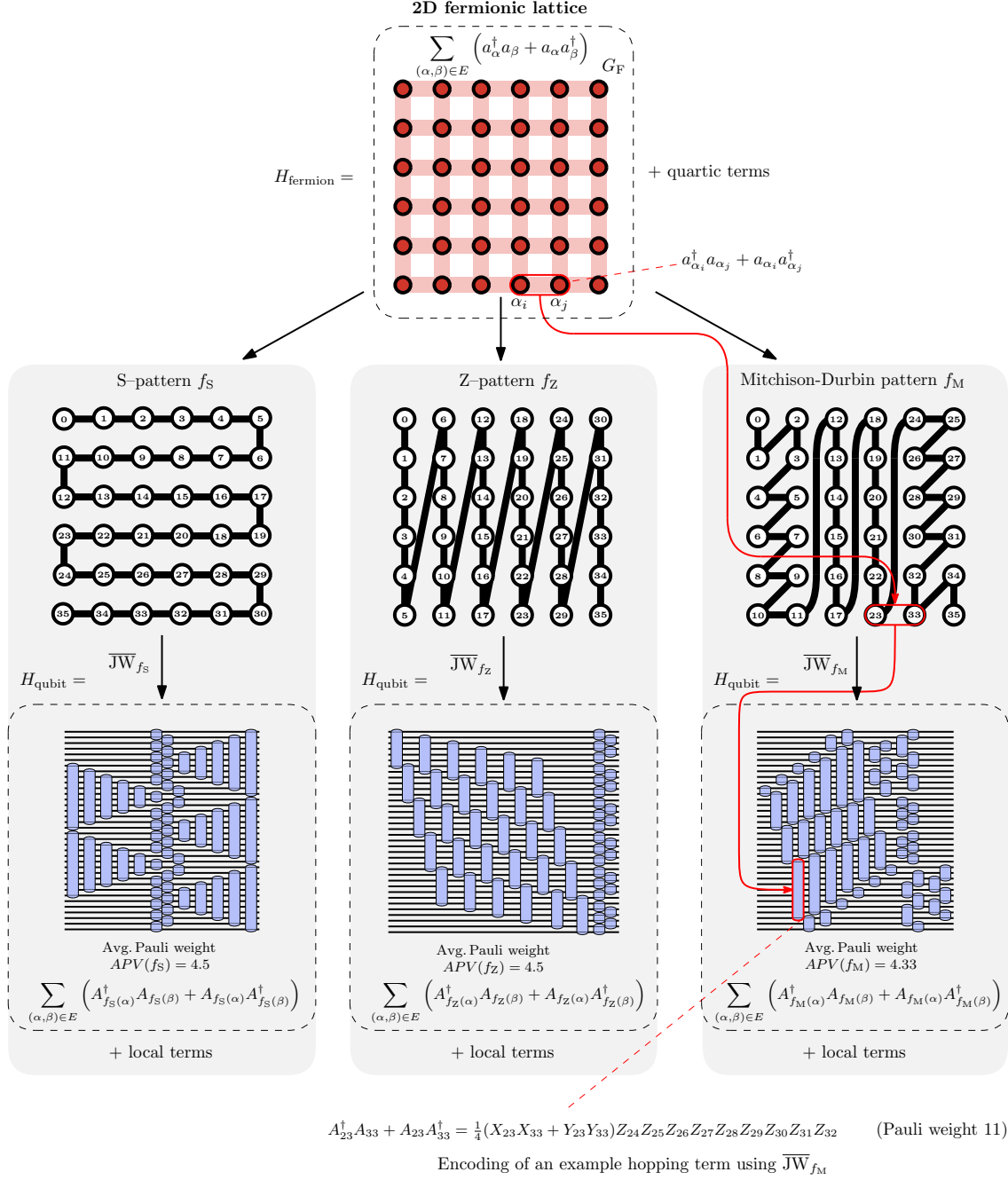


Figure 7: The Jordan–Wigner transformation $\overline{\text{JW}}_f$ produces qubit Hamiltonians that depend on the choice of enumeration scheme f . If the fermionic Hamiltonian contains hopping terms that form a square lattice, the Mitchison–Durbin pattern produces qubit Hamiltonians with hopping terms of the minimum possible average weight.

Pauli measurement depth of H_{qubit} hopping terms

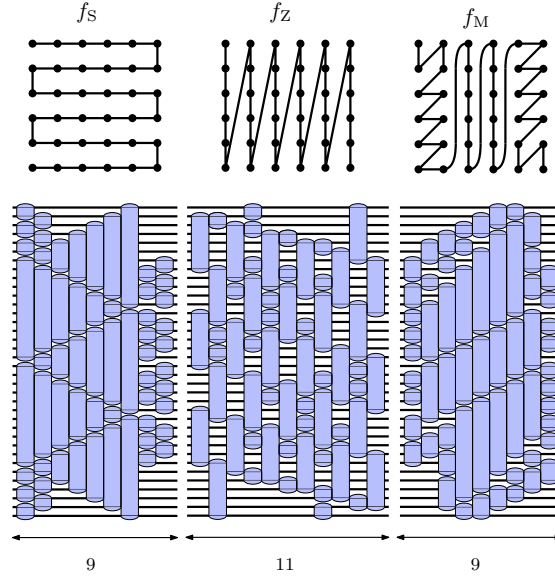


Figure 8: Comparison of the Pauli measurement depth of the hopping terms in qubit Hamiltonians $H_{\text{qubit}} = \overline{\text{JW}}_f(H_{\text{fermion}})$ produced by three different enumeration schemes on a 6×6 square lattice of fermions.

which corresponds to the NP-hard bandwidth problem from Section 2.7. However, for fermionic Hamiltonians H_{fermion} with hopping terms on a square-lattice G_{F} , it is straightforward to see that any fermionic enumeration scheme with $C^\infty(f) = N$ will minimise the maximum Pauli weight of the qubit Hamiltonian. One such enumeration scheme is the Z-pattern f_Z .

Pauli measurement depth (Example 6). Finding Jordan-Wigner transformations with minimum Pauli measurement depths is beyond the scope of this work. Figure 8 demonstrates the variation of Pauli measurement depth of $H_{\text{qubit}} = \overline{\text{JW}}_f(H_{\text{fermion}})$, where the fermionic interaction graph G_{F} is the 6×6 lattice, for different enumeration schemes: f_S , f_Z , and f_M .

Other properties. One may also consider other cost functions. For example, if the qubits have a connectivity graph G_{Q} , it may be desirable to make the Pauli strings in H_{qubit} as local as possible on G_{Q} . A discussion of this optimisation appears in Section 5.2.

3.4 Jordan-Wigner transformations of square-lattice fermionic Hamiltonians with minimum average Pauli weight

Consider fermionic problem Hamiltonians H_{fermion} of the form in Equation 48 with interaction graphs G_{F} equal to the $N \times N$ square lattice. Prior to this work, the default way to enumerate the fermionic modes, regardless of target cost function, has been to number them row-by-row in either a zig-zagging or snake-like pattern, as in Figure 8 variations [17, 37]. The solution to the edgesum problem for G_{F} is related to the work of Graeme Mitchison and Richard Durbin, from their studies of the organisation of nerve cells in the brain cortex [40]. Figure 9 displays the Mitchison-Durbin pattern f_M , which is dramatically different to these more conventional patterns. The proof of our main result below, Theorem 1, makes use of this curious arrangement to construct a Jordan-Wigner transformation with minimum average Pauli weight.



Figure 9: Graeme Mitchison’s sculpture of the optimal numbering of a 7×7 array. Reproduced with the permission of Richard Durbin.

Theorem 1. (*Jordan–Wigner transformations of square–lattice fermionic Hamiltonians with minimum average Pauli weight.*) Given a system of $n = N^2$ fermionic modes, suppose that the system has a Hamiltonian H_{fermion} of the form in Equation 48 with a square–lattice interaction graph G_F . Then, the fermion–qubit mapping $\overline{\text{JW}}_{f_M}$ is a Jordan–Wigner transformation with minimum average Pauli weight for H_{fermion} , where f_M is the Mitchison–Durbin pattern.

Proof. Proof in Section B. □

Remark 3. Finding Jordan–Wigner transformations with minimum average Pauli weight for arbitrary Hamiltonians H_{fermion} of the form in Equation 48 is NP–hard. By extension, this applies to the general class of Hamiltonians in Equation 1.

Remark 4 details all known scenarios to date where the optimal fermionic enumeration scheme is solvable in $\text{poly}(n)$ time.

Remark 4. (*Solutions for other graph types G_F .*) If the Hamiltonian H_{fermion} is as defined in Theorem 1, and if G_F belongs to any of the graph families in Figure 5, then a classical computer can efficiently find the Jordan–Wigner transformation with minimum average Pauli weight for H_{fermion} .

Corollary 2. Using the Mitchison–Durbin pattern f_M in a Jordan–Wigner transformation for a fermionic system with square–lattice–interacting hopping terms produces Pauli strings in the qubit Hamiltonian H_{qubit} with an average weight of $\frac{1}{3}(4 - \sqrt{2}) \approx 0.86$ times the corresponding average Pauli weight that the Z–pattern f_Z and the S–pattern f_S produce.

Proof. On an $N \times N$ lattice, the Mitchison–Durbin pattern f_M and the S–pattern f_S have edgesums

$$C^1(f_Z) = N^3 - N, \quad (53)$$

$$C^1(f_S) = N^3 - N, \quad (54)$$

$$C^1(f_M) = N^3 - xN^2 + 2x^2N - \frac{2}{3}x^3 + N^2 - xN - 2N + \frac{2}{3}x, \quad (55)$$

respectively. The edgesum $C^1(f_Z)$ is straightforward to calculate; see Appendix A for the derivation of $C^1(f_S)$, and Section B for the derivation of $C^1(f_M)$. In Equation 55, the

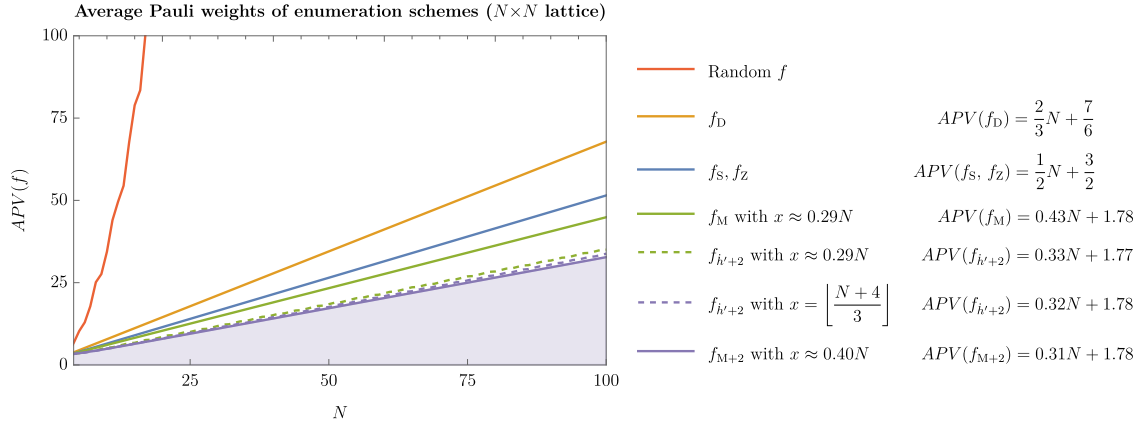


Figure 10: Average Pauli weights $APV(f)$ of enumeration schemes f on $N \times N$ lattices. Random f is a randomly-generated enumeration scheme.

value of x is the closest integer to $N - \frac{1}{2}\sqrt{2N^2 - 2N + \frac{4}{3}}$. Using Equation 51 and the number of hopping terms $|G_F| = 2N(N - 1)$, the average Pauli weights are

$$APV(f_Z) = APV(f_S) = \frac{1}{2}N + \frac{3}{2} \quad (56)$$

and, for large N ,

$$APV(f_M) \approx \frac{1}{6}(4 - \sqrt{2})N + \frac{1}{12}(20 + \sqrt{2}) = 0.43N + 1.78. \quad (57)$$

For small N , explicit calculation verifies that $APV(f_S) > APV(f_M)$ for $N \geq 6$. The ratio of average Pauli weights is thus $APV(f_M)/APV(f_S) = APV(f_M)/APV(f_Z) \approx \frac{1}{3}(4 - \sqrt{2}) \approx 0.86$. \square

We can conclude from Corollary 2 that, simply by labelling the fermionic modes using the Mitchison–Durbin pattern rather than the S–pattern as proposed in [17] or Z–pattern, we can produce a qubit Hamiltonian with terms that are 13.9% more local on average. Our proposal immediately translates to a reduction by the same amount in the number of single–qubit measurements required in a VQE protocol. Even in the case of simulating small fermionic systems, this method provides a worthwhile advantage. For example, in Figure 7 where $N = 6$, the ratio of the average Pauli weight using f_M versus f_S is $4.33/4.5 \approx 0.96$. That is, even for the 6×6 lattice, applying Theorem 1 will reduce the number of Pauli measurements by 4%.

For $2 \leq N \leq 100$, Figure 10 shows the resulting average Pauli weights of various enumeration schemes on $N \times N$ lattices. Even for small lattices, the Mitchison–Durbin pattern can yield a meaningful reduction: for $N = 20$, $C^1(f_M)/C^1(f_S) = \frac{7140}{7980} \approx 89.5\%$.

3.5 Reducing the average Pauli weight for cellular fermionic lattices

Theorem 1 reduces the average Pauli weight of qubit Hamiltonians by making judicious use of the solutions to the edgesum problem. Remark 4 refers to the scarce number of other graph families for G_F for which edgesum solutions are known. It is tempting to think that there is not much use for our approach if the fermionic interaction graph G_F does not belong to one of these families. In this section, however, we show example fermionic

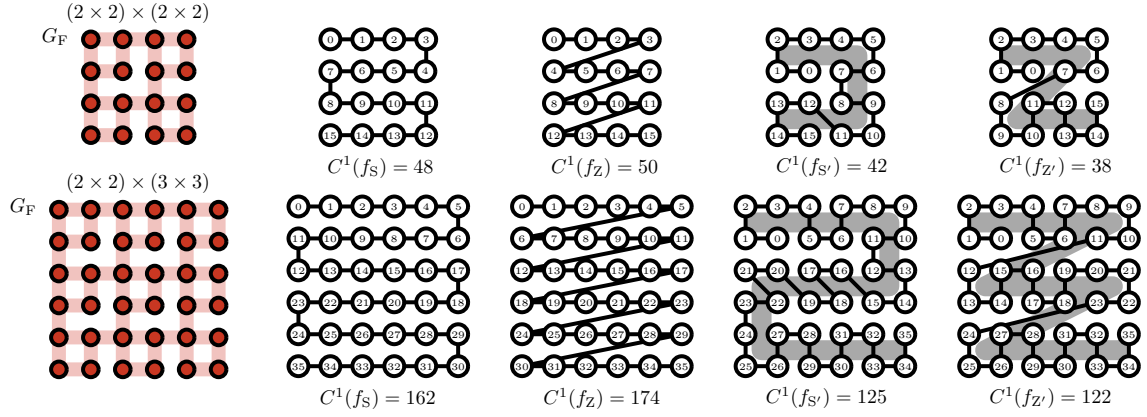


Figure 11: Edgesums for some enumeration schemes of $(n \times n) \times (N \times N)$ cellular arrangement patterns.

Hamiltonians for which the enumeration schemes arising from approximate edgesum solutions can provide order-of-magnitude reductions in the average Pauli weight of the qubit Hamiltonians.

Consider fermionic Hamiltonians of the form in Equation 48 with hopping terms between modes such that G_F is an $(n \times n) \times (N \times N)$ cellular arrangement of square lattices, where each $n \times n$ sub-lattice connects to adjacent sub-lattices via a single edge. Here we use the cellular pattern in Figure 11, where the connections are from each $n \times n$ lattice's top left vertex to the two closest vertices from neighbouring $n \times n$ lattices.

It is possible to enumerate the fermionic modes with the Z-pattern f_Z or the S-pattern f_S from Section 3.4, treating the whole graph G_F as a single square lattice. As Figure 11 shows, another way of enumerating the modes is to enumerate each sub-lattice locally before moving on to the next, progressing through the entire graph via an S- or Z-pattern. We call these two enumeration procedures $f_{S'}$ and $f_{Z'}$, respectively.

The edgesums of these schemes on the cellular arrangement graph are:

$$C^1(f_S) = \begin{cases} (Nn)^3 - Nn - N(N-1)(n-1) - \sum_{k=0}^{N-1} \sum_{i=kn+2}^{(k+1)n} (2i-1), & n \text{ even} \\ (Nn)^3 - Nn - N(N-1)(n-1) - \sum_{k=0}^{N-1} \sum_{i=kn+1}^{(k+1)n-1} (2i-1), & n \text{ odd,} \end{cases} \quad (58)$$

$$C^1(f_Z) = (Nn)^3 - Nn - N(N-1)(n-1) - nN^2(n-1)(N-1), \quad (59)$$

$$C^1(f_{Z'}) = \begin{cases} N^3n^2 + n^3N^2 - n^2N^2 - 2nN^2 - n^2N + 2N^2 + 2nN + n^2 - 2N - n, & n \text{ even} \\ N^3n^2 + n^3N^2 - n^2N^2 - nN^2 - n^2N + N^2 + 2nN + n^2 - 2N - 2n + 1, & n \text{ odd,} \end{cases} \quad (60)$$

and while the value of $C^1(f_{S'})$ also depends on the parities of n and N , it is strictly greater than $C^1(f_{Z'})$.

By using $f_{Z'}$ rather than f_Z , the edgesum of a large cellular arrangement graph reduces by an order of magnitude:

$$\lim_{N \rightarrow \infty} \frac{C^1(f_{Z'})}{C^1(f_Z)} = \frac{n^2}{n^3 - n^2 + n} = \mathcal{O}\left(\frac{1}{n}\right); \quad (61)$$

$$\lim_{n \rightarrow \infty} \frac{C^1(f_{Z'})}{C^1(f_Z)} = \frac{1}{N}. \quad (62)$$

If $n = \mathcal{O}(N)$, then the system has $\mathcal{O}(N^4)$ fermionic modes. From choosing $f_{Z'}$ rather than f_Z , the $\mathcal{O}(1/N)$ factor reduction in the average Pauli weight of the qubit Hamiltonian is thus proportional to the fourth root of the number of fermionic modes. This is much more

Enumeration scheme f	$C^1(f)$	$C^p(f), p > 1$
Mitchison-Durbin pattern f_M 	$N^3 - xN^2 + 2x^2N - 2x^3/3 + N^2 - xN - 2N + 2x/3$	Includes terms $\geq \sim 2x^{p+1}N^p \sim 2k^{p+1}N^{2p+1}$ where $x = kN$
S-pattern f_S 	$N^3 - N$	$(N-1) \left(\sum_{k=1}^{N-1} (2k+1)^p + N+1 \right) \sim \frac{2^p}{p+1} N^{p+2} + \mathcal{O}(N^{p+1})$
Z-pattern f_Z 	$N^3 - N$	$(N-1) (N^{1+p} + N) = N^{p+2} - N^{p+1} + N^2 - N$
Diagonal pattern f_D 	$4N^3/3 - N^2 - N/3$	$2 \left(\sum_{k=1}^{N-2} (2k+1)(k+1)^p + (N-1)N^p + 1 \right) \sim \frac{4}{p+2} N^{p+2} + \mathcal{O}(N^{p+1})$
		Theoretical limit $\sim \frac{4}{2^p(p+2)} N^{p+2} + \text{smaller...}$

Figure 12: Results for the minimum p -sum problem for the square lattice for $p \geq 1$. While the Mitchison–Durbin pattern f_M minimises $C^p(f)$ for $p = 1$, it performs the worst of all the options for $p > 1$. The diagonal pattern f_D performs better than the rest for $p > 2$.

striking than the constant-factor improvement proffered by Corollary 2, even though there is no proof that f_Z is an optimal enumeration scheme for this type of fermionic interaction graph G_F .

3.6 Reducing the average p th power of Pauli weight for a square lattice

Section 3.3 introduced the average p th power of Pauli weight for $p > 1$ as a cost function for the qubit Hamiltonian. For a fermionic Hamiltonian H_{fermion} with interaction graph G_F , consider the task of finding an enumeration scheme f that minimises the p -sum

$$C^p(f) = \left(\sum_{(u,v) \in G_F} |f(u) - f(v)|^p \right)^{1/p}. \quad (63)$$

While the $p = 1$ and $p = \infty$ cases correspond to metrics that seem physically motivated, we are not yet aware if current quantum algorithm designers would consider penalising finite powers $p > 1$ of Pauli weight. The $p = 1$ case is the edgesum problem and via Remark 3 is NP-hard. George and Pothen showed that the minimum 2-sum problem is also NP-hard [52]. They develop spectral approaches to solving the minimum 1-sum and 2-sum problems for *any* graph G_F . Separately, Mitchison and Durbin [40] explored the minimum p -sum problem for square lattices, and conclude with Proposition 1:

Proposition 1. (Mitchison and Durbin’s results for the minimum p -sum problem on an $N \times N$ lattice [40]) *Let G be the $N \times N$ square lattice. Then the following are the lower limits for the value of $C^p(f)$:*

- (a) *If $0 < p < \frac{1}{2}$, then there exists an enumeration scheme f with $C^p(f) = \mathcal{O}(N^2)$.*
- (b) *If $\frac{1}{2} < p < 1$, then $C^p(f) \geq \frac{1}{2^{p+1}} N^{1+2p} + \mathcal{O}(N^{2p})$.*
- (c) *If $p = 1$, then f_M gives the minimum value as shown in Theorem 1.*
- (d) *If $p > 1$, then $C^p(f) \geq \frac{4}{2^p(p+2)} N^{p+2}$.*

The lower bounds in (b) and (d) are theoretical limits, and to date there are no known enumeration schemes that achieve their low coefficients. However, the “diagonal pattern” f_D has edgesum

$$C(f_D) \approx \frac{4}{p+2} N^{p+2} + \mathcal{O}(N^{p+1}), \quad (64)$$

which has the same order of magnitude in N as the theoretical limit in (d).

Proof. See Propositions 2–4 of [40]. □

Remark 5. (Best known results for the minimum p -sum problem on a square lattice, $p \geq 1$)

Figure 12 provides a table of known results for four enumeration schemes f_S , f_M , f_Z , and f_D (the diagonal pattern) in the regimes $p = 1$ and $p > 1$. The diagonal pattern is the solution to the bandwidth problem (from Section 2.7) on rectangles [40], and is the best-performing pattern for the minimum p -sum problem for $p > 1$, $N \rightarrow \infty$.

4 Improving beyond optimality with ancilla qubits

The fermion–qubit mappings in Definitions 1–4, Examples 1–3, and in Section 3 are all mappings between n -mode fermionic systems and n -qubit systems. Theorem 1, for example, details the Jordan–Wigner mapping with minimum average Pauli weight when using N^2 qubits to simulate a fermionic system on N^2 modes. However, there is a storied interplay between the qubit count of a fermion–qubit mapping and the locality of its Hamiltonian. As both qubits and quantum gates are costly with current technology, the tradeoff begs the question: what is the maximum benefit a mapping could gain by using an extra one or two qubits?

In Section 4.1, we describe Steudtner and Wehner’s template for auxiliary qubit mappings [37]. In Section 4.2, we give an example of this process in the form of a new auxiliary qubit mapping. We augment the Mitchison–Durbin pattern to produce an auxiliary qubit mapping $\overline{JW}_{f_{M+2}}$ which achieves a 37.9% reduction over the average Pauli weight of \overline{JW}_{f_S} , using only two extra qubits. Thus, taking advantage of the Mitchison–Durbin pattern we see that a constant number of additional qubits almost triples the advantage provided by Theorem 1, thus improving our earlier results ‘beyond optimality’.

4.1 Background: auxiliary qubit mappings

Moll et al. [58] show how to reduce the number of qubits required by a Jordan–Wigner transformation at the cost of introducing more terms into the molecular Hamiltonian. Auxiliary qubit mappings [17, 37, 36, 35, 59] show the converse: that by introducing more qubits into a simulation of H_{fermion} , it is possible to vastly simplify the qubit Hamiltonian H_{qubit} . Verstraete and Cirac demonstrated a fermion–qubit mapping between a fermionic Hamiltonian H_{fermion} with a square–lattice interaction graph G_F [17] and a qubit Hamiltonian H_{qubit} on $2N^2$ qubits consisting of only local terms. That is, rather than producing long strings of Pauli terms of weight $\mathcal{O}(N)$ that wind around the qubit lattice (as in, for example, Figure 15), the auxiliary qubit mappings produce operations of weight $\mathcal{O}(1)$.

Steudtner and Wehner’s formulation of auxiliary qubit mappings [37] is thus: suppose that a fermion–qubit mapping produces the qubit Hamiltonian

$$H_{\text{fermion}} \mapsto H_q := H_{\text{qubit}} = \sum_{h \in \Lambda} c_h h, \quad (65)$$

where $\Lambda \subseteq \{\mathbb{1}, X, Y, Z\}^{\otimes n}$, and the $c_h \in \mathbb{C}$ ensure that H_q is Hermitian. Denote by the subscript ‘dat’ the n -qubit data system upon which the Hamiltonian H_q acts. Given a state $|\psi\rangle_{\text{dat}}$ of the data system, the goal is to reduce the complexity of simulating the time-evolved state $e^{-iH_q t} |\psi\rangle_{\text{dat}}$. An auxiliary qubit mapping achieves this goal by instead mapping

$$H_{\text{fermion}} \longmapsto \tilde{H}_q, \quad (66)$$

where \tilde{H}_q is a simplified qubit Hamiltonian that acts on both the data register and ancilla qubits in an auxiliary register, denoted ‘aux’. The following three steps detail how to construct Steudtner and Wehner’s type of auxiliary qubit mapping.

1. Choose a subset $\Lambda_{\text{non-loc}} \subseteq \Lambda$ of terms in the Hamiltonian H_q . These are the terms which will be shorter in \tilde{H}_q . For each $h \in \Lambda_{\text{non-loc}}$, choose a Pauli string p^h where $h = h_{\text{loc}} p^h$ such that the weight of h_{loc} is less than that of h . In total, only use r distinct p -strings. That is, several $h \in \Lambda_{\text{non-loc}}$ may contain the same p^h .

Denote the set of all p^h by $\{p_i\}_{i=1}^r$. That is, for any $h \in \Lambda_{\text{non-loc}}$, then $p^h = p_i$ for some $i \in \{1, \dots, r\}$.

2. Introduce r ancilla qubits in the auxiliary register, and devise a unitary mapping

$$V : |\psi\rangle_{\text{dat}} |0\rangle_{\text{aux}}^{\otimes r} \longmapsto |\tilde{\psi}\rangle_{\text{dat,aux}} \quad (67)$$

where $|\tilde{\psi}\rangle_{\text{dat,aux}}$ is such that for each $i \in \{1, \dots, r\}$, there exists $\sigma_i \in \{\mathbb{1}, X, Y, Z\}$ acting on the i th auxiliary qubit such that

$$((p_i)_{\text{dat}} \otimes (\sigma_i)_{\text{aux}}) |\tilde{\psi}\rangle_{\text{dat,aux}} = |\tilde{\psi}\rangle_{\text{dat,aux}}. \quad (68)$$

The $p_i \otimes \sigma_i$ are the *stabilisers* of the combined data and auxiliary system.

Requirement 1: The choice of $\{p_i\}_{i=1}^r$ must allow for the existence of $|\tilde{\psi}\rangle_{\text{dat,aux}}$ obeying Equation 68. A necessary but insufficient condition is that $[p_i, p_j] = 0$ for all $i, j \in \{1, \dots, r\}$.

3. Modify each $h \in \Lambda$ via

$$h_{\text{dat}} \longmapsto h_{\text{dat}} \otimes \kappa_{\text{aux}}^h, \quad (69)$$

where κ^h is a Pauli string acting on the auxiliary qubits such that

$$[h_{\text{dat}} \otimes (\kappa^h)_{\text{aux}}, (p_i)_{\text{dat}} \otimes (\sigma_i)_{\text{aux}}] = 0 \quad (70)$$

for all $i \in \{1, \dots, r\}$. The rationale for this step is as follows: Suppose that $h = h_{\text{loc}} p^h$, where $p^h = p_i$. Then, we can multiply each $h = h_{\text{loc}} p^h \in \Lambda_{\text{non-loc}}$ by its corresponding stabiliser, thus producing a lower-weight Hamiltonian term, $((h_{\text{loc}})_{\text{dat}} \otimes (\sigma_i)_{\text{aux}})$:

$$(h_{\text{dat}} \otimes \mathbb{1}_{\text{aux}}) |\tilde{\psi}\rangle_{\text{dat,aux}} = ((h_{\text{loc}} p^h)_{\text{dat}} \otimes \mathbb{1}_{\text{aux}}) |\tilde{\psi}\rangle_{\text{dat,aux}} \quad (71)$$

$$= ((h_{\text{loc}} p_i)_{\text{dat}} \otimes \mathbb{1}_{\text{aux}}) |\tilde{\psi}\rangle_{\text{dat,aux}} \quad (72)$$

$$= ((h_{\text{loc}} p_i)_{\text{dat}} \otimes \mathbb{1}_{\text{aux}}) ((p_i)_{\text{dat}} \otimes (\sigma_i)_{\text{aux}}) |\tilde{\psi}\rangle_{\text{dat,aux}} \quad (73)$$

$$= ((h_{\text{loc}})_{\text{dat}} \otimes (\sigma_i)_{\text{aux}}) |\tilde{\psi}\rangle_{\text{dat,aux}}. \quad (74)$$

To replicate the time evolution $e^{-iH_q t} |\psi\rangle_{\text{dat}}$ of the system, it is necessary to be able to generate any stabiliser $((p_j)_{\text{dat}} \otimes (\sigma_j)_{\text{aux}})$ at the step in Equation 73 and commute

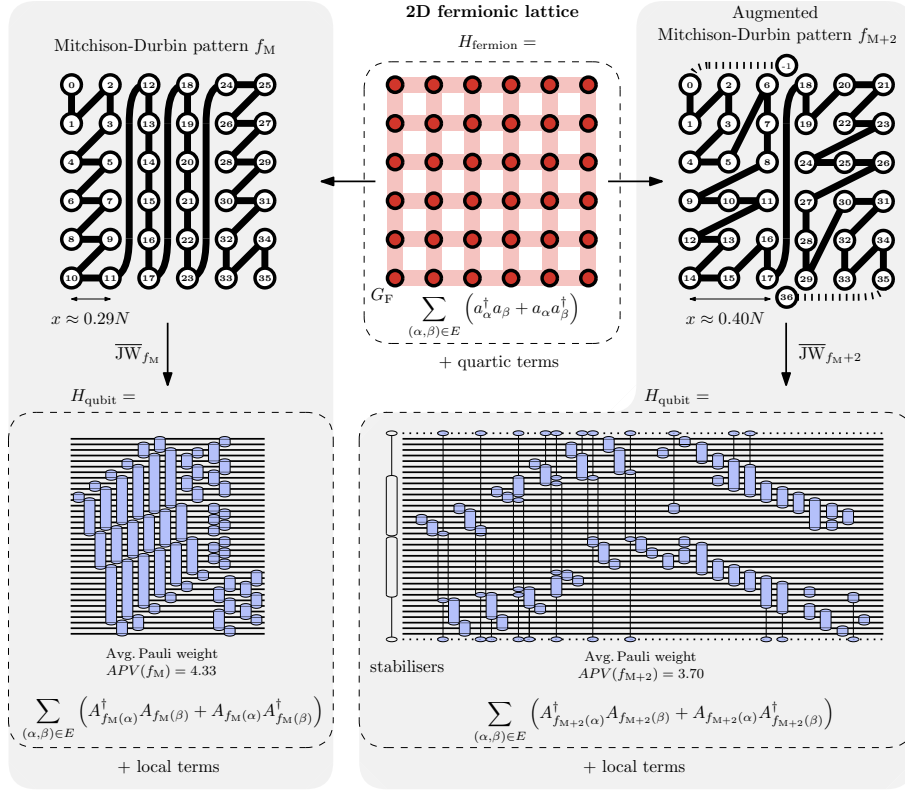


Figure 13: Comparison between the average Pauli weights of Jordan–Wigner mappings generated by the Mitchison–Durbin pattern f_M (left) and our auxiliary qubit pattern f_{M+2} (right). The bottom right image shows the reduction of the Pauli weight of long hopping terms after multiplication by stabilisers. Terms that partially overlap the stabilisers must also be adjusted.

it past *any* Hamiltonian term $h_{\text{dat}} \otimes \mathbb{1}_{\text{aux}}$ where h can now be any element of Λ . If $[h_{\text{dat}} \otimes \mathbb{1}_{\text{aux}}, (p_j)_{\text{dat}} \otimes (\sigma_j)_{\text{aux}}] = [h, p_j] \neq 0$, then application of the Hamiltonian term produces a state

$$|\tilde{\psi}'\rangle_{\text{dat,aux}} = (h_{\text{dat}} \otimes \mathbb{1}_{\text{aux}}) |\tilde{\psi}\rangle_{\text{dat,aux}} \quad (75)$$

that no longer satisfies Equation 68 for all i , and thus it is impossible to generate and apply more stabilisers as required by Equation 73.

Requirement 2: Crucially, the κ^h must be such that they preserve the time evolution of the data system. That is,

$$V^\dagger (h_{\text{dat}} \otimes (\kappa^h)_{\text{aux}}) |\tilde{\psi}\rangle_{\text{dat,aux}} = h |\psi\rangle_{\text{dat}} \otimes |0\rangle_{\text{aux}}^{\otimes r}. \quad (76)$$

Otherwise, the system would not retain any useful information. The requirement for the existence of κ^h for $h \in \Lambda$ places a restriction on V .

After satisfying the above three steps, observe that

$$\left(e^{-iH_{\text{q}}t} |\psi\rangle_{\text{dat}} \right) \otimes |0\rangle_{\text{aux}}^{\otimes r} = \left(V^\dagger e^{-i\tilde{H}_{\text{q}}t} \right) |\tilde{\psi}\rangle_{\text{dat,aux}}, \quad (77)$$

where the effective qubit Hamiltonian \tilde{H}_{q} achieves the goal of reducing the Pauli weight of the strings in $\Lambda_{\text{non-loc}}$, and acts on both the data and auxiliary systems:

$$\tilde{H}_{\text{q}} = \sum_{h \in \Lambda_{\text{non-loc}}} c_h ((h_{\text{loc}})_{\text{dat}} \otimes (\kappa^h \sigma^h)_{\text{aux}}) + \sum_{h \in \Lambda \setminus \Lambda_{\text{non-loc}}} c_h (h_{\text{dat}} \otimes (\kappa^h)_{\text{aux}}). \quad (78)$$

In Equation 78, the Pauli matrix σ^h is the matrix σ_i from the stabiliser $p_i \otimes \sigma_i$ corresponding to $h = h_{\text{loc}} p^h$ via $p^h = p_i$. Assuming the cost of implementing V is insignificant compared to cost of implementing time evolution by \tilde{H}_q , then Equation 77 shows the advantage of the auxiliary qubit mapping: $V^\dagger e^{-i\tilde{H}_q t}$ is less costly to implement than $e^{-iH_q t}$.

Note that this is not the most general form of auxiliary qubit mapping. An example of one that does not fit this template is the Verstraete–Cirac mapping, which uses stabilisers that are of the form $p_{\text{dat}} \otimes \tau_{\text{aux}}$ where τ_{aux} acts on more than one qubit [17].

4.2 Using 2 ancilla qubits to reduce average Pauli weight by 37.9% compared to the S–pattern

By modifying the proposal in Theorem 1, it is possible to use techniques inspired by the Mitchison–Durbin pattern to produce a ‘super-efficient’ fermion–qubit mapping $\overline{\text{JW}}_{f_{M+2}}$ for problem Hamiltonians H_{fermion} , with interaction graphs G_F equal to the $N \times N$ square lattice, using just $N^2 + 2$ qubits. This auxiliary Jordan–Wigner transformation has an average Pauli weight approximately 37.9% less than that of the original $\overline{\text{JW}}_{f_S}$ presented in [17], and 27.9% less than our result $\overline{\text{JW}}_{f_M}$ presented in Theorem 1, which was provably optimal for n –mode to n –qubit Jordan–Wigner transformations of the form in Definition 2.

At this point, we direct our reader to Appendix C for the full creation process of f_{M+2} , and derivation of its average Pauli weight

$$\text{APV}(f_{M+2}) \approx 0.31N + 1.68. \quad (79)$$

Comparing our auxiliary qubit mapping to the S–pattern of [17] and the Mitchison–Durbin pattern of Theorem 1,

$$\lim_{N \rightarrow \infty} \frac{\text{APV}(f_{M+2})}{\text{APV}(f_S)} \approx 0.62 \quad (80)$$

$$\lim_{N \rightarrow \infty} \frac{\text{APV}(f_{M+2})}{\text{APV}(f_M)} \approx 0.72, \quad (81)$$

yielding a 37.9% improvement over the Z– and S–patterns.

Figure 10 shows the average Pauli weights of fermion–qubit mappings $\overline{\text{JW}}_f$ using all the enumeration schemes f for the $N \times N$ fermionic lattice discussed in this paper.

Figure 13 concludes by demonstrating the advantage of our auxiliary qubit mapping $\overline{\text{JW}}_{M+2}$ for simulating fermionic Hamiltonians H_{fermion} with G_F equal to the 6×6 lattice. When $N = 6$ and $x = 3$, the qubit Hamiltonian \tilde{H}_q has a total Pauli weight of 222^1 . Using $\overline{\text{JW}}_{M+2}$ produces a qubit Hamiltonian \tilde{H}_q with an average Pauli weight of $\frac{222}{60} = 3.70$, which is a 14.6% improvement on the result $\frac{260}{60} = 4.33$ of $\overline{\text{JW}}_{f_M}(H_{\text{fermion}})$, which is optimal for n –mode to n –qubit mappings. It is also a 17.8% improvement on the average of $\frac{270}{60} = 4.5$ for $\overline{\text{JW}}_{f_Z}(H_{\text{fermion}})$ and $\overline{\text{JW}}_{f_S}(H_{\text{fermion}})$.

5 Discussion

5.1 Summary of results

By identifying the inherent place of fermion enumeration schemes in all n –fermionic mode to n –qubit mappings, we identified novel methods for creating new and improved map-

¹This differs from direct substitution into Equation 150 in Appendix C, as the 6×6 lattice has no region D and some hopping terms benefit from multiplication by both stabilisers.

pings, demonstrating two main results.

The first (Section 3): when used as enumeration schemes for fermionic modes in Jordan–Wigner transformations of a broad class of n -mode problem fermionic Hamiltonians, solutions to well-known graph problems can minimise practical cost functions of the qubit Hamiltonians. Theorem 1 illustrates the effect for fermionic Hamiltonians with hopping terms forming a square lattice of interactions, and identifies an n -qubit Jordan–Wigner transformation that uses the Mitchison–Durbing pattern to produce a qubit Hamiltonian with the minimum possible average Pauli weight. This is an improvement of 13.9% compared to previous methods using the S-pattern. Even for fermionic interaction graphs without known edgesum solutions, classical heuristic techniques may provide enumeration schemes that drastically reduce the average Pauli weight, as in the case of cellular arrangements in Section 3.5.

The second result combines our fermionic enumeration technique with the common strategy of employing auxiliary qubits to further preserve locality of interactions. In Section 4, we provide an improved Jordan–Wigner transformation for fermionic Hamiltonians with square-lattice interactions. Unlike all other auxiliary qubit mappings in the literature, this mapping requires only two auxiliary qubits, regardless of the number of fermionic modes n , and thus can be compared with the results of Theorem 1, which it improves upon by reducing the average Pauli weight by 37.9% compared to previous methods using the S-pattern.

Summarising our results, Table 1 compares Verstraete and Cirac’s S-pattern to our optimal ancilla-free mapping using f_M , and our low-ancilla mapping f_{M+2} . Auxiliary qubit mappings with scalable numbers of ancilla qubits are included for comparison.

5.2 Nonlinear qubit architectures and qubit routing

Most results involving the Jordan–Wigner and Bravyi–Kitaev transformations rely on qubits with connectivity constraints. In particular, Verstraete and Cirac [17] pursue a Jordan–Wigner type auxiliary qubit mapping to transform a local Hamiltonian on a fermionic lattice to a local Hamiltonian on a qubit lattice. Subsequent works have followed suit, usually working towards preserving geometric locality between the fermions and qubits, where the assumption is that the qubit architecture is the same as the fermionic graph [36, 59, 37, 35].

Fermionic enumeration schemes influence the distribution of quantum gates throughout nonlinear qubit architectures. To see this, consider decomposing a fermion–qubit mapping from a fermionic graph G_F to a qubit graph G_Q into two components: 1) the *enumeration* of the fermionic modes, which projects the fermionic connectivity graph G_F onto a 1D array of qubits, and then 2) the *embedding* of the 1D array of qubits into the qubit architecture G_Q . Figure 14 visualises the distinction between the two processes.

Verstraete and Cirac’s approach is to introduce the S-pattern to enumerate the fermions, and to use an S-pattern embedding to weave Pauli strings into the qubit lattice, as in the top row of Figure 15. In this work we emphasise that these are two distinct processes, and the choice of fermionic enumeration scheme can be done in an entirely separate way to the method of the embedding process. Indeed, as the second row of Figure 15 shows, the path of the fermionic enumeration scheme need not follow the connectivity of the qubit architecture at all to provide a valid mapping.

As mentioned in Section B.1, it is possible to conceive of metrics for qubit Hamiltonians that depend on qubit architectures. For example, the qubit routing problem concerns the distribution of Pauli strings on a nonlinear qubit connectivity G_Q [60]. The cost function for qubit routing should penalise strings of Pauli gates that spread through G_Q sparsely,

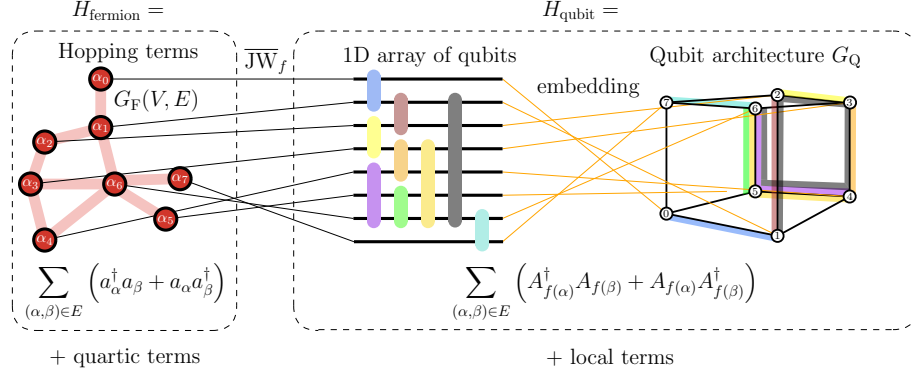


Figure 14: Fermionic enumeration techniques can influence the layout of Pauli strings on nonlinear qubit architectures.

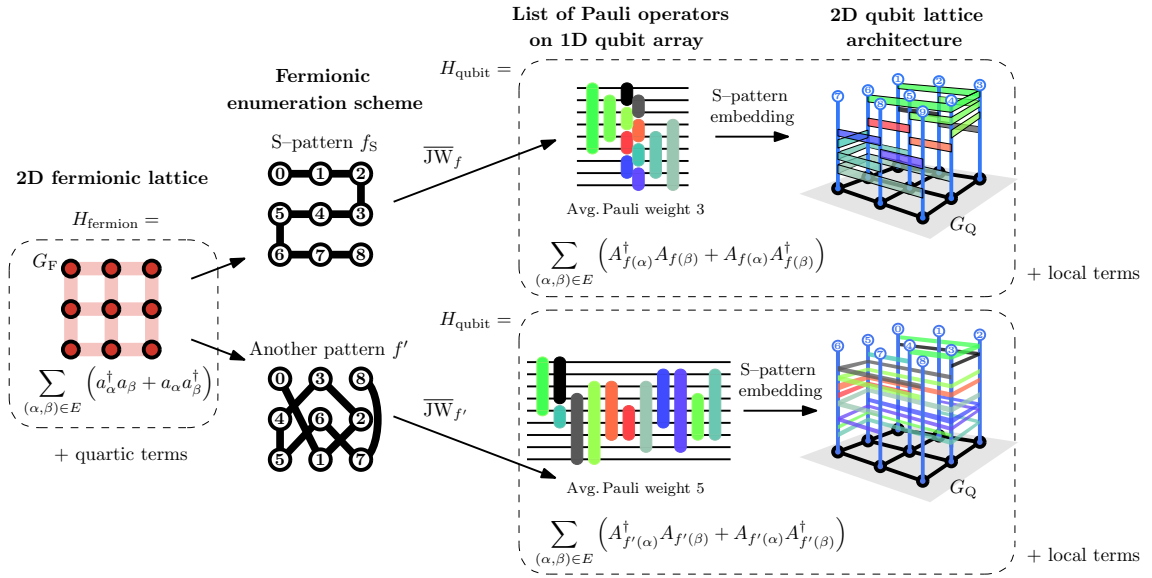


Figure 15: When working with elaborate qubit architectures such as the 2D lattice, the fermionic enumeration scheme need not follow the underlying qubit connectivity. This figure highlights the freedom to choose any scheme to enumerate fermions, yielding averages for the Pauli weights independent of the actual qubit connectivity.

and reward clustered Pauli strings. This poses a different problem to minimising the average Pauli weight of the qubit Hamiltonian, as the optimal enumeration scheme for the fermion–qubit mapping will need to cluster the Pauli strings of the qubit Hamiltonian while also minimising their weight. We expect that finding optimal enumeration schemes for cost functions that incorporate qubit architecture is a much more difficult family of problems than simply minimising a cost function of the Pauli weight as we have done here.

Sections 3 and 4 only concerned Jordan–Wigner transformations of the form in Definition 2. A more general class of mappings to search over would be the general Jordan–Wigner transformation in Example 1. The potential of using enumeration schemes as a method to define optimal Bravyi–Kitaev or ternary–tree mappings of the forms in Example 2 and 3 is completely unexplored and the subject of our upcoming work [47].

Table 1: Fermion–qubit mappings for $H_{\text{fermion}} = N \times N$ square lattice

	\overline{JW}_{f_S} [17]	\overline{JW}_{f_M} (3)	$\overline{JW}_{f_{M+2}}$ (4)	BK superfast [39]	VC [17]	AQM [37]
	(S–pattern)	(pattern from [40])	(+2 qubits)			
Qubit number	N^2	N^2	$N^2 + 2$	$2N^2 - 2N$	$2N^2$	$2N^2 - N$
Qubit/mode ratio	1	1	$1 + \frac{2}{N^2}$	$2 - \frac{2}{N}$	2	$2 - \frac{1}{N}$
Avg. $X\dots X$ weight	$\frac{1}{2}N + \frac{3}{2}$	$0.43N + 1.78$	$0.31N + 1.78$	$\mathcal{O}(1)$	$\mathcal{O}(1)$	$\mathcal{O}(1)$

Comparison between fermion–qubit mappings based on the number of qubits required and the average Pauli weight of hopping terms of the form $XZZ\dots ZX$ in the qubit Hamiltonian. In this case, the comparison is for fermionic Hamiltonians of N^2 –mode systems where hopping terms form a square lattice of interactions. The mapping from Section 3 gives the minimum average Pauli weight without the assistance of ancilla qubits, and the mapping from Section 4 improves this result while also maintaining a qubit/mode ratio of $1 + \mathcal{O}(\frac{1}{N^2})$. In comparison, BK superfast, VC and AQM use twice as many qubits as ancilla–free mappings to reduce the weight of Hamiltonian terms, albeit to terms of weight $\mathcal{O}(1)$. Which mapping is best ultimately depends on factors such as how many qubits are available.

Acknowledgements MC is funded by Cambridge Australia Allen and DAMTP Scholarship and the Royal Society PhD studentship. SS acknowledges support from the Royal Society University Research Fellowship scheme.

A Edgesum of the S-pattern

Lemma 2. On an $N \times N$ lattice, the S-pattern f_S has edgesum $C^1(f_S) = N^3 - N$.

Proof. Figure 16 displays the S-pattern enumeration procedure for an $N \times N$ square lattice, as well as the differences between adjacent vertices' indices.

Regardless of whether N is odd or even, the cost is thus

$$C^1(f_S) = (N - 1) \times \text{no. of rows} + \sum_{i=1}^N (2i - 1) \times (\text{no. of rows} - 1) \quad (82)$$

$$= N^2 - N + (N - 1)(N(N + 1) - N) \quad (83)$$

$$= N^2 - N - N^2 + N + N(N^2 - 1) \quad (84)$$

$$= N^3 - N. \quad \square$$

The average Pauli weight for the S-pattern on a square lattice is then

$$\text{APV}(f_S) = \frac{C^1(f_S)}{|E|} + 1 = \frac{N^3 - N}{2N(N - 1)} + 1 = \frac{1}{2}N + \frac{3}{2}. \quad (85)$$

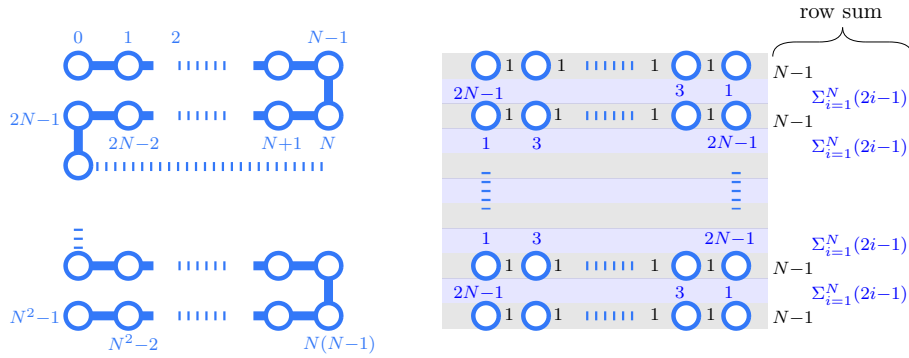


Figure 16: **Top:** S-pattern enumeration on the $N \times N$ square lattice. **Bottom:** Differences between vertex labels using the S-pattern enumeration, with row totals on the far right.

B Proof of Theorem 1

This section contains a more elaborate version of the original proof [40] that the Mitchison–Durbin pattern f_M solves the edgesum problem for an $N \times N$ lattice. Figure 17 chronicles the proof, which starts with an arbitrary enumeration scheme for the N^2 vertices before performing five sequential modifications (Proposition 2 and Lemmas 3–6) which exhaust all possible ways to reduce the edgesum, to give the Mitchison–Durbin pattern f_M .

The edgesum problem is the minimum- p -sum problem described in Section 2.7 with $p = 1$. The first part of the proof, Proposition 2, holds for all $p \geq 1$; the rest of the proof concerns only the case $p = 1$.

Given a graph $G = (V, E)$ and an enumeration scheme $f : V \rightarrow \{0, 1, \dots, N^2 - 1\}$ for G , the cost function $C^p(f)$ for the minimum p -sum problem is

$$(C^p(f))^p = \sum_{(\alpha, \beta) \in E} |f(\alpha) - f(\beta)|^p. \quad (86)$$

In the case that G is a square lattice, the edge set E consists of pairs of horizontally and vertically adjacent vertices, leading to horizontal and vertical contributions:

$$(C^p(f))^p = \sum_{\substack{(\alpha,\beta)\in E; \\ \text{horizontally adjacent}}} |f(\alpha) - f(\beta)|^p + \sum_{\substack{(\alpha,\beta)\in E; \\ \text{vertically adjacent}}} |f(\alpha) - f(\beta)|^p. \quad (87)$$

Definition 6. Let $G = (V, E)$ be the $N \times N$ square lattice, and let f be an enumeration scheme for G . Say f is *horizontally ordered* if, for any vertex $\alpha \in V$, $f(\beta) > f(\alpha)$ for all vertices β to the right of α , and say f is *vertically ordered* if $f(\beta) > f(\alpha)$ for all vertices β below α .

Proposition 2. Let $G = (V, E)$ be the $N \times N$ square lattice, let $p \geq 1$, and let f be an enumeration scheme f for G . Then there exists a horizontally and vertically ordered enumeration scheme g such that $C^p(g) \leq C^p(f)$.

Proof. From f , construct the enumeration scheme f_h by permuting each row of the lattice so that vertex index values ascending from left to right. Call f_h the *horizontal ordering of f* . Similarly, construct f_{hv} from f_h by permuting vertex labels under f_h within each column to increase from top to bottom. Call f_{hv} the *vertical ordering of f_h* . We will prove Proposition 2 via the statements S1 and S2 below:

S1. $C^p(f_h) \leq C^p(f)$.

S2. The enumeration scheme f_{hv} is horizontally ordered.

To prove S1, first consider the impact of horizontal ordering on the horizontal contributions to $C^p(f)$ in Equation 87.

Claim: The horizontal contributions to $C^p(f_h)$ are less than or equal to the horizontal contributions to $C^p(f)$.

Proof: (See Figure 18.) Suppose f is not horizontally ordered, and so there is a row of the lattice consisting of vertices $\alpha_0, \alpha_1, \dots, \alpha_{N-1}$ such that $f(\alpha_i) > f(\alpha_{i+1})$ for some $0 < i \leq N - 1$. The horizontal contributions to $C^p(f)$ from this row are

$$\begin{aligned} & |f(\alpha_0) - f(\alpha_1)|^p + \dots + |f(\alpha_{i-1}) - f(\alpha_i)|^p \\ & \quad + |f(\alpha_i) - f(\alpha_{i+1})|^p \\ & \quad + \dots + |f(\alpha_{N-2}) - f(\alpha_{N-1})|^p. \end{aligned} \quad (88)$$

Consider the enumeration scheme \tilde{f} that is identical to f save that $\tilde{f}(\alpha_i) = f(\alpha_{i+1})$ and $\tilde{f}(\alpha_{i+1}) = f(\alpha_i)$, i.e. \tilde{f} swaps the labels on vertices α_i and α_{i+1} so that $\tilde{f}(\alpha_i) < \tilde{f}(\alpha_{i+1})$. Thus, \tilde{f} is at least ‘partially’ horizontally ordered, moreso than f . The horizontal contributions to $C^p(\tilde{f})$ from this row are:

$$\begin{aligned} & |\tilde{f}(\alpha_0) - \tilde{f}(\alpha_1)|^p + \dots + |\tilde{f}(\alpha_{i-1}) - \tilde{f}(\alpha_{i+1})|^p \\ & \quad + |\tilde{f}(\alpha_{i+1}) - \tilde{f}(\alpha_i)|^p \\ & \quad + \dots + |\tilde{f}(\alpha_{N-2}) - \tilde{f}(\alpha_{N-1})|^p. \end{aligned} \quad (89)$$

The difference between the horizontal contributions to $C^p(f)$ and to $C^p(\tilde{f})$ is thus

$$|\tilde{f}(\alpha_{i+1}) - \tilde{f}(\alpha_i)|^p + |\tilde{f}(\alpha_{i-1}) - \tilde{f}(\alpha_{i+1})|^p \quad (90)$$

$$\begin{aligned} & - |f(\alpha_i) - f(\alpha_{i+1})|^p - |f(\alpha_{i-1}) - f(\alpha_i)|^p \\ & = |\tilde{f}(\alpha_{i-1}) - \tilde{f}(\alpha_{i+1})|^p - |f(\alpha_{i-1}) - f(\alpha_i)|^p \end{aligned} \quad (91)$$

$$\begin{aligned} & = |f(\alpha_{i-1}) - f(\alpha_i)|^p - |f(\alpha_{i-1}) - f(\alpha_i)|^p \\ & < 0, \end{aligned} \quad (92)$$

Finding a solution to the edgsum problem: constructing the Mitchison-Durbin pattern

Goal: find enumeration scheme f to minimise $C^1(f) = \sum_{(i,j) \in E} |f(i) - f(j)|$
 $G(V, E) = N \times N$ square lattice

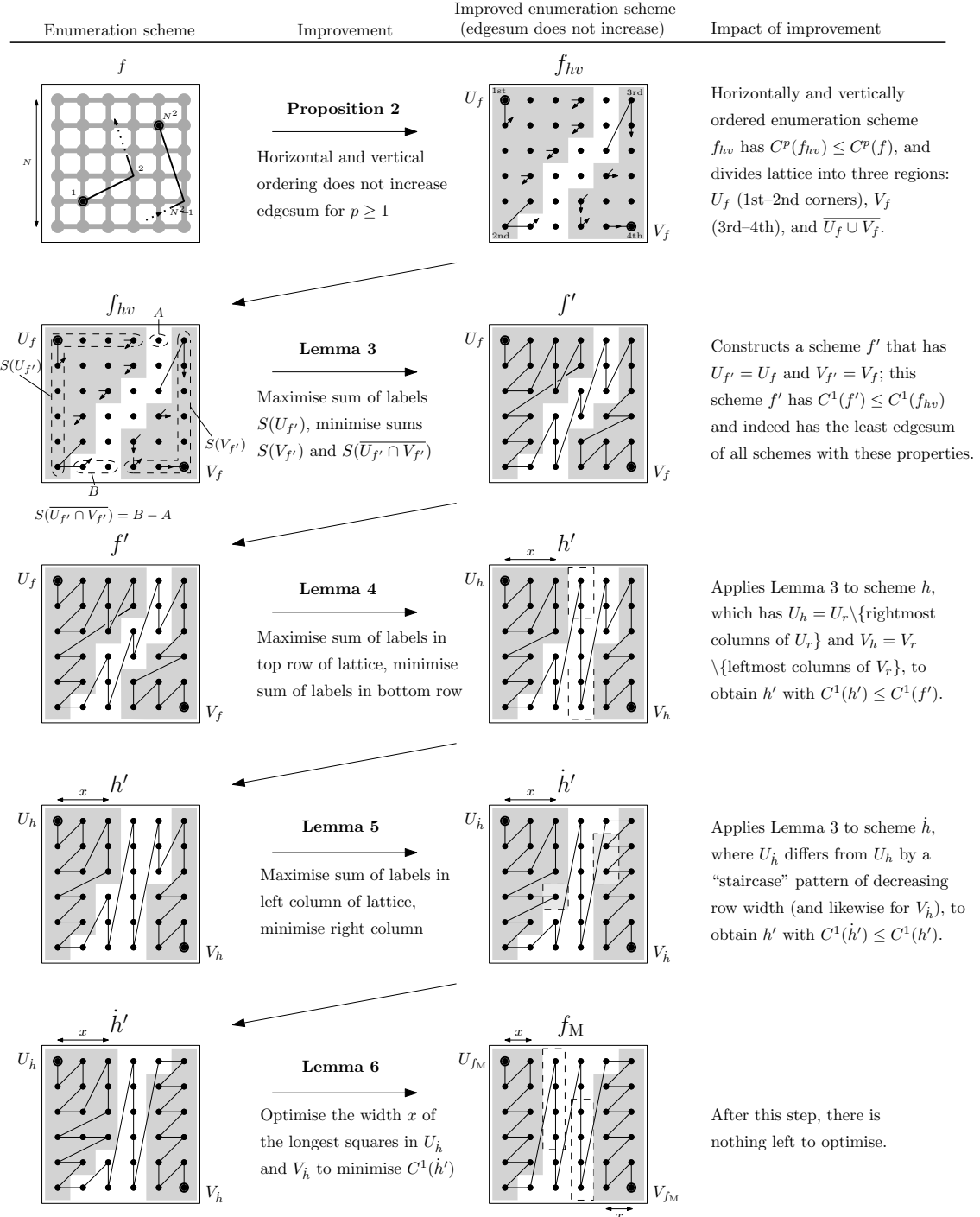


Figure 17: Overview of the proof that the Mitchison–Durbin pattern is a solution to the edgsum problem for the square lattice.

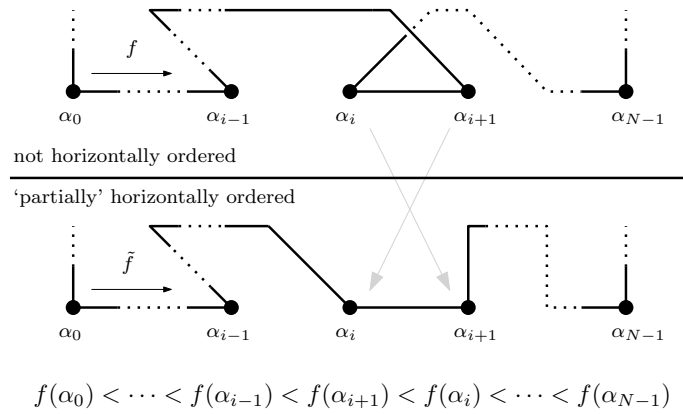


Figure 18: Swapping the labels of vertices in a row of the $N \times N$ square lattice as part of the process of constructing a horizontally ordered enumeration scheme.

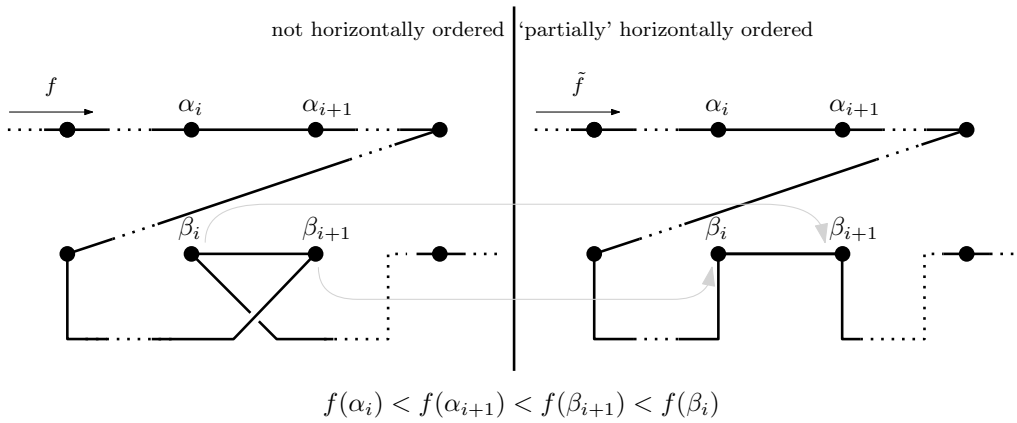


Figure 19: Swapping vertex labels within a row will affect some of the contributions to the p -sum of the enumeration scheme from vertically adjacent vertices.

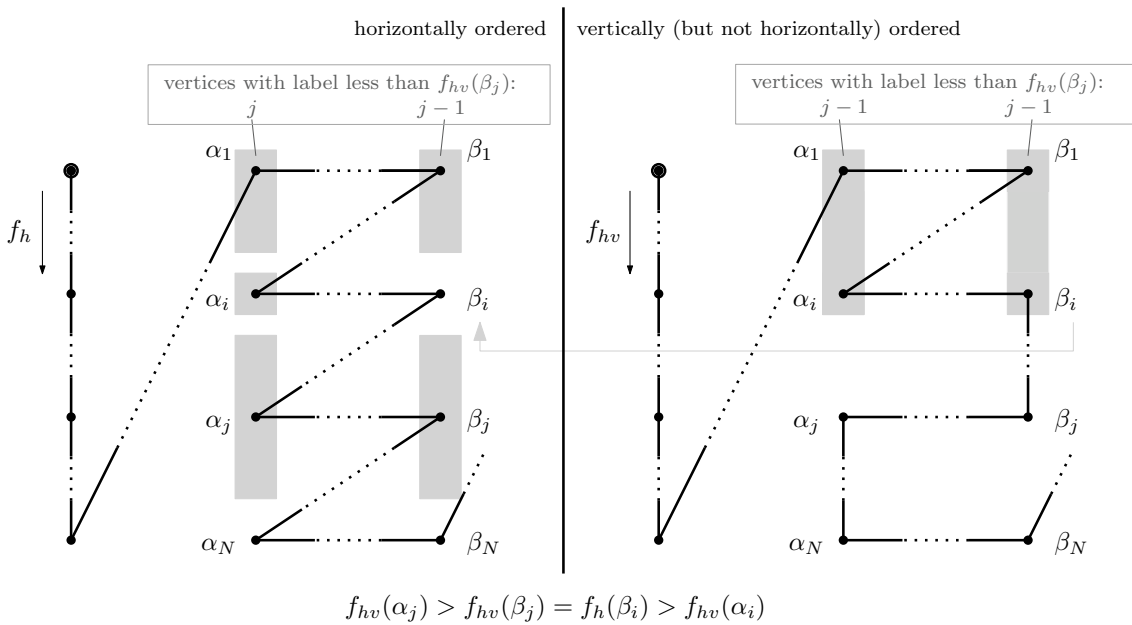


Figure 20: Illustration of the contradiction that would arise if a vertical ordering f_{hv} of a horizontally ordered enumeration scheme f_h were not itself horizontally ordered.

since $p \geq 1$ and $f(\alpha_{i-1}) < f(\alpha_{i+1}) < f(\alpha_i)$.

To construct f_h is to perform as many swaps of the above form (transforming f into \tilde{f}) as is necessary in order to label all N vertices in each row of the lattice in ascending order. Thus, the horizontal contributions to $C^p(f_h)$ are less than the horizontal contributions to $C^p(f)$, with equality if and only if $f = f_h$. ■

To finish proving S1, consider the impact of horizontal ordering on the vertical contributions to $C^p(f)$ in Equation 87.

Claim: The vertical contributions to $C^p(f_h)$ are less than or equal to the vertical contributions to $C^p(f)$.

Proof: (See Figure 19.) Suppose that f is not horizontally ordered, and that we are in the process of constructing f_h from f by re-ordering vertex labels row-by-row. Then there is a row of the lattice consisting of vertices $\beta_0, \beta_1, \dots, \beta_{N-1}$ such that $f(\beta_i) > f(\beta_{i+1})$ for some i . Let α_i and α_{i+1} be the vertices directly above vertices β_i and β_{i+1} , respectively; thus $f(\alpha_i) < f(\alpha_{i+1})$.

The vertical contributions to $C^p(f)$ from these four vertices is

$$|f(\beta_i) - f(\alpha_i)|^p + |f(\beta_{i+1}) - f(\alpha_{i+1})|^p. \quad (93)$$

Because $f(\alpha_i) < f(\alpha_{i+1})$ and $f(\beta_i) > f(\beta_{i+1})$, the values $|f(\alpha_i) - f(\beta_i)|^p$ and $|f(\alpha_{i+1}) - f(\beta_{i+1})|^p$ in Equation 93 are unequal, with the latter being less than the former.

Consider the enumeration scheme \tilde{f} that arises by swapping the labels of vertices β_i and β_{i+1} , so $\tilde{f}(\beta_i) = f(\beta_{i+1})$ and $\tilde{f}(\beta_{i+1}) = f(\beta_i)$. The vertical contributions to $C^p(\tilde{f})$ from the four vertices is

$$|f(\alpha_i) - f(\beta_{i+1})|^p + |f(\alpha_{i+1}) - f(\beta_i)|^p. \quad (94)$$

Note that for $p > 1$, if $a + b$ is a constant value then $a^p + b^p$ reduces in value the closer in value a is to b . Therefore, the vertical contributions to $C^p(\tilde{f})$ in Equation 94 are less than the vertical contributions to $C^p(f)$ in Equation 93. If $p = 1$, the contributions are equal. This proves the claim, and furthermore S1. ■

To prove S2, consider the horizontally ordered enumeration scheme f_h , as in Figure 20. Suppose that f_h is not vertically ordered, and let f_{hv} be the vertical ordering of f_h . It remains to show that f_{hv} is horizontally ordered. Suppose that it is not horizontally ordered: thus, there exists $j \in \{0, \dots, N-1\}$ such that the j th row of the lattice contains vertices α_j, β_j , with β_j to the right of α_j and $f_{hv}(\alpha_j) > f_{hv}(\beta_j)$.

Denote vertices in the column with β_j by $\beta_0, \dots, \beta_{N-1}$, and similarly define the vertices $\alpha_0, \dots, \alpha_{N-1}$ as those sharing the column of α_j . Because f_{hv} is vertically ordered, then $f_{hv}(\alpha_j) > f_{hv}(\alpha_k)$ and $f_{hv}(\beta_j) > f_{hv}(\beta_k)$ for all $0 \leq k \leq j-1$. As $f_{hv}(\alpha_j) > f_{hv}(\beta_j)$, then under f_{hv} , both the $j-1$ vertices above α_j and the $j-1$ vertices above β_j have labels less than $f_{hv}(\beta_j)$. Since all that separates f_h and f_{hv} is a permutation of vertex labels that fixes the labels within columns of the lattice, then there should be exactly $j-1$ vertices with labels less than $f_{hv}(\beta_j)$ in both the $\alpha_0, \dots, \alpha_{N-1}$ and $\beta_0, \dots, \beta_{N-1}$ columns of the lattice under enumeration scheme f_h as well.

Because f_h is horizontally ordered, $f_h(\alpha_j) < f_h(\beta_j)$. Therefore at least one of α_j and β_j will have a different label under f_h than under f_{hv} . Suppose, without loss of generality, that the vertex β_j satisfies this: that $f_h(\beta_j) \neq f_{hv}(\beta_j)$ and thus there exists some $i \in \{0, \dots, N-1\}$ such that $f_h(\beta_i) = f_{hv}(\beta_j)$. Under f_h , there are $j-1$ vertices in the $\beta_0, \dots, \beta_{N-1}$ column with label less than $f_{hv}(\beta_j)$, as was the case under f_{hv} . However, consider the vertices in the $\alpha_0, \dots, \alpha_{N-1}$ column. Each vertex α_k to the left of a vertex β_k with $f_h(\beta_k) < f_{hv}(\beta_j)$ also satisfies $f_h(\alpha_k) < f_{hv}(\beta_j)$ due to horizontal ordering; there

are $j - 1$ of these vertices. Distinct from these vertices, there is also the vertex α_i to the left of β_i which must also have $f_h(\alpha_i) < f_h(\beta_i) = f_{hv}(\beta_j)$. This is the contradiction.

This proves S2 and hence Proposition 2. \square

Section 3.6 discusses the case $p > 1$. Henceforth, this proof of Theorem 1 only concerns the case $p = 1$.

Let $G = (V, E)$ be the $N \times N$ square lattice. As a result of Proposition 2, we need only consider horizontally and vertically ordered enumeration schemes in the search for the solution to the edgesum problem for G . Let f_{hv} be the horizontal and vertical ordering of a vertex enumeration scheme f for G . Let $\alpha_{i,j}$ denote the vertex of G in the i th row and j th column, using matrix index notation so that the top-left vertex is $\alpha_{1,1}$. Then the edgesum of f_{hv} is

$$C^1(f_{hv}) = \sum_{i,j=1}^{N-1} (f_{hv}(\alpha_{i+1,j}) - f_{hv}(\alpha_{i,j}) + f_{hv}(\alpha_{i,j+1}) - f_{hv}(\alpha_{i,j})) \quad (95)$$

$$= 2f_{hv}(\alpha_{N,N}) + \sum_{i=2}^{N-1} f_{hv}(\alpha_{i,N}) + \sum_{j=2}^{N-1} f_{hv}(\alpha_{N,j}) - \sum_{i=2}^{N-1} f_{hv}(\alpha_{i,1}) \quad (96)$$

$$- \sum_{j=2}^{N-1} f_{hv}(\alpha_{1,j}) - 2f_{hv}(\alpha_{1,1})$$

$$= \sum_{\alpha \in V_b} f_{hv}(\alpha) + \sum_{\alpha \in V_r} f_{hv}(\alpha) - \left(\sum_{\alpha \in V_l} f_{hv}(\alpha) + \sum_{\alpha \in V_t} f_{hv}(\alpha) \right), \quad (97)$$

where V_l , V_r , V_t , V_b are the vertices in the left column, right column, top row and bottom row of the square lattice, respectively. This result greatly simplifies the calculation of $C^1(f_{hv})$ for the square lattice.

Due to horizontal and vertical ordering, $f_{hv}(\alpha_{1,1}) = 0$ and $f_{hv}(\alpha_{N,N}) = N^2 - 1$. Without loss of generality, assume that $f_{hv}(\alpha_{N,1}) < f_{hv}(\alpha_{1,N})$. As detailed in Figure 17, define U_f to be the set of vertices with labels between $f_{hv}(\alpha_{1,1}) = 0$ and $f_{hv}(\alpha_{N,1})$, and let V_f be the set of vertices with labels between $f_{hv}(\alpha_{N,1})$ and $f_{hv}(\alpha_{N,N}) = N^2 - 1$. Define $S(U_f)$ and $S(V_f)$ to be the sums of the labels of vertices on the boundary of the lattice in the regions U_f and V_f , respectively, and define $S(\overline{U_f \cap V_f})$ to be the difference between the sum of labels of vertices in $\overline{U_f \cap V_f}$ in the bottom and top rows of the lattice. By Equation 97, these quantities completely determine the edgesum:

$$C^1(f_{hv}) = S(V_f) + S(\overline{U_f \cap V_f}) - S(U_f). \quad (98)$$

The task now is to identify an improved enumeration scheme f' with the least edgesum of all schemes g that have $U_g = U_f$ and $V_g = V_f$. That is, find an enumeration scheme f' such that

$$f' = \arg \min_{\substack{\text{enumerations } g \\ U_g=U_f, V_g=V_f}} C^1(g) = \arg \min_{\substack{\text{enumerations } g \\ U_g=U_f, V_g=V_f}} \left(S(V_g) + S(\overline{U_g \cap V_g}) - S(U_g) \right). \quad (99)$$

Note that if f is such that U_f and V_f are the same regions as those yielded by a solution to the edgesum problem, then any f' satisfying Equation 99 is a solution to the edgesum problem. Lemma 3 details how to construct an f' given f ; using this result, Lemmas 4–6 detail how to set f such that this f' is a solution to the edgesum problem, completing the proof.

Lemma 3. Let $G = (V, E)$ be the $N \times N$ square lattice, with $\alpha_{i,j} \in V$ denoting the vertex in the i th row and j th column. Let f_{hv} be the horizontal and vertical ordering of an enumeration scheme f for G , dividing the lattice into regions U_f , V_f and $\overline{U_f \cap V_f}$ as defined above. Then, the steps below construct a horizontally and vertically ordered enumeration scheme f' that satisfies Equation 99. Note that while $U_{f'} = U_f$, $S(U_{f'})$ may not be equal to $S(U_f)$ and so on.

1. To maximise $S(U_{f'})$:

Rule A: starting at the beginning of a row $\alpha_{1,j}$ (resp. column $\alpha_{i,1}$), the enumeration scheme f' proceeds rightwards along the row (resp. downwards along the column) into the interior of U_f as far as possible without violating horizontal and vertical ordering.

Rule B: once the enumeration scheme f' has proceeded along a row or column as far as successive applications of Rule A permits, it must begin afresh at the start of the next-topmost row or the next-rightmost column, whichever is longest.

Mathematically: suppose that Rule A terminates at the vertex $\alpha_{i,j}$. Let $i' > i$ and $j' > j$ denote the indices of the topmost row and rightmost columns, respectively, that are *yet to be enumerated*, i.e. that consist entirely of vertices with labels greater than $f'(\alpha_{i,j})$. Then, let the number of vertices that are both in the (i') th row and also contained within U_f be $n_r(i')$, and similarly let $n_c(j')$ denote the number of vertices in the (j') th column that are also contained within U_f . The following recursive rule describes the process of maximising $S(U_{f'})$ with Rule A and Rule B:

$$f'(\alpha_{i,j}) + 1 = \begin{cases} f'(\alpha_{i,j+1}) & \text{if } \alpha_{i,j+1} \in U_f \text{ and } f'(\alpha_{i-1,j}) < f'(\alpha_{i,j}), \\ f'(\alpha_{i+1,j}) & \text{if } \alpha_{i+1,j} \in U_f \text{ and } f'(\alpha_{i,j-1}) < f'(\alpha_{i,j}), \\ f'(\alpha_{1,j'}) & \text{else if } n_c(j') \geq n_r(i'), \\ f'(\alpha_{i',1}) & \text{else } n_r(i') > n_c(j'). \end{cases} \quad (100)$$

2. To minimise $S(\overline{U_{f'} \cap V_{f'}})$: have the enumeration scheme f' begin at the topmost vertex of each column in $\overline{U_f \cap V_f}$ and fill down to the lowest vertex in that column of $\overline{U_f \cap V_f}$.
3. To minimise $S(V_{f'})$: perform the inverse procedure for maximising $S(U_{f'})$.

Proof. Begin by noting that maximising $S(U_{f'})$, minimising $S(\overline{U_{f'} \cap V_{f'}})$ and minimising $S(V_{f'})$ are three independent tasks, thus the Lemma's sequential approach is conceptually valid. Next, with $f'(\alpha_{1,1}) = 0$, it must be the case that either $f'(\alpha_{1,2}) = 1$ or $f'(\alpha_{2,1}) = 1$. Without loss of generality, take $f'(\alpha_{1,2}) = 1$.

1. To maximise $S(U_{f'})$: Rule A and Rule B, as described in Equation 100, work in tandem to label vertices the interior of U_f with the lowest indices possible. As illustrated in Figure 21, this ensures that the vertices on the boundary of the lattice, i.e. the vertices contributing to $S(U_{f'})$, have as high an index as possible.
2. To minimise $S(\overline{U_{f'} \cap V_{f'}})$, label the vertices in the columns of $\overline{U_f \cap V_f}$ in ascending order from top-to-bottom. This places labels with the least possible value in the bottom row of the lattice, and labels with the greatest possible value in the top row of the lattice, while preserving horizontal and vertical ordering.
3. As in step 1, a symmetric argument applies to minimising $S(V_{f'})$. □

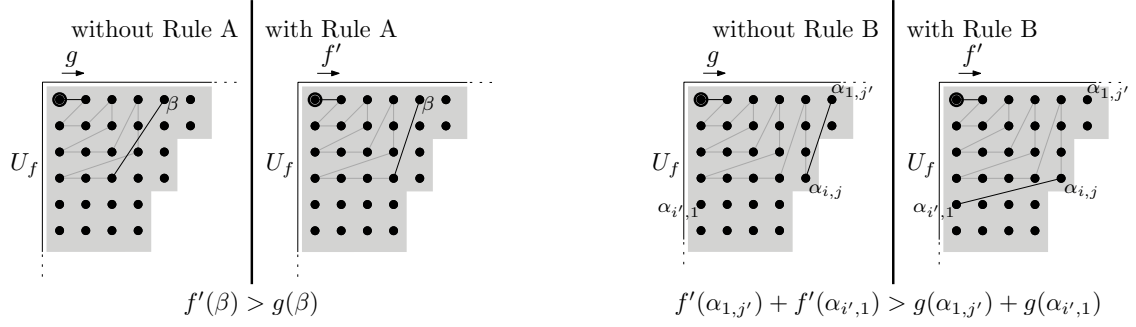


Figure 21: Rules in Lemma 3 for constructing the enumeration scheme f' so that it has the least edgesum of all enumeration schemes g with $U_g = U_f$ and $V_g = V_f$.

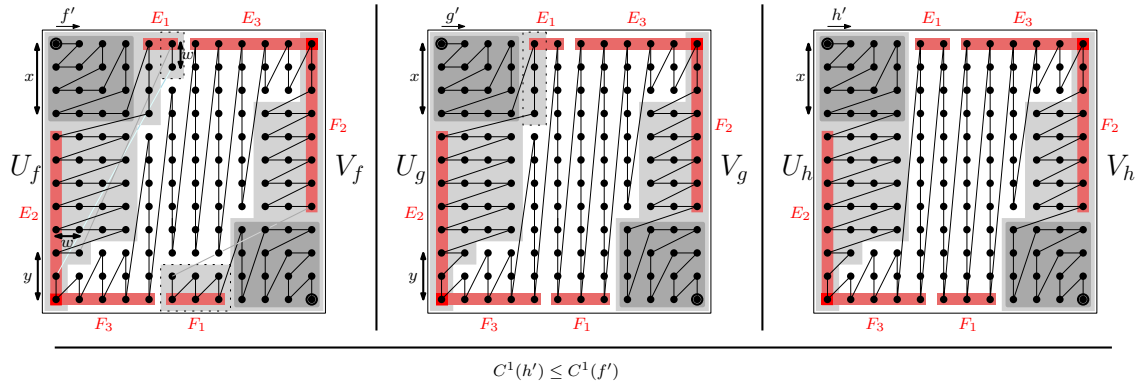


Figure 22: Illustration of Lemma 4: starting with an enumeration scheme f' , intermediate scheme g' , and final scheme h' demonstrating shapes of U_h and V_h that allow for a lower edgesum.

By the definition in Equation 99, there must exist a particular shape for regions U_f and V_f such that the f' described in Lemma 3 is a solution to the edgesum problem. There is an $x \times x$ square region of vertices in the top-left region of U_f , where x is the greatest integer for which the statement “the topmost x rows of U_f contain at least x vertices” is true. We will call this region the *largest square of U_f* ; define the *largest square of V_f* similarly.

Lemma 4. Let $G = (V, E)$ be the $N \times N$ square lattice, and let f be a horizontally and vertically ordered enumeration scheme for G , dividing the lattice into regions U_f , V_f and $\overline{U_f \cap V_f}$ as defined above. Let f' be the enumeration scheme resulting from applying Lemma 3 to f .

Now, consider an enumeration scheme h that divides the lattice into regions U_h , V_h and $\overline{U_h \cap V_h}$ where $U_h \subseteq U_f$ consists of all the vertices in U_f except for those to the right of the largest square of U_f , and where $V_h \subseteq V_f$ consists of all the vertices in V_f except for those to the left of the largest square of V_f . The vertices in $U_f \setminus U_h \cup V_f \setminus V_h$ are thus in $\overline{U_h \cap V_h}$. Let h' be the scheme resulting from applying Lemma 3 to h . Then, $C^1(h') \leq C^1(f')$.

Proof. As in Figure 22, define E_1 to be the set containing the topmost vertices in U_f that are to the right of the largest square in U_f , E_2 to be the set containing the leftmost vertices in U_f beneath the largest square of U_f , and E_3 to be set containing the topmost vertices of the lattice that are outside of U_f . Define F_1 , F_2 and F_3 analogously.

While E_1, \dots, F_3 refer to fixed sets of vertices defined by the enumeration scheme f , let $E_1(g), \dots, F_3(g)$ refer to the sums of the labels of those same vertex sets under any

enumeration scheme g . Using the shorthand $(E_1 + E_2)(g) = E_1(g) + E_2(g)$, we have via Equation 97,

$$C^1(f') = ((F_1 + F_2 + F_3) - (E_1 + E_2 + E_3))(f') \quad (101)$$

+ labels under f' of boundary vertices of largest squares of U_f and V_f ,

where f' is the enumeration scheme that arises from applying Lemma 3 to f .

Claim: With the description of h and h' from Lemma 4,

$$(E_1 + E_2 + E_3)(h') \geq (E_1 + E_2 + E_3)(f'). \quad (102)$$

Proof: Consider an enumeration scheme g that has $U_g = U_f$ and $V_g = V_h$, and let g' be the enumeration scheme that arises from applying Lemma 3 to g . Then, $E_1(g') = E_1(f')$ and $E_2(g') = E_2(f')$ as the vertex labels are unchanged. However, $E_3(g') > E_3(f')$: this is because there are more vertices in $\overline{U_g} \cap \overline{V_g}$ than in $\overline{U_f} \cap \overline{V_f}$.

Next, redefine g such that $V_g = V_h$ and U_g is equal to U_f with its rightmost column removed, as in Figure 22. Define g' to be the scheme arising from applying Lemma 3 to g .

Let x be the side length of the largest square in U_f , let w be the number of vertices in the rightmost column of U_f and let y be the number of rows in U_f with no more than w vertices.

The labels of the bottom-most y vertices in E_2 under g' are each w less than those same vertices under f' , and so $E_2(g') = E_2(f') - wy$. Meanwhile, $E_1(g') > E_1(f')$ because of the new label for the topmost vertex of column that was removed from U_f to make U_g . The label of this vertex increases by at least xy , and so $(E_1 + E_2)(g') \geq (E_1 + E_2)(f') + xy - wy \geq (E_1 + E_2)(f')$, as $xy - wy = (x - w)y \geq 0$ because $x \geq w$ (with equality iff. $U_g = U_f$).

Repeating the process of deleting the rightmost column of U_f will continue to increase $(E_1 + E_2 + E_3)(g')$. Note that E_3 does not change during the course of this procedure, which terminates when $g = h$, giving

$$(E_1 + E_2 + E_3)(h') \geq (E_1 + E_2 + E_3)(f'). \quad (103)$$

■

By the symmetric structure of enumeration patterns that arise from Lemma 3, this claim also demonstrates that $(F_1 + F_2 + F_3)(h') \leq (E_1 + E_2 + E_3)(f')$. Therefore,

$$((F_1 + F_2 + F_3) - (E_1 + E_2 + E_3))(h') \leq ((F_1 + F_2 + F_3) - (E_1 + E_2 + E_3))(f'), \quad (104)$$

which, via Equation 101, implies $C^1(h') \leq C^1(f')$. □

At this stage, the only part of U_h left to scrutinise is its bottom-left corner: Lemma 5 details a shape for it to take (and vice-versa for the top-right corner of V_h) in order to produce a new enumeration scheme \dot{h}' with $C^1(\dot{h}') \leq C^1(h')$.

Lemma 5. Let $G = (V, E)$ be the $N \times N$ square lattice, and let h be a horizontally and vertically ordered enumeration scheme for G arising from applying Lemma 4 to some enumeration scheme f . Let h' be the enumeration scheme resulting from applying Lemma 4 to h .

Let x be the side length of the largest square in U_h . Then, consider a new enumeration scheme \dot{h} such that $U_{\dot{h}}$ differs from U_h by the following: modify U_h by imposing a length of x vertices on all rows down to a height x above the bottom row, and then give the row at height $y < x$ a length of y or $y - 1$ for all $y = x - 1, \dots, 1$. Define $V_{\dot{h}}$ similarly. Apply Lemma 3 to \dot{h} to obtain \dot{h}' . Then, $C^1(\dot{h}') \leq C^1(h')$.

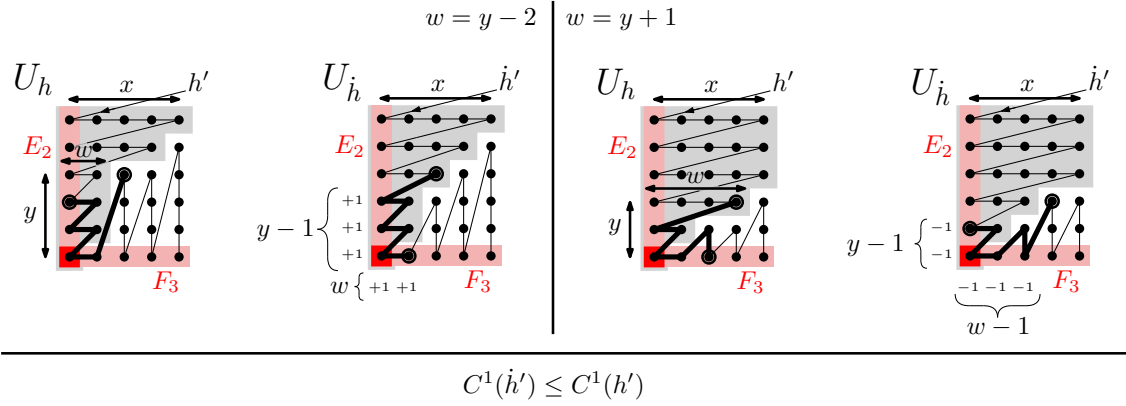


Figure 23: Finding an improvement $U_{\dot{h}}$ to the region U_h in Lemma 5, and hence an improved enumeration scheme \dot{h}' which has a lower edgesum than h' . As a visual aid, in both cases $w = y - 2$ and $w = y + 1$, the bolded vertices under scheme h' share the same labels as the bolded vertices under \dot{h}' .

Proof. Using Equation 101,

$$C^1(\dot{h}') - C^1(h') = ((F_3 - E_2) + (F_2 - E_3))(\dot{h}') - ((F_3 - E_2) + (F_2 - E_3))(h') \quad (105)$$

$$= \underbrace{(F_3 - E_2)(\dot{h}') - (F_3 - E_2)(h')}_{\text{involves regions } U_h \text{ and } U_{\dot{h}} \text{ only}} + \underbrace{(F_2 - E_3)(\dot{h}') + (F_2 - E_3)(h')}_{\text{involves regions } V_h \text{ and } V_{\dot{h}} \text{ only}} \quad (106)$$

as the vertices in E_1 and F_1 have the same labels under h' and \dot{h}' .

First, consider the difference in edgesum due to the difference in shape between $U_{\dot{h}}$ and U_h , given in the first line of Equation 106. As in Figure 23, for $y = 1, \dots, N - x$ take the y th row from the bottom of U_h , and let w be the number of vertices it contains. The enumeration scheme \dot{h}' only differs from h' if $w < y - 1$ or $w > y$.

Case $w < y - 1$: Suppose $w = y - 1 - k$ for $k \geq 1$ (Figure 23 contains an example with $y = 4$, $w = 2$, $k = 1$). Choose the number of vertices in the y th row from the bottom of $U_{\dot{h}}$ to be $y - 1$. Then the labels of the $y - 1$ bottom-most vertices in E_2 under \dot{h}' are each greater by k than the same vertices' labels under h' , i.e. $E_2(\dot{h}') - E_2(h') = k(y - 1)$. Similarly, the labels of the w leftmost vertices in F_3 under \dot{h}' are each greater by k than the same vertices' labels under h' , i.e. $F_3(\dot{h}') - F_3(h') = kw$. Thus, the top line of Equation 106 is equal to $k(w - (y - 1)) < 0$.

Case $w > y$: Suppose $w = y + k$ for $k \geq 1$ (Figure 23 contains an example with $y = 3$, $w = 4$, $k = 1$). Choose the number of vertices in the y th row from the bottom of $U_{\dot{h}}$ to be y . Then the labels of the $y - 1$ bottom-most vertices E_2 under \dot{h}' each differ by $-k$ from the same vertices' labels under h' , i.e. $E_2(\dot{h}') - E_2(h') = -k(y - 1)$. Similarly, the labels of the $w - 1$ leftmost vertices in F_3 each differ by $-k$ from the same vertices' labels under h' , i.e. $F_3(\dot{h}') - F_3(h') = -k(w - 1)$. Thus, the top line of Equation 106 is equal to $-k((w - 1) - (y - 1)) < 0$.

Note that, working within the successive restrictions of Lemmas 3 and 4, the maximum number of vertices permitted in any row of $U_{\dot{h}}$ is x . Thus, the rows increase in width from $y = 1$ by one vertex at a time before reaching the maximum width of $y = x$ at $y = x$.

By symmetry, the same rules work to construct the region $V_{\dot{h}}$ such that $C^1(\dot{h}') \leq C^1(h')$. \square

Finally, only one degree of freedom remains: the side lengths of the largest squares in $U_{\dot{h}}$ and $V_{\dot{h}}$. Note that these values only affect the top and bottom lines of Equation 106,

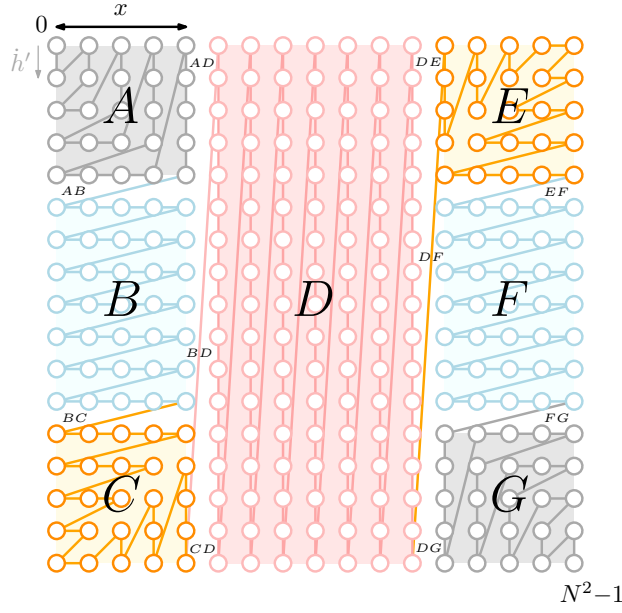


Figure 24: Sections of the $N \times N$ square lattice and an enumeration pattern \hat{h}' that satisfies Lemma 6.

respectively, and hence if there exists an optimal value x for the width of $U_{\hat{h}}$, then it will also be the optimal value for the width of $V_{\hat{h}}$. Thus, we can take the side lengths of the largest squares in $U_{\hat{h}}$ and $V_{\hat{h}}$ to be the same.

Lemma 6 expresses the edgesum of the pattern as a function of N and x . Corollary 3 then provides the optimal value for x and hence the Mitchison–Durbin pattern f_M , a solution to the edgesum problem.

Lemma 6. Let $G = (V, E)$ be the $N \times N$ square lattice, and let \hat{h} be a horizontally and vertically ordered enumeration scheme that arises from applying Lemma 5 to some horizontally and vertically ordered scheme f .

Let x be the side length of the largest squares of $U_{\hat{h}}$ and $V_{\hat{h}}$, and let \hat{h}' be the enumeration scheme that results from applying Lemma 3 to \hat{h} . Then, the edgesum of \hat{h}' is

$$C^1(\hat{h}') = N^3 - xN^2 + 2x^2N - \frac{2}{3}x^3 + N^2 - xN - 2N + \frac{2}{3}x. \quad (107)$$

Proof. See Section B.1. □

Corollary 3. For $N \geq 5$, the value of x that minimises $C^1(\hat{h}')$ in Equation 107 is $x = N - \frac{1}{2}\sqrt{2N^2 - 2N + \frac{4}{3}}$. Round x to the nearest integer to obtain the minimum edgesum over all enumeration schemes for the $N \times N$ square lattice.

Proof. Treat N and x as continuous variables, and use calculus to find that minimum of $C^1(\hat{h}')$ in Equation 107 occurs when $x = N - \frac{1}{2}\sqrt{2N^2 - 2N + \frac{4}{3}}$. □

This completes the proof. The optimal value for x in Corollary 3 is a refinement on the value $x = \left(1 - \frac{1}{\sqrt{2}}\right)N$ that Mitchison and Durbin give in [40]. Rounding this approximate value gives the same integer as $N - \frac{1}{2}\sqrt{2N^2 - 2N + \frac{4}{3}}$ for most values of N .

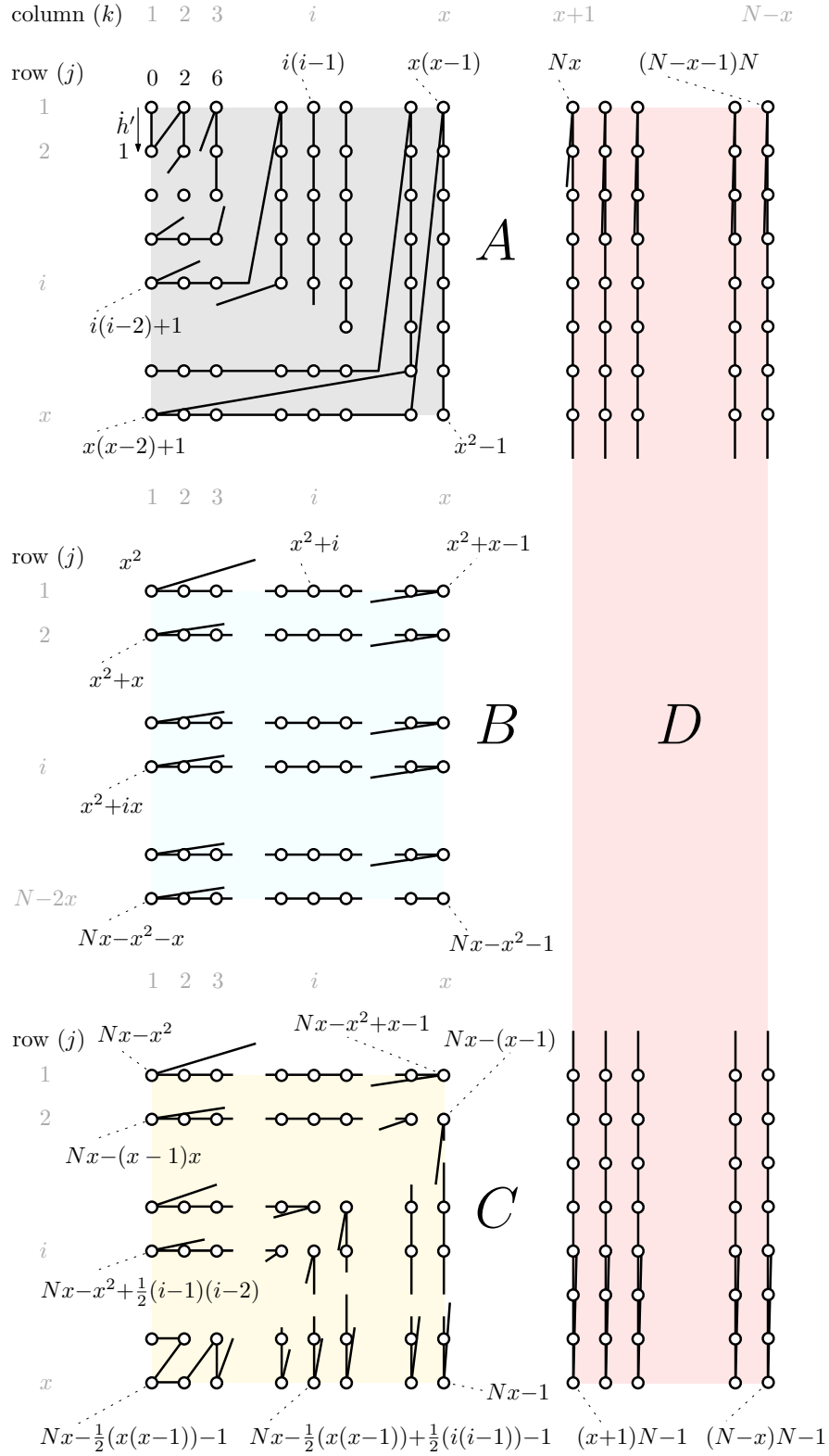


Figure 25: An in-depth look at the enumeration scheme h' that arises from Lemma 6. Vertex labels indicate the value of each vertex under the enumeration scheme.

B.1 Edgesum of the Mitchison–Durbin pattern

This section calculates the edgesum of the enumeration pattern \dot{h}' in Lemma 6. Divide the enumeration pattern on the $N \times N$ grid up into regions A, B, \dots, G as in Figure 24. Let the label of each region also denote its edgesum. Therefore

$$\begin{aligned} C^1(\dot{h}') &= A + B + C + D + E + F + G \\ &\quad + AB + AD + BD + BC + CD \\ &\quad + DE + EF + DF + FG + DG, \end{aligned} \quad (108)$$

where AB, \dots, DG denote the sums of the differences between vertex labels across the interfaces between each pair of regions. Due to the symmetry of \dot{h}' , Equation 108 becomes

$$C^1(\dot{h}) = 2(A + B + C) + D + 2(AB + AD + BC + BD + CD). \quad (109)$$

We can derive expressions for the contributions of each region to $C^1(\dot{h}')$ by observing the patterns in the differences between vertex labels. Figure 25 shows the progression of vertex labels in regions A – D of the square lattice. Within each of these regions, the enumeration scheme is horizontally and vertically ordered. Thus, using Equation 97 on regions A and C gives:

$$A = \left(\sum_{k=1}^{x-1} (x(x-2) + k) + x^2 - 1 + \sum_{j=1}^x (x(x-1) + j - 1) \right) \quad (110)$$

$$\begin{aligned} &\quad - \left(\sum_{k=1}^x (k(k-1)) + \sum_{j=1}^x (j(j-2) + 1) \right) \\ &= \frac{1}{6}(x-1)(6 + x(8x-1)) \end{aligned} \quad (111)$$

$$= C. \quad (112)$$

The other regions' contributions are more straightforward to calculate:

$$B = (N - 2x)(x - 1) + x^2(N - 2x - 1) \quad (113)$$

$$D = N^3 - 2xN^2 - 2xN + 2x - N. \quad (114)$$

The vertex labels in Figure 25 also make it simple to calculate the contributions to $C^1(\dot{h}')$ from the interfaces between the regions:

$$AD = \sum_{j=1}^x \left((x(x-1) + j - 1) - (Nx + j - 1) \right) = Nx^2 - x^3 + x^2 \quad (115)$$

$$AB = 1 - 2x + 2x^2 \quad (116)$$

$$BD = \frac{1}{2}(N^2 + N - 3xN + xN^2 + 2x^2 - 2x - 2x^2N) \quad (117)$$

$$BC = x^2 \quad (118)$$

$$CD = 1 - 2x + xN + x^2. \quad (119)$$

Substituting Equations 111–119 into Equation 109 gives the result,

$$C^1(\dot{h}') = N^3 - xN^2 + 2x^2N - \frac{2}{3}x^3 + N^2 - xN - 2N + \frac{2}{3}x. \quad (120)$$

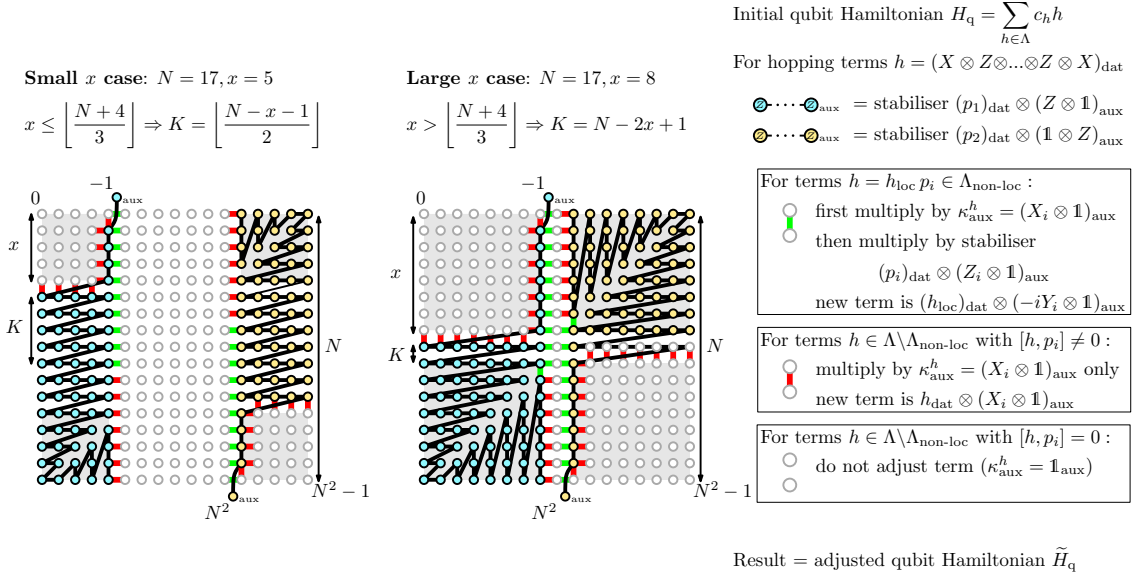


Figure 26: Stabilisers and adjusted Hamiltonian hopping terms for the auxiliary qubit mapping using our augmented Mitchison–Durbin pattern, ‘ $f_{\dot{h}'+2}$ ’. Initialising the (N^2+2) –qubit system in a state stabilised by the strings $p_i \otimes \sigma_i$ nullifies the most costly contributions to the edgesum of the Mitchison–Durbin pattern, resulting in a significantly reduced average Pauli weight for the qubit Hamiltonian \tilde{H}_q . As the text details, setting $x \approx 0.40N$ in the enumeration scheme \dot{h}' yields the minimum average Pauli weight.

C Constructing the enumeration pattern f_{M+2}

Begin with a data register of N^2 qubits, and take a fermionic Hamiltonian H_{fermion} of the form in Equation 48, where $G_F = (V, E)$ is the $N \times N$ square lattice. As the quartic terms become local under any Jordan–Wigner transformation, consider only the hopping terms of the resulting qubit Hamiltonian

$$H_q := \overline{\text{JW}}_{\dot{h}'} \left(\sum_{(\alpha, \beta) \in E} a_\alpha^\dagger a_\beta + a_\alpha a_\beta^\dagger \right) = \sum_{h \in \Lambda} c_h h, \quad (121)$$

where Λ is the set of terms of H_q , and \dot{h}' is the Mitchison–Durbin pattern with a variable value for x , the side–length of the distinctive square in the corners of the pattern, as in Lemma 5. In f_M the value $x \approx 0.29N$; however this only minimises $C^1(f_M)$ for Jordan–Wigner transformations with zero ancilla qubits. Since we are permitting ancillas, as in the proof of Theorem 1, treat $x \in \{1, 2, \dots, N/2\}$ as a variable, its optimal value currently unknown.

Note that the edgesum $C^1(f_M)$ has two costly contributions: the $\mathcal{O}(x^2N)$ –valued difference between adjacent vertices in the AD – and DG –interfaces as labelled in Figure 24. We will construct an auxiliary qubit mapping that reduces the contributions of these edges to $C^1(f_M)$, and hence reduces the average Pauli weight of the qubit Hamiltonian.

The fermion–qubit mapping we construct here uses only two ancilla qubits and takes a similar approach to the E–type auxiliary qubit mapping from [37]. We will follow the formulation of auxiliary qubit mappings from Section 4, making sure our mapping satisfies the two requirements that section lays out:

1. Choose p –strings $\{p_1, p_2\}$ that correspond to the longest individual strings of Pauli

Z matrices of any term $h \in \Lambda$. In this case, we choose

$$p_1 = \begin{pmatrix} xN-1 \\ \otimes & Z_i \\ i=x(x-1)+1 \end{pmatrix} \otimes \begin{pmatrix} \otimes & \mathbf{1}_i \\ \text{other} \end{pmatrix} \quad (122)$$

$$p_2 = \begin{pmatrix} N^2-x^2+x-2 \\ \otimes & Z_i \\ i=(N-x)N \end{pmatrix} \otimes \begin{pmatrix} \otimes & \mathbf{1}_i \\ \text{other } i \end{pmatrix}. \quad (123)$$

These bridge the gaps between the outermost vertices on the AD - and DG -interfaces, respectively. Figure 26 depicts the two p -strings for differing values of x ; the indices of the first and last qubits of each p -string result from inspecting the label guide in Figure 25.

Then, define $\Lambda_{\text{non-loc}}$ to be all of the Hamiltonian terms $h \in \Lambda$ that contain less Z matrices upon multiplication by either p_1 or p_2 . Note that none of the $h \in \Lambda$ would benefit from multiplication by *both* p -strings, unless $x = N/2$ exactly as, in that case, there is no column of vertices separating the stabilisers. Figure 13 shows this in detail with $N = 6$ and $x = 3$. These p -strings trivially satisfy **Requirement 1**'s preliminary condition that $[p_1, p_2] = 0$.

2. Introduce two auxiliary qubits, labelled -1 and N^2 . Define the unitary mapping V to be a cascade of controlled-NOT operations, storing the net parity of the qubits appearing in p_i in the phase of the i th auxiliary qubit. Figure 27 shows a valid circuit for V .

For any state $|\psi\rangle_{\text{dat}}$ of the original N^2 -qubit system, now consider the state

$$|\tilde{\psi}\rangle_{\text{dat,aux}} = V |\psi\rangle_{\text{dat}} |0\rangle_{\text{aux}}^{\otimes 2}. \quad (124)$$

This state has two stabilisers:

$$((p_1)_{\text{dat}} \otimes (Z \otimes \mathbf{1})_{\text{aux}}) |\tilde{\psi}\rangle_{\text{dat,aux}} = |\tilde{\psi}\rangle_{\text{dat,aux}}, \quad (125)$$

$$((p_2)_{\text{dat}} \otimes (\mathbf{1} \otimes Z)_{\text{aux}}) |\tilde{\psi}\rangle_{\text{dat,aux}} = |\tilde{\psi}\rangle_{\text{dat,aux}}. \quad (126)$$

The existence of the stabiliser state $|\tilde{\psi}\rangle_{\text{dat,aux}}$ satisfies **Requirement 1**.

3. To identify which terms $h \in \Lambda$ do not commute with p_1 and p_2 , recall the form of the hopping terms from Equation 43. The only relevant feature of a term h is the location of the endpoint matrices of its non-identity Pauli strings, i.e. its X and Y matrices. For brevity, and without loss of generality, abbreviate the terms to just the Pauli string $XZZ\dots ZX$:

$$h_{\text{dat}} = (X \otimes Z \otimes \dots \otimes Z \otimes X) \otimes \begin{pmatrix} \otimes & \mathbf{1} \\ \text{other} \end{pmatrix}. \quad (127)$$

As p_1 and p_2 comprise only Z matrices, $[h, p_i] = 0$ if and only if the Pauli string $XZZ\dots ZX$ of h intersects completely, or not at all, with the Pauli string $ZZZ\dots Z$ of p_i , because $[X, Z] = -2iY \neq 0$. Thus the vast majority of the hopping terms already commute with both p -strings; it is only the hopping terms with Pauli strings that have one endpoint in p_i and the other not in p_i that need to be modified so that they commute with both stabilisers. If $[h, p_1] \neq 0$, make the adjustment

$$h_{\text{dat}} \longmapsto h_{\text{dat}} \otimes (X \otimes \mathbf{1})_{\text{aux}}; \quad (128)$$

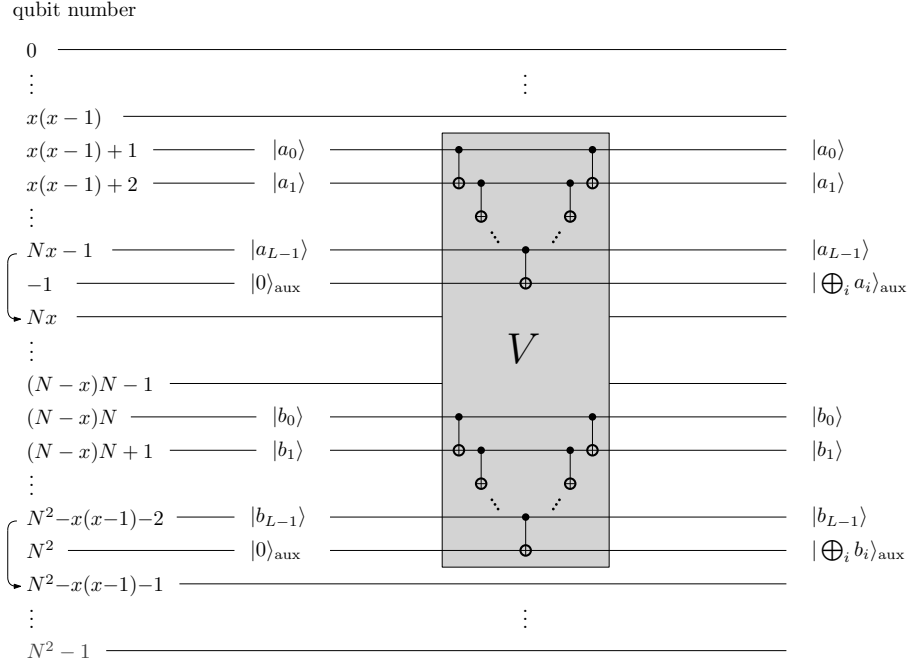


Figure 27: A circuit for V , which initialises the stabiliser state $|\tilde{\psi}\rangle_{\text{dat,aux}}$ from $|\psi\rangle_{\text{dat}} |0\rangle_{\text{aux}}^{\otimes 2}$ while preserving the time–evolution of the underlying data system.

if $[h, p_2] \neq 0$, make the adjustment

$$h_{\text{dat}} \mapsto h_{\text{dat}} \otimes (\mathbf{1} \otimes X)_{\text{aux}} . \quad (129)$$

If $x = N/2$ exactly, then some of the horizontal hopping terms across the BD – and DF –interfaces will not commute with either p_1 or p_2 , and need both adjustments (as depicted in Figure 13). Abbreviating each correction by κ^h , adjusted Hamiltonian terms then satisfy

$$[h_{\text{dat}} \otimes \kappa_{\text{aux}}^h, (p_i)_{\text{dat}} \otimes (\sigma_i)_{\text{aux}}] = 0 \quad (130)$$

for $i = 1, 2$ because $[X_{\text{dat}} \otimes X_{\text{aux}}, Z_{\text{dat}} \otimes Z_{\text{aux}}] = 0$. Figure 26 shows which hopping terms need adjustment in this way.

Finally, check that V and κ^h satisfy **Requirement 2**. Let h be a hopping term that does not commute with p_1 . Consider an arbitrary state for the quantum register

$$|\psi\rangle_{\text{dat}} = \sum_{\vec{a}, \vec{b}, \vec{c}} \gamma |a_0 a_1 \dots, b_0 b_1 \dots, c_0 c_1 \dots\rangle_{\text{dat}} , \quad (131)$$

where $a_j, b_j, c_j \in \{0, 1\}$ such that \vec{a} contains the parities of all the qubits involved in p_1 , \vec{b} contains the parities of the qubits not involved in either p –string, and \vec{c} contains the parities of the qubits involved in p_2 . The coefficients $\gamma \in \mathbb{C}$ depend on the bit strings \vec{a} , \vec{b} and \vec{c} .

As h does not commute with p_1 , one of the X matrices in its Pauli string must act on a qubit in \vec{a} and the other X matrix must act on a qubit in either \vec{b} (if $x < N/2$) or \vec{c} (if $x = N/2$ exactly). Consider the case $x < N/2$ and let the endpoint qubits of the Pauli string of h be the j th and k th qubits in each string, respectively. Therefore,

the output of $h|\psi\rangle_{\text{dat}}$ is

$$h|\psi\rangle_{\text{dat}} = \sum_{\vec{a}, \vec{b}, \vec{c}} \gamma' \left| a_1 \dots \bar{a}_j \dots, b_1 \dots \bar{b}_k \dots, c_1 c_2 \dots \right\rangle_{\text{dat}}, \quad (132)$$

where each γ' is equal to γ up to a sign depending on the effect of the Z matrices in h . Meanwhile, our prescription for κ^h is to apply an X on the first auxiliary qubit. Noting that $V = V^\dagger$, observe that

$$V(h \otimes \kappa^h) |\tilde{\psi}\rangle = V(h \otimes \kappa^h) \sum_{\vec{a}, \vec{b}, \vec{c}} \gamma \left| a_0 a_1 \dots, b_0 b_1 \dots, c_0 c_1 \dots \right\rangle_{\text{dat}} \otimes (|\oplus_l a_l\rangle |\oplus_l c_l\rangle)_{\text{aux}} \quad (133)$$

$$= V \sum_{\vec{a}, \vec{b}, \vec{c}} \gamma' \left| a_0 \dots \bar{a}_j \dots, b_0 \dots \bar{b}_k \dots, c_0 c_1 \dots \right\rangle_{\text{dat}} \otimes (|\oplus_l \bar{a}_l\rangle |\oplus_l c_l\rangle)_{\text{aux}} \quad (134)$$

$$= V \sum_{\vec{a}, \vec{b}, \vec{c}} \gamma' \left| a_0 \dots \bar{a}_j \dots, b_0 \dots \bar{b}_k \dots, c_0 c_1 \dots \right\rangle_{\text{dat}} \otimes (|a_0 \oplus \dots \oplus \bar{a}_j \oplus \dots\rangle |\oplus_l c_l\rangle)_{\text{aux}} \quad (135)$$

$$= \sum_{\vec{a}, \vec{b}, \vec{c}} \gamma' \left| a_0 \dots \bar{a}_j \dots, b_0 \dots \bar{b}_k \dots, c_0 c_1 \dots \right\rangle_{\text{dat}} \otimes (|0\rangle |0\rangle)_{\text{aux}} \quad (136)$$

$$= h|\psi\rangle_{\text{dat}} \otimes |0\rangle_{\text{aux}}^{\otimes 2}, \quad (137)$$

as required. Progressing from Equation 135 to Equation 136 uses fact that V is a cascade of controlled–NOT gates. A symmetric argument follows for all $h \in \Lambda$ which do not commute for p_2 . For the case $x = N/2$, there will also be Hamiltonian terms that flip a_j and c_k , and a similar argument applies.

This establishes a modified qubit Hamiltonian \tilde{H}_q via Equation 78 and hence an auxiliary qubit mapping with two ancilla qubits, which we denote by $\overline{\text{JW}}_{\hat{h}'+2}$:

$$\overline{\text{JW}}_{\hat{h}'+2} : (H_{\text{fermion}} \text{ hopping terms}) \longmapsto \tilde{H}_q. \quad (138)$$

By construction, this mapping follows the rules set out in Section 4.1. The mapping has one degree of freedom: the value of x in the enumeration scheme \hat{h}' , which relates the n fermionic modes to the n data qubits.

As established in Section 3 for n –mode to n –qubit mappings, there are many possible cost functions for the qubit Hamiltonian. In extending this concept to our new n –mode to $(n+2)$ –qubit mapping $\overline{\text{JW}}_{\hat{h}'+2}$, we will determine the optimal value for x in order to minimise the average Pauli weight of \tilde{H}_q .

The *total* Pauli weight of all terms in the modified Hamiltonian \tilde{H}_q is (1) the total Pauli weight of the original H_q , plus (2) the difference between the new and old Z –matrix counts of the terms in $\Lambda_{\text{non-loc}}$ after multiplication by stabilisers, plus (3) the cost of extra operations on the auxiliary qubits from making the κ^h adjustments to terms in $\Lambda \setminus \Lambda_{\text{non-loc}}$. That is,

$$\begin{aligned} & \text{Total Pauli weight of } \tilde{H}_q & (139) \\ & = \quad (1) \text{ Total Pauli weight of } H_q \\ & \quad + (2) \text{ difference in } Z\text{–matrix count of } \tilde{H}_q \text{ and } H_q \\ & \quad + (3) \text{ number of adjusted terms in } \tilde{H}_q \text{ that are not multiplied by stabilisers} \end{aligned}$$

Begin by only considering the effects of the first stabiliser, $(p_1)_{\text{dat}} \otimes (Z \otimes \mathbb{1})_{\text{aux}}$. For (1), recall from Equation 51 that the total Pauli weight of the square lattice qubit Hamiltonian H_q is $C^1(f_M) + 2N(N - 1)$.

For (2): First determine which hopping terms should be multiplied by stabilisers. In the original Hamiltonian H_q , a term $h \in \Lambda$ between vertices α and β of G_F has Pauli weight $|f_M(\alpha) - f_M(\beta)| + 1$; as hopping terms consist of a string of Z matrices between a pair of X or Y matrices, the total number of Z matrices in such a term is then

$$\#(Z \text{ matrices in } h) = |f_M(\alpha) - f_M(\beta)| - 1. \quad (140)$$

Referring to the region labels A, B, \dots, D in Figure 25, it is clear that all of the lengthy hopping terms between vertices on the AD -interface will have less Z matrices after multiplication by the stabiliser $(p_1)_{\text{dat}} \otimes (Z \otimes \mathbb{1})_{\text{aux}}$. Using the labels from Figure 25 in Equation 140, the original number of Z matrices in *each* of these terms is then

$$\#(Z \text{ matrices in each row of } AD, \text{ before}) = Nx - x(x - 1) - 1. \quad (141)$$

By inspection, the topmost hopping term across the AD -interface after multiplication by $(p_1)_{\text{dat}} \otimes (Z \otimes \mathbb{1})_{\text{aux}}$ will consist of a single Z matrix on the first auxiliary qubit. For the hopping terms across the AD -interface in the j th row beneath the top row, there will be $2j$ Z matrices *after* multiplication by $(p_1)_{\text{dat}} \otimes (Z \otimes \mathbb{1})_{\text{aux}}$, including the one on the auxiliary qubit. Thus, the correction term for the AD -interface is

$$\begin{aligned} \Delta[\#(Z \text{ matrices in } AD)] & \quad (142) \\ & = 1 - (Nx - (x(x - 1))) + \sum_{j=1}^{x-1} \left(2j - (Nx - (x(x - 1))) \right). \end{aligned}$$

Hopping terms across the BD -interface and the first row of the CD -interface may benefit from multiplication by $(p_1)_{\text{dat}} \otimes (Z \otimes \mathbb{1})_{\text{aux}}$. Call the collection of these hopping terms the $(BC)D$ -interface, and consider its i th row: once again, the labels from Figure 25 in Equation 140 yield

$$\#(Z \text{ matrices in } i\text{th row of } (BC)D, \text{ before}) = Nx + x - 1 + i - (x^2 + ix - 1) - 1. \quad (143)$$

By inspection, these terms will have $(2 + i)x + i - 2$ Z matrices *after* multiplication by the stabiliser $(p_1)_{\text{dat}} \otimes (Z \otimes \mathbb{1})_{\text{aux}}$, including the Z matrix on the auxiliary qubit.

As Figure 26 shows, if x is large enough then it is possible that a small number of vertical hopping terms within the region C will benefit from stabiliser multiplication as well. Although this reduces the average Pauli weight of the qubit Hamiltonian even further, its effect is negligible compared to the savings across the $(BC)D$ -interface, and we omit it for simplicity. The correction term for the $(BC)D$ -interface is thus

$$\begin{aligned} \Delta[\#(Z \text{ matrices in } (BC)D)] & \quad (144) \\ & = \sum_{i=1}^K \left((2 + i)x + i - 2 - (Nx + x - 1 + i - (x^2 + ix - 1) - 1) \right). \end{aligned}$$

The value K depends on the size of x , as Figure 26 illustrates. From a naïve inspection of Equation 144, the i th row of the $(BC)D$ -interface hopping terms will observe a reduction

in Z -matrix count after stabiliser multiplication as long as

$$(2+i)x+i-2 < Nx+x+i-(x^2+ix+1) \quad (145)$$

$$i < \frac{1}{2x} + \frac{N-x-1}{2} \quad (146)$$

$$\leq \frac{N-x-1}{2}. \quad (147)$$

This might tempt us to set $K = \lfloor (N-x-1)/2 \rfloor$. However, there are $N-2x+1$ rows in the $(BC)D$ -interface, so the expression in Equation 144 is only valid if

$$K = \min \left\{ \left\lfloor \frac{N-x-1}{2} \right\rfloor, N-2x+1 \right\}. \quad (148)$$

These two values are equal if $x = \lfloor (N+4)/3 \rfloor$. Figure 26 shows the two scenarios where x is above or below this threshold value.

For (3), note that we must adjust all of the hopping terms h that do not commute with p_1 by multiplication by κ^h , which is a single X matrix targeting the first auxiliary qubit. However, in (2) we have already accounted for the cost of an extra auxiliary Z matrix on each of the terms in the AD - and BD -interfaces that benefited from stabiliser multiplication. This Z matrix will become $(-iY)$ upon prior adjustment by κ^h (premultiplication by X). We therefore need only count hopping terms that partially overlap with p_1 : by inspection of Figure 26, the total number of such terms is

$$\begin{aligned} \#(X \text{ matrices from correction to terms}) &= 2x-1 + (N-x-K-1) \\ &= N+x-K-1. \end{aligned} \quad (149)$$

As the Mitchison–Durbin pattern is symmetric, the same rules apply when considering the effects of the second stabiliser, $(p_2)_{\text{dat}} \otimes (\mathbf{1} \otimes Z)_{\text{aux}}$. We can now finally substitute these values into Equation 139 and express the total Pauli weight of \tilde{H}_q . Note that the factor of 2 in Equation 150 takes into account both stabilisers:

$$\begin{aligned} \text{Total Pauli weight of } \tilde{H}_q &= C^1(f_M) + 2N(N-1) \\ &+ 2 \left((1 - (Nx - x(x-1)) - 1) + \sum_{j=1}^{x-1} (2j - (Nx - x(x-1))) \right) \\ &+ \sum_{i=1}^K \left(((2+i)x+i-2) - (Nx+x+i-(x^2+ix+1)) \right) \\ &+ N+x-K-1 \Big). \end{aligned} \quad (150)$$

For example, using the value for $x \approx 0.29N$ from the original Mitchison–Durbin pattern f_M and dividing the total Pauli weight by the number of hopping terms, $2N(N-1)$, the average Pauli weight of our auxiliary qubit mapping, here nicknamed ‘ $f_{h'+2}$ ’, produces a dramatic improvement:

$$\text{APV} \left(f_{h'+2} \Big|_{x \approx 0.29N} \right) \approx 0.33N + 1.77 \quad (151)$$

However, in the scenario $x \leq \lfloor (N+4)/3 \rfloor$ with $K = \lfloor (N-x-1)/2 \rfloor$, the extremum $x = \lfloor (N+4)/3 \rfloor$ actually minimises the expression in Equation 150. The average Pauli

weight for large N in this instance is:

$$\text{APV} \left(f_{h'+2} \Big|_{x=\lfloor \frac{N+4}{3} \rfloor} \right) \approx \frac{26}{81}N + \frac{289}{162} = 0.32N + 1.78. \quad (152)$$

But there is a better value yet for x : in the other scenario, where $x > \lfloor (N+4)/3 \rfloor$, the value of K is $N - 2x + 1$. An approximately optimal value for x to minimise the total Pauli weight in this instance is

$$x = \frac{1}{8} \left(7 + N + \sqrt{\frac{15N^2 - 18N - 53}{3}} \right) \quad (153)$$

$$\approx \frac{1}{8} (1 + \sqrt{5}) N \quad (154)$$

$$= 0.40N, \quad (155)$$

which is the result of replacing floor brackets with normal parentheses in Equation 150. It is for this reason that we define our new pattern f_{M+2} to have x equal to the rounded value of that in Equation 153, i.e. $x \approx 0.40N$. For large N , this yields an average Pauli weight of

$$\text{APV}(f_{M+2}) = \text{APV} \left(f_{h'+2} \Big|_{x \approx 0.40N} \right) \approx 0.31N + 1.68. \quad (156)$$

This analysis does not include the cost of initialising the stabiliser state $|\tilde{\psi}\rangle_{\text{dat,aux}}$ via the unitary operation V . It is possible to implement V using fewer gates than the circuit in Figure 27 at the cost of more ancilla qubits [61]. However, even adding the cost of the circuit in Figure 27, which is $4(L-1) + 2 = 4((Nx-1) - (x(x-1) + 1) - 1) + 2 = 4Nx - x^2 + \mathcal{O}(x)$ CNOTs, to Equation 150 has negligible effects on the calculations in this section. The value $x \approx 0.40N$ in Equation 155 still holds.

References

- [1] Dave Wecker, Matthew B Hastings, Nathan Wiebe, Bryan K Clark, Chetan Nayak, and Matthias Troyer. “Solving strongly correlated electron models on a quantum computer”. *Physical Review A* **92**, 062318 (2015).
- [2] Giacomo Mauro D’Ariano, Franco Manessi, Paolo Perinotti, and Alessandro Tosini. “The feynman problem and fermionic entanglement: Fermionic theory versus qubit theory”. *International Journal of Modern Physics A* **29**, 1430025 (2014).
- [3] Nicolai Friis, Antony R Lee, and David Edward Bruschi. “Fermionic-mode entanglement in quantum information”. *Physical Review A* **87**, 022338 (2013).
- [4] Panagiotis Kl Barkoutsos, Nikolaj Moll, Peter WJ Staar, Peter Mueller, Andreas Fuhrer, Stefan Filipp, Matthias Troyer, and Ivano Tavernelli. “Fermionic hamiltonians for quantum simulations: a general reduction scheme” (2017). [arXiv:1706.03637](https://arxiv.org/abs/1706.03637).
- [5] Benjamin P Lanyon, James D Whitfield, Geoff G Gillett, Michael E Goggin, Marcelo P Almeida, Ivan Kassal, Jacob D Biamonte, Masoud Mohseni, Ben J Powell, Marco Barbieri, et al. “Towards quantum chemistry on a quantum computer”. *Nature chemistry* **2**, 106–111 (2010).
- [6] Manfred Salmhofer. “Renormalization in condensed matter: Fermionic systems—from mathematics to materials”. *Nuclear Physics B* **941**, 868–899 (2019).
- [7] Christina Verena Kraus. “A quantum information perspective of fermionic quantum many-body systems”. PhD thesis. Technische Universität München. (2009).

- [8] Ali Hamed Moosavian and Stephen Jordan. “Faster quantum algorithm to simulate fermionic quantum field theory”. *Physical Review A* **98**, 012332 (2018).
- [9] Joshua J. Goings, Alec White, Joonho Lee, Christofer S. Tautermann, Matthias Degroote, Craig Gidney, Toru Shiozaki, Ryan Babbush, and Nicholas C. Rubin. “Reliably assessing the electronic structure of cytochrome p450 on today’s classical computers and tomorrow’s quantum computers”. *Proceedings of the National Academy of Sciences* **119**, e2203533119 (2022). [arXiv:https://www.pnas.org/doi/pdf/10.1073/pnas.2203533119](https://www.pnas.org/doi/pdf/10.1073/pnas.2203533119).
- [10] Kaoru Hagiwara, K Hikasa, Kenzo Nakamura, M Tanabashi, M Aguilar-Benitez, C Amsler, RMichael Barnett, PR Burchat, CD Carone, C Caso, et al. “Review of particle physics”. *Physical Review D (Particles and Fields)* **66** (2002).
- [11] Matthew B. Hastings and Ryan O’Donnell. “Optimizing strongly interacting fermionic hamiltonians”. In *Proceedings of the 54th Annual ACM SIGACT Symposium on Theory of Computing*. Page 776–789. STOC 2022 New York, NY, USA (2022). Association for Computing Machinery.
- [12] Alán Aspuru-Guzik, Anthony D Dutoi, Peter J Love, and Martin Head-Gordon. “Simulated quantum computation of molecular energies”. *Science* **309**, 1704–1707 (2005).
- [13] Hefeng Wang, Sabre Kais, Alán Aspuru-Guzik, and Mark R Hoffmann. “Quantum algorithm for obtaining the energy spectrum of molecular systems”. *Physical Chemistry Chemical Physics* **10**, 5388–5393 (2008).
- [14] Ivan Kassal and Alán Aspuru-Guzik. “Quantum algorithm for molecular properties and geometry optimization”. *The Journal of chemical physics* **131**, 224102 (2009).
- [15] Ivan Kassal, Stephen P Jordan, Peter J Love, Masoud Mohseni, and Alán Aspuru-Guzik. “Polynomial-time quantum algorithm for the simulation of chemical dynamics”. *Proceedings of the National Academy of Sciences* **105**, 18681–18686 (2008).
- [16] Jarrod R McClean, Ryan Babbush, Peter J Love, and Alán Aspuru-Guzik. “Exploiting locality in quantum computation for quantum chemistry”. *The journal of physical chemistry letters* **5**, 4368–4380 (2014).
- [17] Frank Verstraete and J Ignacio Cirac. “Mapping local hamiltonians of fermions to local Hamiltonians of spins”. *Journal of Statistical Mechanics: Theory and Experiment* **2005**, P09012 (2005).
- [18] Ivan Kassal, James D Whitfield, Alejandro Perdomo-Ortiz, Man-Hong Yung, and Alán Aspuru-Guzik. “Simulating chemistry using quantum computers”. *Annual review of physical chemistry* **62**, 185–207 (2011).
- [19] Julia Kempe, Alexei Kitaev, and Oded Regev. “The complexity of the local Hamiltonian problem”. *Siam journal on computing* **35**, 1070–1097 (2006).
- [20] Ryan Babbush, Peter J Love, and Alán Aspuru-Guzik. “Adiabatic quantum simulation of quantum chemistry”. *Scientific reports* **4**, 1–11 (2014).
- [21] Gerardo Ortiz, James E Gubernatis, Emanuel Knill, and Raymond Laflamme. “Quantum algorithms for fermionic simulations”. *Physical Review A* **64**, 022319 (2001).
- [22] Alexei Y. Kitaev. “Quantum measurements and the abelian stabilizer problem”. *Electron. Colloquium Comput. Complex.* **TR96** (1995). url: <https://api.semanticscholar.org/CorpusID:17023060>.
- [23] Daniel S Abrams and Seth Lloyd. “Quantum algorithm providing exponential speed increase for finding eigenvalues and eigenvectors”. *Physical Review Letters* **83**, 5162 (1999).
- [24] Alberto Peruzzo, Jarrod McClean, Peter Shadbolt, Man-Hong Yung, Xiao-Qi Zhou, Peter J Love, Alán Aspuru-Guzik, and Jeremy L O’Brien. “A variational eigenvalue solver on a photonic quantum processor”. *Nature communications* **5**, 1–7 (2014).

- [25] Jarrod R McClean, Jonathan Romero, Ryan Babbush, and Alán Aspuru-Guzik. “The theory of variational hybrid quantum-classical algorithms”. *New Journal of Physics* **18**, 023023 (2016).
- [26] Matthew B Hastings, Dave Wecker, Bela Bauer, and Matthias Troyer. “Improving quantum algorithms for quantum chemistry”. *Quantum Information & Computation* **15**, 1–21 (2015).
- [27] Pascual Jordan and Eugene Paul Wigner. “Über das Paulische Äquivalenzverbot”. *Zeitschrift für Physik* **47**, 631–651 (1928).
- [28] Elliott Lieb, Theodore Schultz, and Daniel Mattis. “Two soluble models of an anti-ferromagnetic chain”. *Annals of Physics* **16**, 407–466 (1961).
- [29] Rami Barends, L Lamata, Julian Kelly, L García-Álvarez, Austin G Fowler, A Megrant, Evan Jeffrey, Ted C White, Daniel Sank, Josh Y Mutus, et al. “Digital quantum simulation of fermionic models with a superconducting circuit”. *Nature communications* **6**, 1–7 (2015).
- [30] Yu-An Chen, Anton Kapustin, and Đorđe Radičević. “Exact bosonization in two spatial dimensions and a new class of lattice gauge theories”. *Annals of Physics* **393**, 234–253 (2018).
- [31] Yu-An Chen and Anton Kapustin. “Bosonization in three spatial dimensions and a 2-form gauge theory”. *Physical Review B* **100**, 245127 (2019).
- [32] Yu-An Chen. “Exact bosonization in arbitrary dimensions”. *Physical Review Research* **2**, 033527 (2020).
- [33] Yu-An Chen, Yijia Xu, et al. “Equivalence between fermion-to-qubit mappings in two spatial dimensions”. *PRX Quantum* **4**, 010326 (2023).
- [34] Kanav Setia, Sergey Bravyi, Antonio Mezzacapo, and James D Whitfield. “Superfast encodings for fermionic quantum simulation”. *Physical Review Research* **1**, 033033 (2019).
- [35] Zhang Jiang, Jarrod McClean, Ryan Babbush, and Hartmut Neven. “Majorana loop stabilizer codes for error mitigation in fermionic quantum simulations”. *Physical Review Applied* **12**, 064041 (2019).
- [36] Charles Derby and Joel Klassen. “Low weight fermionic encodings for lattice models” (2020). [arXiv:2003.06939](https://arxiv.org/abs/2003.06939).
- [37] Mark Steudtner and Stephanie Wehner. “Quantum codes for quantum simulation of fermions on a square lattice of qubits”. *Physical Review A* **99**, 022308 (2019).
- [38] Zhang Jiang, Amir Kalev, Wojciech Mruzekiewicz, and Hartmut Neven. “Optimal fermion-to-qubit mapping via ternary trees with applications to reduced quantum states learning”. *Quantum* **4**, 276 (2020).
- [39] Sergey B Bravyi and Alexei Y Kitaev. “Fermionic quantum computation”. *Annals of Physics* **298**, 210–226 (2002).
- [40] Graeme Mitchison and Richard Durbin. “Optimal numberings of an $N \times N$ array”. *SIAM Journal on Algebraic Discrete Methods* **7**, 571–582 (1986).
- [41] Michael R Garey, David S Johnson, and Larry Stockmeyer. “Some simplified NP-complete problems”. In Proceedings of the sixth annual ACM symposium on Theory of computing. Pages 47–63. (1974).
- [42] Michael R Garey, Ronald L Graham, David S Johnson, and Donald Ervin Knuth. “Complexity results for bandwidth minimization”. *SIAM Journal on Applied Mathematics* **34**, 477–495 (1978).
- [43] Michael R Garey and David S Johnson. “Computers and intractability; a guide to the theory of np-completeness”. *W. H. Freeman & Co. USA* (1990).

- [44] John Hubbard and Brian Hilton Flowers. “Electron correlations in narrow energy bands”. *Proceedings of the Royal Society of London. Series A. Mathematical and Physical Sciences* **276**, 238–257 (1963). [arXiv:https://royalsocietypublishing.org/doi/pdf/10.1098/rspa.1963.0204](https://royalsocietypublishing.org/doi/pdf/10.1098/rspa.1963.0204).
- [45] Michael A. Nielsen. “The fermionic canonical commutation relations and the jordan-wigner transform”. url: https://futureofmatter.com/assets/fermions_and_jordan_wigner.pdf.
- [46] Aaron Miller, Zoltán Zimborás, Stefan Knecht, Sabrina Maniscalco, and Guillermo García-Pérez. “Bonsai algorithm: Grow your own fermion-to-qubit mappings”. *PRX Quantum* **4**, 030314 (2023).
- [47] Mitchell Chiew and Sergii Strelchuk. “To appear”.
- [48] Andrew Tranter, Peter J Love, Florian Mintert, and Peter V Coveney. “A comparison of the bravyi–kitaev and jordan–wigner transformations for the quantum simulation of quantum chemistry”. *Journal of chemical theory and computation* **14**, 5617–5630 (2018).
- [49] Jacob T Seeley, Martin J Richard, and Peter J Love. “The Bravyi-Kitaev transformation for quantum computation of electronic structure”. *The Journal of chemical physics* **137**, 224109 (2012).
- [50] Tjalling C Koopmans and Martin Beckmann. “Assignment problems and the location of economic activities”. *Econometrica: journal of the Econometric Society* Pages 53–76 (1957).
- [51] Martin Juvan and Bojan Mohar. “Optimal linear labelings and eigenvalues of graphs”. *Discrete Applied Mathematics* **36**, 153–168 (1992).
- [52] Alan George and Alex Pothen. “An analysis of spectral envelope reduction via quadratic assignment problems”. *SIAM Journal on Matrix Analysis and Applications* **18**, 706–732 (1997). [arXiv:https://doi.org/10.1137/S089547989427470X](https://doi.org/10.1137/S089547989427470X).
- [53] Steven Bradish Horton. “The optimal linear arrangement problem: algorithms and approximation”. PhD thesis. School of Industrial and Systems Engineering, Georgia Institute of Technology. (1997).
- [54] Yung-Ling Lai and Kenneth Williams. “A survey of solved problems and applications on bandwidth, edgesum, and profile of graphs”. *Journal of graph theory* **31**, 75–94 (1999).
- [55] Greg N Frederickson and Susanne E Hambrusch. “Planar linear arrangements of outerplanar graphs”. *IEEE transactions on Circuits and Systems* **35**, 323–333 (1988).
- [56] Fan-Rong King Chung. “On optimal linear arrangements of trees”. *Computers & mathematics with applications* **10**, 43–60 (1984).
- [57] James B Saxe. “Dynamic-programming algorithms for recognizing small-bandwidth graphs in polynomial time”. *SIAM Journal on Algebraic Discrete Methods* **1**, 363–369 (1980). [arXiv:https://doi.org/10.1137/0601042](https://doi.org/10.1137/0601042).
- [58] Nikolaj Moll, Andreas Fuhrer, Peter Staar, and Ivano Tavernelli. “Optimizing qubit resources for quantum chemistry simulations in second quantization on a quantum computer”. *Journal of Physics A: Mathematical and Theoretical* **49**, 295301 (2016).
- [59] James D Whitfield, Vojtěch Havlíček, and Matthias Troyer. “Local spin operators for fermion simulations”. *Phys. Rev. A* **94**, 030301 (2016).
- [60] Alexander Cowtan, Silas Dilkes, Ross Duncan, Alexandre Krajenbrink, Will Simmons, and Seyon Sivarajah. “On the Qubit Routing Problem”. In Wim van Dam and Laura Mancinska, editors, 14th Conference on the Theory of Quantum Computation, Communication and Cryptography (TQC 2019). Volume 135 of *Leibniz International*

Proceedings in Informatics (LIPIcs), pages 5:1–5:32. Dagstuhl, Germany (2019). Schloss Dagstuhl–Leibniz-Zentrum fuer Informatik.

- [61] Jiaqing Jiang, Xiaoming Sun, Shang-Hua Teng, Bujiao Wu, Kewen Wu, and Jialin Zhang. “Optimal space-depth trade-off of CNOT circuits in quantum logic synthesis”. In Proceedings of the Fourteenth Annual ACM-SIAM Symposium on Discrete Algorithms. Pages 213–229. SIAM (2020).